X-ray Absorption Spectroscopy of Copper: Characterization of the Human Copper Chaperone to Superoxide Dismutase

Jay Paul Stasser
B.S., Chemistry, The Evergreen State College (1993)

A dissertation submitted to the faculty of the
OGI School of Science & Engineering
at Oregon Health & Science University
in partial fulfillment of the
requirements for the degree

Doctor of Philosophy
in
Biochemistry and Molecular Biology

March 2006

The dissertation "X-ray Absorption Spectroscopy of Copper: Characterization of the Human Copper Chaperone to Superoxide Dismutase" by Jay Paul Stasser has been examined and approved by the following examination committee:

Ninian J. Blackburn, Research Advisor
Professor

Bradley M. Tebo
Professor

Pierre Moënne-Loccoz
Assistant Professor

Arthur Glasfeld
Professor
Reed College

Acknowledgments

I would like to thank my advisor, Dr. Ninian Blackburn, for the opportunity he gave me by accepting me as one of his students and for his guidance, advice and patience. And I would like to thank my wife and kids, Diana, Regina, and Ariel, for their love and support and the much needed distraction they provided.

I would also like to acknowledge the members of the Blackburn lab, past and present, who helped me out through the years, specifically: Martina Ralle, for her help on the beamline and her advice afterwards; Amanda Barry, for the discussions about CCS and other things; Mary Mayfield-Gambill, for her plasmids; Frank Rhames and Shula Jaron, for helping to get me settled into the lab.

Table of Contents

List of Tables

List of Figures

Abstract

X-ray Absorption Spectroscopy of Copper:
Characterization of the Human Copper Chaperone
to Superoxide Dismutase

Jay Paul Stasser, B.S.

Ph. D., OGI School of Science and Engineering
at Oregon Health & Science University

March 2006

Thesis Advisor: Dr. Ninian J. Blackburn

The human copper chaperone to superoxide dismutase (hCCS) is a zinc and copper containing protein that delivers copper to the active site of the cytoplasmic protein superoxide dismutase (SOD). hCCS is a three domain protein with three possible copper binding sites: Domain I is called the Atx-like domain and contains the copper binding motif MXCXXC; Domain II is the SOD-like domain and includes the slightly altered histidine rich copper binding site seen in SOD; and Domain III is a short C-terminal tail that has the copper binding motif of CXC. Studies of the WT protein using EXAFS showed that the protein contained a binuclear copper-sulfur cluster. Initially, it was unknown whether this cluster was formed between domain I and domain II of the protein or formed intermolecularly between two hCCS monomers. Further studies, on the cysteine to serine

mutants of the residues in the Domain I and Domain II motifs, showed that while the Domain I motif is capable of binding Cu(I), it is Domain III that is the site of the copper cluster and the cluster is formed between two hCCS monomers. Additional studies with cysteine to alanine mutants of the residues in the copper binding motifs of Domain I and Domain III, showed that Domain III is not only the site of the copper cluster but also the site of transfer of copper from hCCS to SOD and also a dimerization interface for hCCS. While Domain I can bind copper and may play a role in regulation of activity, it is Domain III that contains the activity of hCCS.

CHAPTER 1
INTRODUCTION

1.1 OVERVIEW

The goal of this thesis is to characterize the copper-binding sites of the human copper chaperone to superoxide dismutase (hCCS). The copper chaperone to superoxide dismutase (CCS) is a copper-binding protein that acquires copper in the cytosol and delivers it to the copper-utilizing enzyme Cu, Zn superoxide dismutase [Culotta et al. 1997]. This introduction contains a review of copper in human biology as well a focus on the known human copper-containing enzymes, with an emphasis on Cu, Zn superoxide dismutase. Next the introduction covers the transport and regulation of copper in the cell, with an emphasis on copper chaperones. Finally the human copper chaperone to superoxide dismutase is covered in depth concluding with the introduction of the heterodimer mechanism. In this mechanism, it is proposed that a monomer of CCS binds a single atom of copper(I) with three ligating cysteine residues found within domain I and domain III of the protein. The copper-loaded CCS then interacts with a monomer of SOD via domain II to form the heterodimer. Once the heterodimer is formed transfer of copper can take place from CCS to SOD [Torres et al. 2001].

Chapter 2 covers the methods and techniques used within the thesis, first covering the development of the expression systems used to purify hCCS and its mutants. Next the physical techniques are covered with an emphasis on Extended X-ray Absorption Fine Structure (EXAFS), the main form of spectroscopy used in this thesis. In chapter 3, we begin to characterize the copper binding site of wild type hCCS, showing that copper

binds to hCCS in the form of a binuclear copper-sulfur cluster, this finding differing from previous assumptions that CCS binds copper in a single three or four coordinate sulfur site. Chapter 4 covers the first mutational studies of hCCS with the study of single and double cysteine to serine mutants. Our findings from these studies show that the active copper-sulfur cluster is most likely formed by interactions between two domain III binding sites from separate CCS monomers and that the activity of CCS is dependent on the formation of the cluster. This brings into question the heterodimer mechanism which is based on the active form of CCS being a single CCS monomer with a copper site formed by the interaction of domain I and domain III. Instead we propose that the active site of hCCS is most likely a dimer of hCCS with the copper site being formed by interactions solely between two domain III motifs.

In Chapter 5 we return to studies of the wild type CCS from an intein expression system as well as various cysteine to alanine mutants. The localization of the copper cluster to domain III and the dependence of copper transfer activity on cluster formation are both confirmed for the untagged protein. This chapter includes reconstitution studies undertaken to study CCS loaded with substoichiometric levels of copper. Gel filtration on these reconstituted samples show a much more complex monomer-dimer equilibrium than that put forth in the heterodimer mechanism. The research done in this chapter suggests that the active form of hCCS is a dimer formed through the intermolecular interaction of domain III to form the copper-sulfur cluster, very different from the monomer of hCCS present as the starting species for the heterodimer mechanism. Chapter 6 presents the final conclusions of the thesis as well as suggestions for future studies including residues of interest for mutation and use of intein mediated protein ligation for the incorporation of selenocystiene into the active site of hCCS to allow the use of Se-EXAFS for further structural studies of hCCS as well as its interactions with hSOD.

1.2 COPPER IN HUMAN BIOLOGY

Copper (Cu) is a transition metal with the atomic number of 29 and an atomic weight of 63.55. It is in group IB of the periodic table which includes gold and silver. There is very little similarity between these metals but all commonly form the +1 ion to completely empty their 4*s* shell. In aqueous environments, copper is found mainly as two ions; the reduced or cuprous form, copper(I) and the oxidized or cupric form, copper(II). Free copper(I) can be unstable in aqueous environments and will spontaneously disproportionate into copper(II) and copper(0), this reaction, however, is inhibited in the presence of complexing agents that favor copper(I), such as CN^-, I^- and S^{2-}. Copper can also form the copper(III) oxidation state, but this ion is extremely unstable due to its strong oxidizing ability [Cotton et al. 1980; Shriver et al. 1990].

Copper is an essential trace element for all species of the phylogenic tree. It is defined as an essential trace metal because some level must be maintained to sustain biological function, but high levels are toxic. Therefore, the levels of copper must be under homoeostatic control to balance between essential need and toxicity. In humans, the recommended dietary allowance is 0.9 mg/day. Foods high in copper include nuts, beans, grains, liver, shellfish, oysters, and chocolate [Trumbo et al. 2001]. The requirements for copper as an essential nutrient were first suggested by Josephs, in 1931. His studies showed that copper deficiency could account for the iron unresponsive anemia in a population of milk-fed infants [Josephs 1931]. From that time the nutritional requirement of copper was debated until work done by Cardano et al. in the 1960's on a population in Peru, which helped to characterize the classical signs of copper deficiency and establish copper as a micro nutrient [Cordano et al. 1964; Cordano 1998]. Since then it has been shown that copper performs many important functions in the human body, including oxygen chemistry, iron regulation, connective tissue production, hormone and neurotransmitter production, blood cell maturation, brain development, and immune function [Klinman 1996; Harris et al. 1998; Keen et al. 1998; Percival 1998; Rucker et al. 1998; Hellman et al. 2002; Lewis et al. 2004].

1.2.1 WHOLE BODY COPPER METABOLISM

There is little known about the exact route of copper absorption into the body. It is known that copper absorption is closely balanced with zinc absorption. Zinc is absorbed into the gut by use of small metallothioneins, general metal binding proteins, that are capable of binding copper. If copper concentration increases, it competes with zinc binding to the metallothioneins, and if the zinc concentration decreases, the excess metallothionein binds copper, thereby inhibiting its absorption. High levels of zinc can cause the production of high levels of metallothioneins and further inhibit the absorption of copper [Lonnerdal 1998].

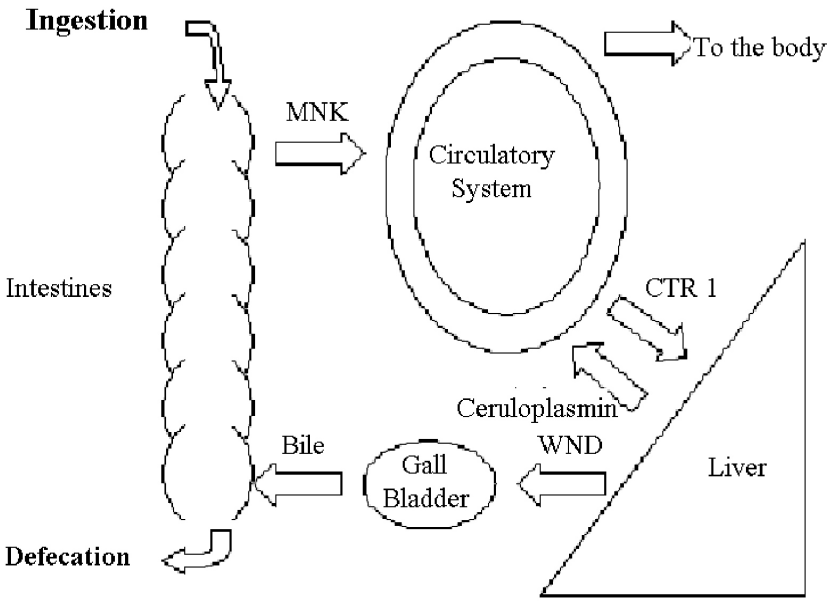

Figure 1.1: Copper cycling through the human body.

Copper is mainly absorbed in the absorptive cells in the intestinal mucosa of the small intestine by an unknown mechanism. At low concentrations, the transport of copper appears to be energy dependent, but there is evidence that at high concentrations transport can happen by non-carrier diffusion [Crampton et al. 1965; Bronner et al. 1985]. The exact proteins involved in transfer into the cells of the intestinal wall are not well defined. It has been suggested that transfer might be promoted by the transporter

protein, CTR1 [Zhou et al. 1997]. CTR1 is known to be the route of copper entry into cells elsewhere in the body [Dancis et al. 1994]. It has also been suggested that DMT1, a NRAMP2-like divalent cation transporter, might be responsible [Gunshin et al. 1997], but to date no studies have been conclusive regarding the route of entry into the intestinal walls [Zerounian et al. 2003]. How copper moves across the basolateral membrane into the blood has been determined, and that is done by the ATP7A transporter called the Menke's protein [Greenough et al. 2004]. Studies have shown that the regulated step of copper absorption is the transfer of copper from the basolateral cells into the blood [Linder 1991]. After release into the blood stream, copper is known to bind nonspecifically to the protein albumin as well as free amino acids, mainly histidine [Sarkar 1981]. Once in the blood stream, copper is delivered to all the cells of the body.

The major source of copper excretion from the body is release into the bile and then out through the digestive tract. The hepatocytes transfer copper to the bile canaliculi where copper is incorporated into the bile [Tao et al. 2003; Wijmenga et al. 2004]. Copper is known to be transported into the hepatic cells by the copper transporter CTR1, a high-affinity copper uptake protein [Tao et al. 2003]. In the liver, copper is transferred into the Golgi network of the hepatocytes via the ATP7B transporter known as the Wilson's disease protein [Wijmenga et al. 2004]. In the Golgi network, copper is either incorporated into ceruloplasmin, a plasma ferroxidase containing 6 atoms of copper, or released into the bile canaliculi. The bile canaliculi are capillaries which join together to form the bile duct and transport bile from the liver to the intestines and gall bladder. Copper excretion from the body is the main source of regulating copper levels as dietary levels of copper rarely change [Barceloux 1999]. Renal release of copper is rare, except in the case of kidney damage.

Copper deficiency can lead to anemia, due to low levels of ceruloplasmin, which is important in iron regulation, neutropenia, a reduction in the blood neutrophil count, and bone abnormalities [Watts 1989; Percival 1998]. The liver usually stores large amounts of copper making copper deficiency unusual, but it has been reported in case of extreme malnutrition, diarrhea, and most commonly Menke's disease [Olivares et al. 1996]. Menke's disease results from the inability of the body to transport copper across

the intestinal wall due to the genetic mutation of a transporter protein, the Menke's disease protein, ATP7A. Menkes disease is an X-linked mutation which mainly affects males. The symptoms of Menke's disease are present in one in 50,000 live births and can be characterized by neurodegeneration, connective tissue abnormalities and eventually death [Mercer 1998].

1.2.2 COPPER ENZYMES

Historically, copper sites in proteins have been divided into three main categories: Type I, Type II, and Type III (Figure 1.2). Blue, or type I, copper proteins are spectroscopically characterized by their intense absorption at 600 nm, resulting from a sulfur to copper ligand to metal charge transfer. Typically, type I copper sites exhibit a trigonal planar coordination geometry with the sulfur of one cysteine residue and two nitrogens from histidine residues. Often, there are one or two weakly bound ligands in the axial positions. Type I sites are usually electron transfer sites. Type II sites are, generally, four or five coordinate structures of distorted tetrahedral or tetragonal geometry, respectively, and have strictly nitrogen or oxygen donors as ligands. Also, type II sites generally have very weak optical spectra but do have a very characteristic

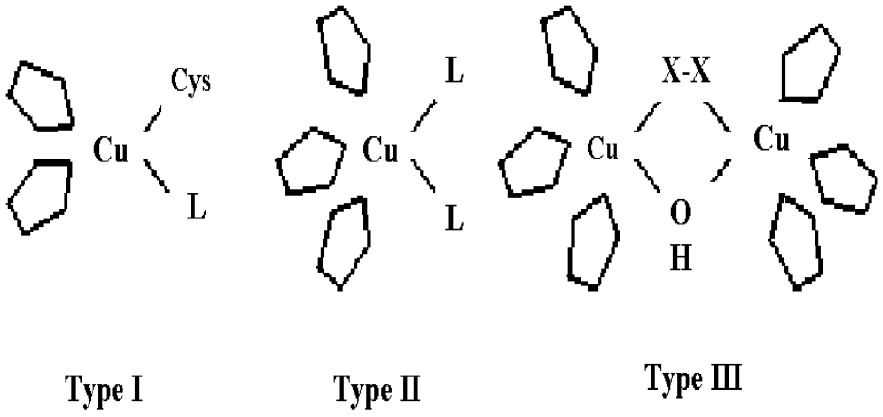

Figure 1.2: The three types of copper sites

Table 1.1: Copper-containing enzymes in human biology

Protein	Function	Thesis Section
Ceruloplasmin	Iron oxidase important in iron transport	1.2.2.1
Cytochrome *c* oxidase	Terminal end of the electron transfer chain in respiration, catalyzes the 4 e^- reduction of O_2 to H_2O	1.2.2.2
Peptidylglycine α-hydoxylating monooxygenase	Catalyzes the first step of a two-step process that activates peptide hormones by the amidation of the C-terminus	1.2.2.3
Dopamine β-monooxygenase	Catalyzes the conversion of dopamine to norepinephrine	1.2.2.4
Amine Oxidase	Catalyzes the oxidation of amines to aldehydes	1.2.2.5
Lysyl Oxidase	Catalyzes the crosslinking of collagen and elastin	1.2.2.5
Tyrosinase	Catalyzes the oxidation of phenols and catechols to ortho-quinones	1.2.2.6
Superoxide Dismutase	Catalyzes the dismutation of superoxide to oxygen and water	1.2.3

EPR spectrum. Type II copper sites are catalytically active sites, carrying out oxygen activation. A Type III or coupled dinuclear site, contains two electronic coupled copper atoms generally involved in oxygen binding or oxygen activation [Roat-Malone 2002].

Below are reviews of the main copper containing enzymes found in humans, absent from this list is Cu, Zn superoxide dismutase (SOD) which is covered in more detail in section 1.3.

1.2.2.1 Ceruloplasmin. Ceruloplasmin is part of the family of multicopper oxidases that includes laccase and ascorbate oxidase, notable because they contain all three of the types of copper sites (Figure 1.3) [Messerschmidt et al. 1990]. Ceruloplasmin is a plasma protein that is produced in the Golgi network of hepatocytes and released into the blood stream [Aldred et al. 1987]. Ceruloplasmin accounts for 95% of all serum copper and is known to be an important component in iron metabolism [Hellman et al. 2002]. A homologue of ceruloplasmin, hephaestin, has recently been discovered and has been shown to be responsible for regulation of iron transport across the placental barrier [Vulpe et al. 1999].

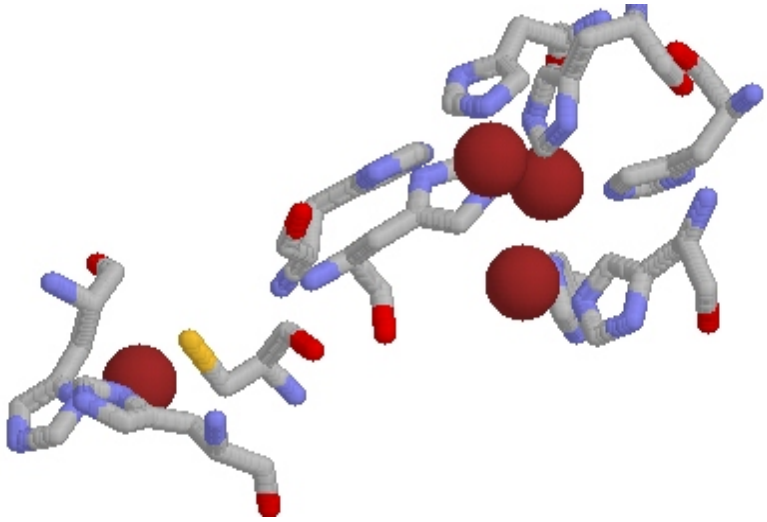

Figure 1.3: The three copper sites of ceruloplasmin. The coordinates for this structure were taken from the protein data bank file 1KCW.

Ceruloplasmin is a six domain protein that contains five Type I copper sites as well as one Type II site and one Type III site closely related in a trinuclear cluster. Ceruloplasmin oxidizes Fe^{2+} to Fe^{3+} coupled to the 4 e^- reduction of oxygen to water via the following reaction:

$$4\ Fe^{2+} + O_2 + 4\ H^+ \rightarrow 4\ Fe^{3+} + 2\ H_2O$$

This step of iron oxidation is crucial to the import of iron into the cell. The Type I sites are implicated as the sites of iron oxidation while the trinuclear cluster is believed to be the site of oxygen reduction [Calabrese et al. 1989; Palmer et al. 2002].

1.2.2.2 Cytochrome c oxidase. Cytochrome *c* oxidase (COX) is a heme/ copper protein found in the mitochondria. COX is the terminal end of the electron transfer chain that couples metabolism to ATP formation in respiration. COX accepts electrons from cytochrome *c* and performs the 4 e^- reduction of dioxygen to water, coupled with the movement of protons across the mitochondrial inner membrane:

$$\text{Cyt } c \text{ (red)} + O_2 + 8H^+_{in} \rightarrow \text{Cyt } c \text{ (ox)} + 2H_2O + 4H^+_{out}$$

It is this movement of protons that creates the protomotive force that drives the production of ATP.

COX contains three copper atoms in two copper sites and two heme sites (Figure 1.4) [Tsukihara et al. 1995]. The first site, Cu_A, is a dinuclear copper site that is

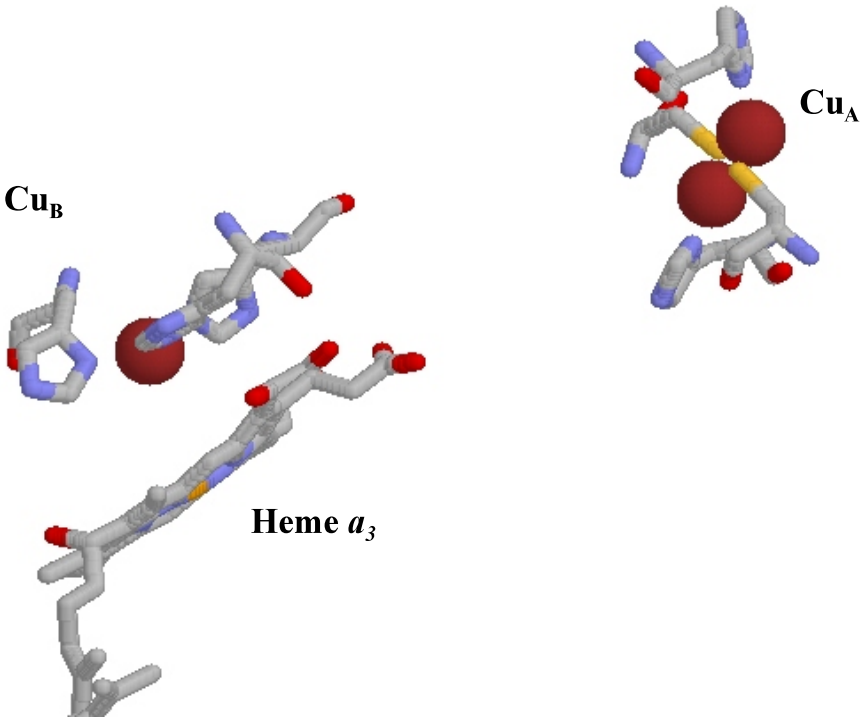

Figure 1.4: The Cu_A and Cu_B-heme a_3 sites of cytochrome *c* oxidase. The coordinates for this structure were taken from the protein data bank file 2OCC.

responsible for electron transfer. The second site, Cu_B, is a mononuclear copper site that is bridged to a heme a_3 cofactor and is the site of oxygen reduction [Beinert 1995]. The electron transfer chain in COX follows the path:

$$\text{Cyt } c \rightarrow Cu_A \rightarrow \text{heme } a \rightarrow \text{heme } a_3 - Cu_B \rightarrow O_2$$

1.2.2.3 Peptidylglycine α-hydroxylating monooxygenase. Peptidylglycine α-hydroxylating monooxygenase (PHM) is a copper containing monooxygenase, so called because it inserts one oxygen atom from the dioxygen into its substrate and reduces the other oxygen atom to water [Klinman 1996]. PHM is expressed and targeted to vacuoles in neural and endocrine cells. PHM activates peptide hormones by catalyzing the first step of a two-step process which lyses the carbon–nitrogen bond in a C-terminal glycine residue leaving an α-NH_2 moiety on the C-terminus of the peptide hormone [Eipper et al. 1988]. PHM starts the lysis reaction by hydroxylating the α-carbon of the glycine

residue. The lysis of the carbon–nitrogen bond is then performed by peptidylhydroxyglycine α-amidating lyase (PAL), a zinc and iron containing enzyme [Young et al. 1989; Prigge et al. 1999].

PHM contains two copper sites separated by 11 Å, the Cu_H site coordinated by three histidines and one solvent molecule in the oxidized form and the Cu_M site coordinated by two histidines and two solvent molecules in the oxidized form (Figure 1.5) [Prigge et al. 1997]. The Cu_M site is so named because upon reduction it binds the sulfur of a nearby methionine residue [Boswell et al. 1996]. The mechanism of PHM first involves the two e^- reduction of both copper atoms followed by the insertion of one oxygen atom onto the terminal glycine of the peptide substrate:

$$R\text{-}NH\text{-}CH_2\text{-}COO^- + O_2 + 2H^+ \rightarrow R\text{-}NH\text{-}CHOH\text{-}COO^- + H_2O$$

Substrate binding and oxygen insertion are known to happen at the Cu_M site while the Cu_H site is thought to play a role in oxygen activation or electron transfer.[Jaron et al. 1999].

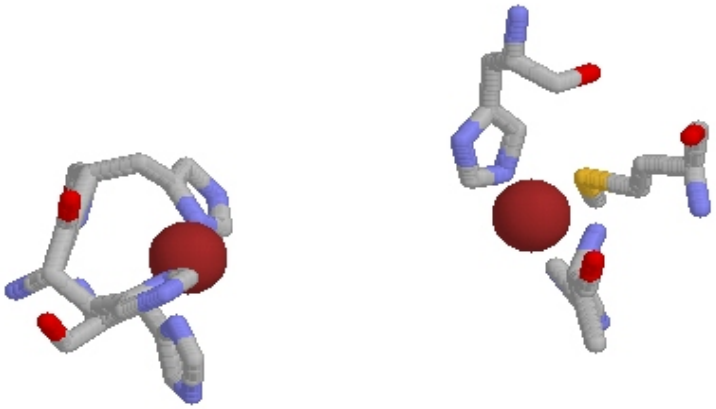

Figure 1.5: The oxidized forms of the CuH and CuM sites of peptidylglycine α-hydroxylating monooxygenase. The cooridinates for this structure were taken from the protein data bank file 1PHM.

1.2.2.4 Dopamine β-monoxygenase. Dopamine β-monooxygenase (DBM) is a copper containing monoxygenase that is very similar to PHM. Like PHM, DBM contains two copper sites and like PHM, DBM catalyzes the insertion of one

oxygen atom from dioxygen into its substrate. The reaction catalyzed by DBM is the conversion of dopamine to norepinephrine:

$$PhCH_2CH_2NH_2 + O_2 + 2H^+ \rightarrow PhCHOHCH_2NH_2 + H_2O$$

Although less work has been done on DBM it is assumed that its mechanism is the same as PHM [Klinman 1996; Klinman 2005].

1.2.2.5 Amine Oxidases. Copper containing amine oxidases (CuAO) are a class of enzymes that contain a copper ion as well as the organic cofactor 2,4,5 – trihydroxyphenylalanine quinone (TPQ), a modified tyrosine residue [Klinman 1996]. These enzymes include diamine oxidase, an intracellular membrane-bound protein responsible for the breakdown of histamine; cell surface and serum CuAOs, such as VAP1, the vascular adhesion protein; and the closely related lysyl oxidase, an extracellular enzyme responsible for the cross linking of the extracellular matrix [Rucker et al. 1998; Salmi et al. 2002; Klinman 2003].

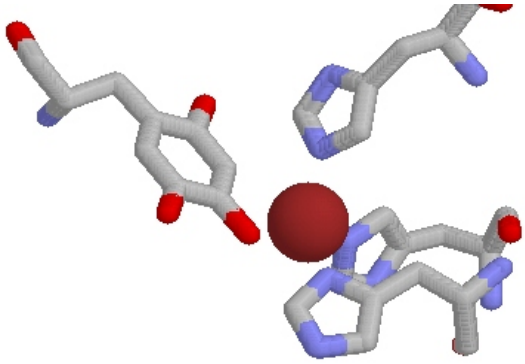

Figure 1.6: The copper site with the TPQ cofacter of vascular adhesion protein, an amino oxidase. The coordinates for this structure were taken from the protein data bank file 1PU4.

The copper active site (Figure 1.6) is known to play a role in the biogenesis of the TPQ, but whether or not it is involved in the catalytic oxidation of amines to aldehydes is still debated. Initially, the protein is expressed as an inactive protein with a copper site

containing three histidine ligands and a nearby tyrosine residue [Cai et al. 1994]. The first step of the protein biogenesis is oxidation of the tyrosine to TPQ by the copper site:

$$Cu(His)_3 + 2O_2 + H_2O + Tyr\text{-}E \rightarrow Cu(His)_3(H_2O)_2 + H^+ + H_2O_2 + TPQ\text{-}E$$

This leaves the active protein containing a five-coordinate copper site with a nearby TPQ residue. The reaction catalyzed by the active protein can be broken down into two steps: the oxidation of the amine to an aldehyde and the reduction of oxygen to hydrogen peroxide [McGuirl et al. 1999; Whittaker 1999]:

$$E_{ox} + RCH_2NH_3^+ \rightarrow E_{red}\text{-}NH_3^+ + RCHO$$

$$E_{red}\text{-}NH_3^+ + O_2 \rightarrow E_{ox} + H_2O_2 + NH_3^+$$

Although it has been determined that copper plays no role in the oxidation of the amine, it is still debated if copper is the site of oxygen binding in the second step of the reaction [Dawkes et al. 2001].

Lysyl oxidase (LO) is an enzyme similar to the CuAOs, except that it contains a lysyl tyrosyl quinine (LTQ) instead of a TPQ cofactor (Figure 1.7). LO catalyzes the cross linking of collagen and elastin in the extracellular matrix by the reduction of peptidyl lysine to peptidyl α-aminoadipic-δ-semialdehyde (AAS). Once formed, AAS can spontaneously condense with peptidyl lysine to form cross linkages [Smith-Mungo et al. 1998]. LTQ is itself formed by a cross-link between lysine and tyrosine. In LO, as in CuAOs, copper is known to play a role in the biogenesis of the cofactor, but its role in the catalytic cycle is unknown [Kagan et al. 2003].

1.2.2.6 Tyrosinase Tyrosinase is a copper containing enzyme that catalyzes the oxidation of phenols and catechols to ortho-quinones. Ortho-quinones nonenzymatically react to form the precursors of melanin production [Mason 1948]. In mammals, tyrosinase is selectively expressed in the neural crest cells in the skin and retina of the eye. Tyrosinase contains a type III copper site containing two coupled copper atoms [Gerdemann et al. 2002]. The typical reaction catalyzed by tyrosinase is the oxidation of dopaquinone via the insertion of an oxygen atom from molecular oxygen:

$$\text{Tyrosine} + O_2 \rightarrow \text{Dopaquinone} + H_2O$$

The oxygen is activated by bridging between the two coppers in the type III site [Land et al. 2003].

1.2.3 SUPEROXIDE DISMUTASE

Most aerobic life forms produce energy by a process called respiration. The reaction at the heart of respiration is the four electron reduction of dioxygen to water:

$$O_2 + 4e^- + 4H^+ \rightarrow 2H_2O$$

The energy released with the reduction of the double bond in oxygen makes it a good source of energy for aerobic life. It also makes oxygen highly reactive and can lead to toxicity through Reactive Oxygen Species (ROS). ROS arise from the partial reduction of oxygen and side reactions. ROS include hydrogen peroxide, hydroxyl radical, peroxynitrite, lipid peroxides and the superoxide radical.

Superoxide is formed from the one electron reduction of oxygen. The toxicity of superoxide in biological systems has been debated [Ullrich et al. 2000], but it has been shown that superoxide can be harmful to many biological systems [Fridovich 1986]. Superoxide is known to react with thiols, ascorbate, catcholamines, tocopherols, phenols, and flavins [Fridovich 1983]. It is also known to inactivate catalases, peroxidases and iron sulfur centers [Odajima et al. 1972; Kono et al. 1983]. Also, the toxicity of the superoxide anion is implied by the ubiquitous presence of superoxide dismutases in all aerobic forms of life.

Superoxide dismutases are a family of enzymes that catalyze the disproportionation of the superoxide radical. There are four main types of SODs: manganese, iron, nickel and copper, zinc [McCord et al. 1968; Keele et al. 1970; Yost et al. 1973; Youn et al. 1996]. With the exception of MnSOD and FeSOD, there is no structural homology within this family of enzymes, but all catalyze the oxidation of

superoxide to hydrogen peroxide followed by the reduction of superoxide to oxygen [Zelko et al. 2002]:

$$M^{+n} + O_2^- \rightarrow M^{+n-1} + O_2$$

$$M^{+n-1} + O_2^- + 2H^+ \rightarrow M^{+n} + H_2O_2$$

When Cu,Zn superoxide dismutase was originally discovered, its enzymatic function was unknown. It was not until work done by Fridovich and McCord in 1968, that the activity of SOD was assigned [McCord et al. 1969]. There are two forms of Cu,ZnSOD; a cytosolic dimeric form and a tetrameric extracellular form.

The cytosolic Cu,ZnSOD is a 32 kD homodimeric protein in which each monomer contains one zinc and one copper atom (Figure 1.7) [Abernethy et al. 1974]. In the oxidized form the copper is in a square pyramidal geometry coordinated by four histidine residues and one solvent molecule [Boden et al. 1979; Blackburn et al. 1983; Strange et al. 2005]. The zinc is coordinated by three histidine residues and one aspartate residue in a tetrahedral geometry. One histidine is a ligand to both the metal ions: to the

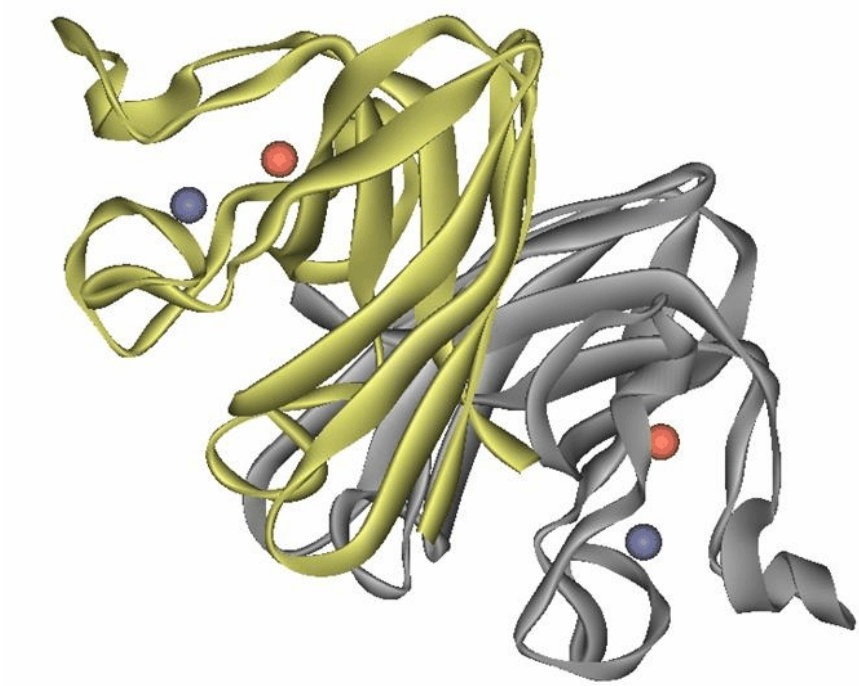

Figure 1.7: The structure of the SOD dimer. The coordinates for this structure were take from the protein data bank file 1HL5.

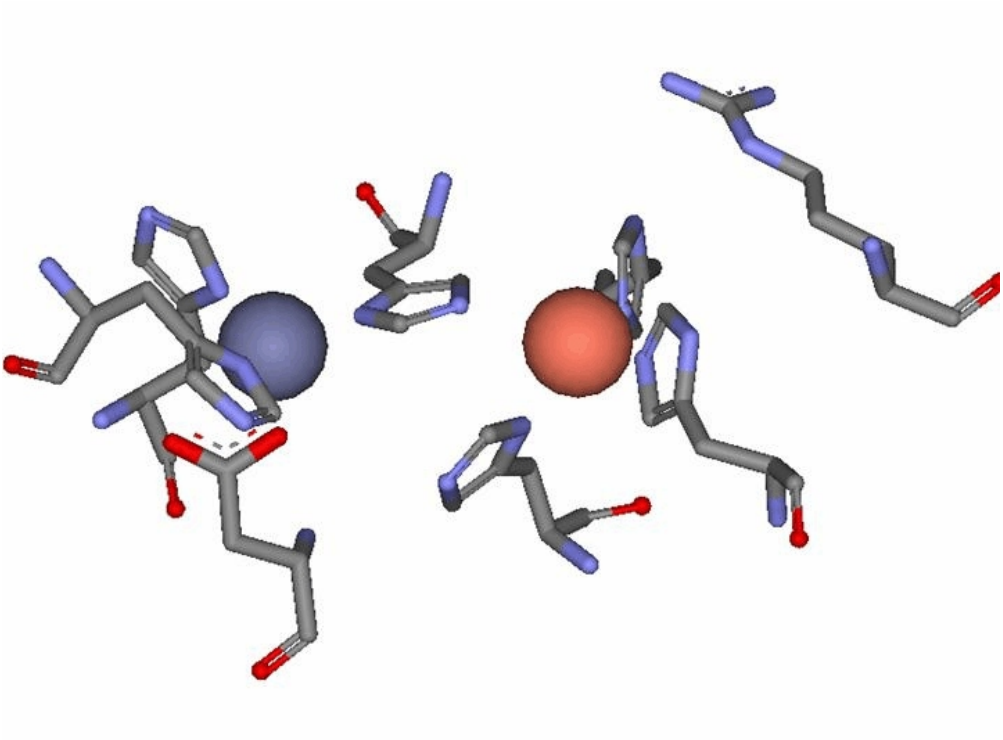

Figure 1.8: The zinc (blue) and copper (red) sites of Cu, Zn SOD.

copper atom through the ϵ-nitrogen and to the zinc through the δ-nitrogen [Richardson et al. 1975]. In the reduced form, the bridge between the zinc and the copper atom is broken as the copper reduces its coordination environment to only three histidine residues in a trigonal planar geometry [McAdam et al. 1977; Blackburn et al. 1984]. Upon reduction the ϵ-nitrogen of the binding histidine, which is ligated to the copper in the oxidized state, becomes protonated [Banci et al. 1994]. The consistent geometry around the zinc site between oxidation and reduction suggests that the zinc site is a structural site. The copper is the site of oxidation of superoxide to oxygen followed by the reduction of superoxide to hydrogen peroxide. It has been shown that when coupled with an external electron donor or acceptor, one step of the reaction with superoxide can be bypassed; meaning that SOD can work solely as a superoxide oxidase or superoxide reductase. Whether this is exploited by the cell to favor one of the superoxide reactions over the other is unknown [Liochev et al. 2000].

The binding of superoxide to copper is stabilized by the electrostatic interactions with a nearby arginine residue [Tainer et al. 1983]. Overall, the SOD protein is negatively charged except for a positively charged channel that ends in the arginine residue near the copper sites. It is believed that this electrostatic interaction is in part what facilitates SOD's high rate of catalysis, which has been shown to approach diffusion-controlled limit [Getzoff et al. 1983; Getzoff et al. 1992].

The tertiary structure of Cu, Zn SOD displays a Greek key β-barrel fold [Tainer et al. 1982]. One important feature in SOD is a region known as the metal binding loop which contains many of the metal binding residues. In the apo-protein the metal binding loop is relaxed, resulting in an unformed copper binding site. Zinc binding to the protein closes this loop and helps to form the copper site. The closing of this loop is further stabilized by the formation of a disulfide bond [Bordo et al. 1994]. The dimer interface of cytosolic Cu,ZnSOD is formed by hydrophobic interactions and has an area of 500 $Å^2$ [Tainer et al. 1982]. SOD is an unusually stable protein and has been shown to resist denaturation by heating up to 100ºC, 1% SDS and 8 M Urea [Lepock et al. 1985]. It has also been shown to be resistant to degradation by trypsin and aminopeptidase M [Senoo

```
Cyto SOD      --ATKAVCVLKGDGP---------------------------------------------
EC SOD        MLALLCSCLLLAAGASDAWTGEDSAEPNSDSAEWIRDMYAKVTEIWQEVMQRRDDDGTLH
                *  . *:* .  *.

Cyto SOD      ------------------VQGIINFEQKESNGPVKVWGSIKGLTEGLHG----FHVHEFGD
EC SOD        AACQVQPSATLDAAQPRVTGVVLFRQLAPRAKLDAFFALEGFPTEPNSSSRAIHVHQFGD
                              * *:: *.*  ... :.:: :::*:.   :.    :***:***

Cyto SOD      NTAGCTSAGPHFNPLSRKHGGPKDEERHVGDLGNVTADKDGVADVSIEDSVISLSGDHCI
EC SOD        LSQGCESTGPHYNPLAVPHP------QHPGDFGNFAVR-DGSLWRYRAGLAASLAGPHSI
               : ** *:***:***:  *       :* **:**.:.  **       . . **:* *.*

Cyto SOD      IGRTLVVHEKADDLGKGGNEESTKTGNAGSRLACGVIGIAQ------------------
EC SOD        VGRAVVVHAGEDDLGRGGNQASVENGNAGRRLACCVVGVCGPGLWERQAREHSERKKRRR
              :**::***   ****:***:  *.:.**** **** *:*:.

Cyto SOD      -------
EC SOD        ESECKAA
```

Figure 1.9: Sequence alignment of human cytosolic SOD (cyto SOD) and extracellular SOD (EC SOD). Alignment done with CLUSTALW.

et al. 1988].

The extracellular form of SOD has some homology to the cytosolic SOD with three main differences (Figure 1.9). First, the metal binding loop is more compact, it is missing a 7 residue region between two metal binding histidines. Second, there is the presence of a N-terminal and a C-terminal tail [Oury et al. 1996]. In the N-terminal region there is a hydrophobic alpha-helix and in the C-terminus there is a cysteine residue and a tryptophan residue; all of these have been implicated in tetramer formation [Stenlund et al. 1997; Stenlund et al. 1999].

1.2.4 COPPER TOXICITY

Although copper is needed for many functions in humans, high levels of copper can be fatal. Toxic effects of copper can be seen after ingestion of one gram. The fatal dose for an adult is estimated at more than 10 grams of copper [Walsh et al. 1977; Haywood et al. 1985]. Acute copper poisoning has the symptoms of diarrhea, circulatory collapse, and hemolysis. Chronic copper poisoning can lead to hepatic failure [Dash 1989; Sandstead 1995]. Wilson's disease is a genetic disorder caused by a mutation of the protein that transports copper out of the liver, the Wilson's disease protein. As a result, copper accumulates in the body, as it cannot be excreted into the bile. The symptoms of Wilson's disease include mental retardation and fulminant hepatic failure [Walshe 1962].

The ability of copper to exist in both the +1 oxidation state and the +2 oxidation state in physiological conditions makes it a potentially toxic substance in biology. In the cell, free Cu(I) can be oxidized to Cu(II) and can undergo Fenton-like reactions, which can generate radicals that may react with and oxidize larger biopolymers and membrane layers [Fridovich 1989]. In 1934, Haber and Weiss published a mechanism by which the extremely toxic hydroxyl radical can be produced from hydrogen peroxide and superoxide anion [Haber et al. 1932]:

$$O_2^{\bullet -} + H_2O_2 \rightarrow HO^{\bullet} + O_2 + HO^-$$

$$H_2O_2 + OH^{\bullet} \rightarrow H_2O + O_2^{\bullet -} + H^+$$

The rate of this reaction was thought to be too slow to have any importance in biology, but previously it was shown that free iron could catalyze this reaction. The Fenton reaction is the generation of hydroxyl radical from hydrogen peroxide [Fenton 1896]:

$$Fe^{2+} + H_2O_2 \rightarrow Fe^{3+} + HO^{\bullet} + HO^{-}$$

In the presence of a reductant like ascorbate the Fe(II) can be regenerated. Therefore, from free iron and hydrogen peroxide the autocatalytic Haber-Weiss cycle can be started and large amounts of hydroxyl radical can be generated. Even though the Fenton cycle describes iron chemistry, it has been shown that other free metal ions such as copper can generate the toxic hydroxyl radical in what has been termed Fenton-like reactions [Stohs et al. 1995].

1.3 COPPER IN THE CELL

1.3.1 COPPER TRANSPORT THROUGH THE CELL

One way the cell counteracts the uncontrolled redox reactions of copper is by importing only copper(I) into the cytosol and maintaining a reducing environment within the cell. It has also been shown that most of the copper in the cytoplasm is in equilibrium bewteen free copper and copper bount to metal binding proteins to reduce the amount of copper free to participate in side reactions [Rae et al. 1999; Outten et al. 2001]. Copper transport through the cell begins with the reduction of Cu(II) to Cu(I) outside of the cell by the extracellular membrane protein, Fre1p. Cu(I) can be transported into the cell by a variety of trans-membrane transporters but the main route is through the Ctr1p transporter. Once inside the cell, copper is generally bound to metallothioneins or delivered to copper-containing enzymes. Finally, copper is exported out of the cytoplasm into the Golgi network by the Wilson's, or Menke's disease protein.

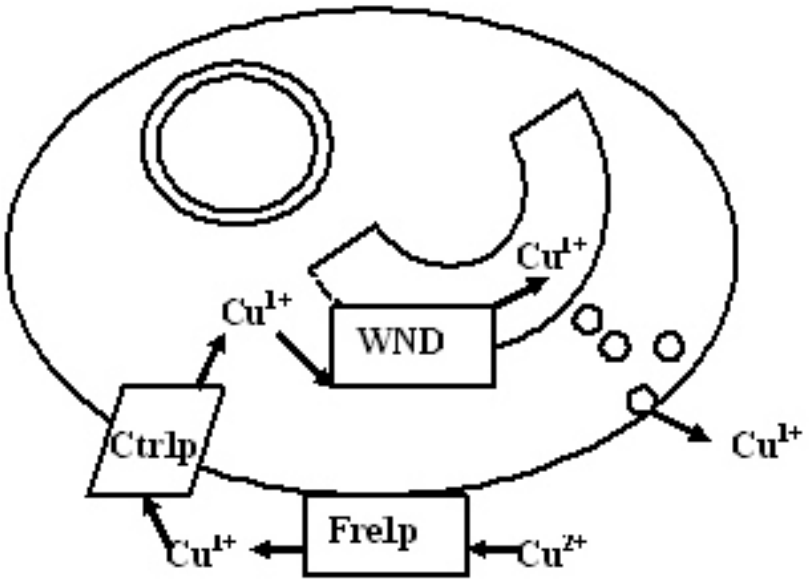

Figure 1.10: Copper cycling through the cell

1.3.1.1 FRE1 Before being transported into the cell, copper must be reduced to the cuprous form. This reduction is done by external membrane protein Fre1p. Very little is known about Fre1p. Originally, it was identified as an iron reductase, before its role in copper reduction was elucidated [Hassett et al. 1995]. It is known to have a flavin cofactor and is believed to accept electrons from NADPH [Dancis et al. 1992]. However, the exact mechanism of Fre1p is still unknown.

1.3.1.2 CTR1 Several copper transporters into the cell have been identified including Ctr2p, Ctr3p, and Fet4p, however the main route of copper's entry into the cell is the Ctr1p protein [Portnoy et al. 2001]. Ctr1p has been identified as the high-affinity copper uptake protein [Zhou et al. 1997; Kuo et al. 2001]. The human Ctr1p contains an N-terminal extracellular tail followed by three trans-membrane domains and finally, a C-terminal tail. The N-terminal tail contains four metal binding regions termed H1 (HSHH), M1 (MGMSYM), H2 (HHH) and M2 (MMMMPM). Although all of the N-terminal binding domains are thought to play a role in sequestering copper, it has been shown that only the M2 domain, the domain closest to the trans-membrane domains, is needed for copper transport [Puig et al. 2002]. The second trans-membrane domain

Table 1.2: Proteins involved in copper transport through the cell and in copper regulation of gene transcription

Protein	Function	Thesis Section
Fre1	Extracellular copper reductase	1.3.1.1
Ctr1	Main copper transporter into the cell	1.3.1.2
Ctr2	Low affinity copper transporter into the cell	1.3.1.2
Ctr3	Low affinity copper transporter into the cell	1.3.1.2
Fet4	Low affinity copper transporter into the cell	1.3.1.2
Cup1	Copper-binding metallothionein	1.3.1.3
Crs5	Copper-binding metallothionein	1.3.1.3
Wilson's/ Menke's disease proteins (WND/MKD)	Copper transporter into the Golgi network	1.3.1.4
Ace1	Gene transcription factor up-regulated by copper	1.3.2
Mac1	Gene transcription factor down-regulated by copper	1.3.2

contains an $M_{150}XXM_{154}$ motif that has been implicated in the transport of copper across the membrane [Puig et al. 2002].

The role of the C-terminal tail is a little less clear. In the human form of Ctr1p, the C-terminal tail is only 11 residues long with few metal binding residues, and mutation of those residues has no effect on copper transport [Eisses et al. 2002]. Conversely, the yeast cytosolic tail is 125 residues long and contains six cysteine residues. XAS studies of the yCtr1c, a truncation containing only the cytosolic tail, showed that the tail formed Cu_4S_6 polynuclear clusters. The best fits for these clusters showed a sulfur shell (N=3) at 2.254 Å, a copper shell (N=2) at 2.715 Å and a copper shell (N=1) at 2.898 Å. However, since the human form of the protein doesn't contain these residues and the human form can rescue the yeast form by complementation, it seems that these clusters may not play a role in copper transport so much as copper buffering or cell signaling [Eisses et al. 2002].

1.3.1.3 Metallothioneins Metallothioneins (MTs) are a class of low molecular weight proteins that are high in cysteine content. Their main role is to bind

free metals either for detoxification of non-biological metals, or possibly, as storage for metals with a biological role [Kagi et al. 1988]. MTs are generally devoid of histidines and aromatic amino acids, but their amino acid content is up to one-third cysteine. The cysteine residues are typically in CXC or CXXC motifs [Kille et al. 1994], and they bind metal in polynuclear thiolate clusters [Arseniev et al. 1988]. The two main copper thioneins in eukaryotes are Cup1 and Crs5 [Butt et al. 1984; Culotta et al. 1994]. Although expression studies suggest that Cup1 is the major protein for copper detoxification, it is interesting that Crs5 actually binds more Cu(I) ions than Cup1, 12 -15 atoms compared to 6-7. It has been proposed that Crs5 might play more of a role in copper regulation than actual detoxification [Jensen et al. 1996].

1.3.1.4 Wilson's and Menke's disease proteins Wilson's disease protein (WND) and the Menke's disease protein (MKD) are both P-type ATPases that are responsible for transporting copper out of the cell via the Golgi network [Lutsenko et al. 1995]. There are many similarities between the two proteins, in fact the main difference is in the organs where the proteins are expressed. WND, or ATP7B is expressed in the liver, kidney and brain, while MKD, or ATP7A, is expressed in all tissues except the liver [Tanzi et al. 1993; Muramatsu et al. 1998]. Both WND and MKD are P-type ATPases, a class of ion transporters that use energy from the hydrolysis of ATP and undergo a structural change upon phosphorylation that leads to ion pumping [Kuhlbrandt 2004].

WND is a 165 kD transmembrane protein [Petrukhin et al. 1994]. It consists of eight transmembrane domains, three cytosolic loops and cytosolic C-terminal and N-terminal tails. The ATP-binding domain is conserved in all ATPases and is the cytosolic loop between the sixth and seventh transmembrane domain. The N-terminal domain contains six metal binding sites of the sequence GM(T/H)CXXC, and each of the metal binding sites is capable of binding a single copper atom, meaning that the N-terminal of WND is capable of binding six coppers [Lutsenko et al. 1997]. It has been shown that the activity of WND/MKD is controlled by copper concentration. Under low copper concentrations, WND is phosphorylated and is in the perinuclear space. When copper

concentrations increase, WND is hyperphosphorylated and relocalized to the Golgi network [Vanderwerf et al. 2001]. It is believed that copper binding to the metal binding domains induces a conformational change that allows copper to bind to the transmembrane domain and allows the phosphorylation that induces ion transport [Lutsenko et al. 2002].

1.3.2 COPPER REGULATION OF PROTEIN EXPRESSION

Copper levels are not only controlled by proteins importing and exporting copper from the cell, but are also controlled on the genetic level by the up- and down-regulation of expression of the proteins that bind and transport copper [Winge et al. 1997]. Most of these methods of regulation have been mapped out for yeast and the process is believed to happen much the same in humans. The first copper-mediated gene regulator discovered was Ace1 [Furst et al. 1988]. When copper binds to Ace1, it is activated to up-regulate the expression of certain genes that express proteins that bind to copper. Cup1, Crs5 and Cu,ZnSOD are three proteins that are up-regulated by Ace1 [Thiele 1988; Buchman et al. 1989]. Ace1 is a three domain protein, an N-terminal Zn-binding domain, a cysteine rich Cu-binding domain, and a C-terminal transactivation domain. The DNA binding site is in the N-terminal Zn-binding domain, although zinc binding does not appear to have a role in the binding of DNA, and up regulation of the transcription is done by the transactivation domain [Furst et al. 1988; Thorvaldsen et al. 1994; Farrell et al. 1996]. The binding of Cu to Ace1 increases the binding of Ace1 to DNA, therefore there is a direct relation between an increase in cellular copper and an increase in the expression of metal binding proteins. Cu binds to the Cys rich regions in the Cu-binding domain to create a Cu_4S_6 cluster [Brown et al. 2002].

Conversely to Ace1, Mac1 binding to DNA is repressed by the binding of copper [Jungmann et al. 1993]. Apo-Mac1 has been shown to up-regulate the expression of Fre1, Ctr1 and other proteins involved in copper import [Hassett et al. 1995]. Mac1 is comprised of an N-terminal Zn-binding domain responsible for the binding of DNA and

a C-terminal cysteine rich copper binding domain. The copper binding to the C-terminal domain of Mac1 forms Cu_4S_6 clusters similar to those found in Ace1 [Brown et al. 2002].

1.4 COPPER CHAPERONES

It has been shown that bacterial cells in metal-depleted medium are able to sequester metals, so that the levels of metals in the cytosol are much higher than in the extracellular medium. If the levels of metals in the medium increases, the cytosolic levels of metals do not increase [Outten et al. 2001]. This is because while cells need metals as nutrients the amount of excess levels must be kept low to decrease their possible toxic side effects. One way that cells keep this equilibrium is by the tight regulation of import and export to and from the cell. But in the case of copper, there is known to be another system in play. It has been shown that even with high levels of cytosolic copper in the yeast cell, most of it exists bound to protein [Rae et al. 1999]. Part of this pool is bound to general metal binding proteins called metallothioneins. But there is another class of proteins in the cytosol called copper chaperones. Copper chaperones perform a dual role of both binding free copper, to inhibit any possible toxic reactions, and they also sequester copper for delivery to proteins that utilize copper. Many copper chaperones have been identified including: Atox1, the chaperone to the

Table 1.3: Proteins classified as copper chaperones

Protein	Function	Thesis Section
Atox1	Copper chaperone to the Wilson's and Menke's disease proteins	1.4.1
Cox17	Copper chaperone to the mitochondria	1.4.2
Sco1	Copper chaperone to the Cu_A site of cytochrome *c* oxidase	1.4.3
Sco2	Unknown function, thought to aid Sco1 with assembly of the Cu_A site of cytochrome *c* oxidase	1.4.3
Cox11	Copper chaperone to the Cu_B site of cytochrome *c* oxidase	1.4.4
Copper chaperone to superoxide dismutase (CCS)	Copper chaperone to Cu,Zn superoxide dimutase	1.5

Wilson and Menke's disease proteins; SCO1, COX11 and COX17, the copper chaperones to cytochrome *c* oxidase; and CCS, the copper chaperone to superoxide dismutase [Glerum et al. 1996; Glerum et al. 1996; Culotta et al. 1997; Klomp et al. 1997; Carr et al. 2003].

The known human copper chaperones are reviewed in this section except for the copper chaperone to superoxide dismutase which is discussed in section 1.4.

1.4.1 ATOX1

Atox1 is the copper chaperone to the Wilson's and the Menke's disease proteins. It is the human homolog of the yeast protein Atx1 [Klomp et al. 1997]. Atx1 was the first copper chaperone ever identified (Figure 1.11), where the copper binding motif MXCXXC, the motif that helped to define copper chaperones, was first discovered [Lin et al. 1997]. Currently, Atx1 is the only copper chaperone shown to interact with Ctr1

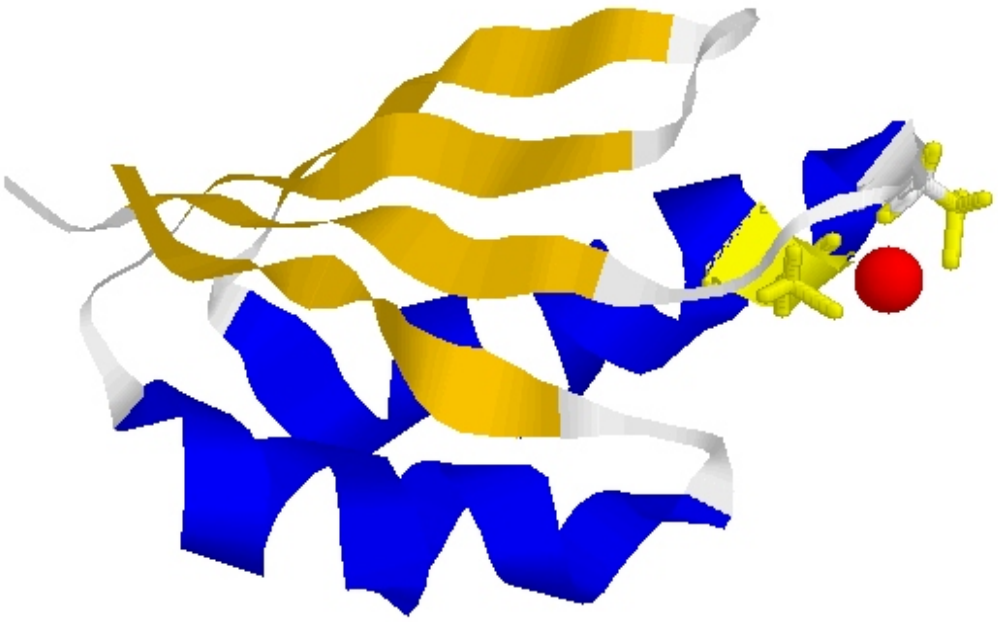

Figure 1.11: The solution structure of Atox1 with copper (red) and ligand cysteines (yellow) shown. The cooridnates for this structure were taken from the data bank file 1TL4.

[Xiao et al. 2002].

Atox1 is a 68 residue protein that binds copper in the MTCGGC motif. Although Atox1 binds copper in a linear geometry, it can switch to a trigonal geometry in the presence of excess thiol ligand [Ralle et al. 2003]. This suggests a mechanism whereby Atox1 delivers copper to the linear copper site in MKD/WND by the formation of a three coordinate intermediate. It has also been shown that docking of Atox1 onto WND/MKD is controlled by electrostatic interactions [Arnesano et al. 2001].

1.4.2 COX17

The first copper chaperone known to be important in the assembly of copper sites in the mitochondrial protein cytochrome c oxidase was the protein Cox17 [Glerum et al. 1996]. It was soon hypothesized that Cox17 was not responsible for direct transfer to COX, but instead, responsible for copper transfer to the mitochondria, because it was found to localize both in the mitochondrial inner membrane space and the cytoplasm [Beers et al. 1997]. Cox17 is responsible for copper delivery to both Sco1 and Cox11, the copper chaperones to the Cu_A and Cu_B sites of COX [Horng et al. 2004].

Cox17 is a 69 residue protein with the Cu(I)-binding motif of CXCC [Heaton et al. 2000]. Cox17 binds three copper(I) atoms per protein and appears to exist in a dimer/tetramer equilibrium. The copper binds in a polyncuclear cluster with a Cu-S distance of 2.25 Å and a Cu-Cu distance of 2.7 Å as determined by EXAFS. This cluster is believed to be the dimer interface in Cox17 [Heaton et al. 2001]. The mode of transfer from Cox17 to Cox11 or Sco1 is unknown. It has been suggested that Cox17 may just help import copper to the mitochondria where it exists as a low molecular complex from which Cox11 and Sco1 pick up their copper, meaning that there is no direct interaction between those proteins and Cox17 [Cobine et al. 2004].

1.4.3 SCO1 and SCO2

Sco1 is a 30 kD protein found as an inner mitochondrial membrane protein. It has been identified in humans, but most of the studies done on Sco1 have been done on the yeast form [Paret et al. 1999]. Sco1 receives its copper from Cox17, or the proposed mitochondrial copper pool, and delivers copper to the Cu_A site in COX [Mattatall et al. 2000]. Sco1 has the conserved metal binding site of CXXCP, where both cysteine residues and a histidine residue are known to be important for copper binding [Glerum et al. 1996].

EXAFS and HPLC gel filtration studies suggest that purified Sco1 binds copper in a trigonal geometry with one copper per monomer and that there are no higher oligomerization states [Nittis et al. 2001]. However, this is in contrast to *in vivo* studies of Sco1. When purified directly from mitochondrial lysates, Sco1 is seen as a higher molecular weight than expected for monomeric Sco1 [Nittis et al. 2001]. An explanation for this higher molecular weight species could be that Sco1 is interacting with another protein, Sco2. The existence of Sco2 has been known for a while and it has the same CXXCP conserved motif as Sco1 [Glerum et al. 1996], but the function of Sco2 has remained unknown. Recently, it has been shown that Sco2 might form a complex with Sco1 and work in conjunction to deliver copper to COX [Leary et al. 2004].

1.4.4 COX11

Cox11 is the copper chaperone that delivers copper to the Cu_B site in COX [Hiser et al. 2000]. Cox11 is a 34 kD protein that is tethered to the inner mitochondrial membrane by a single trans-membrane domain. There are three conserved cysteine residues in Cox11, but none appear in motifs observed in other copper chaperones [Carr et al. 2002]. Cox11 binds one copper atom per monomer but EXAFS studies of the protein from *S. meliloti* show a best fit of three sulfur at 2.23 Å and one copper at 2.70 Å. This data is best represented by dinuclear copper cluster. Further studies on the NMR

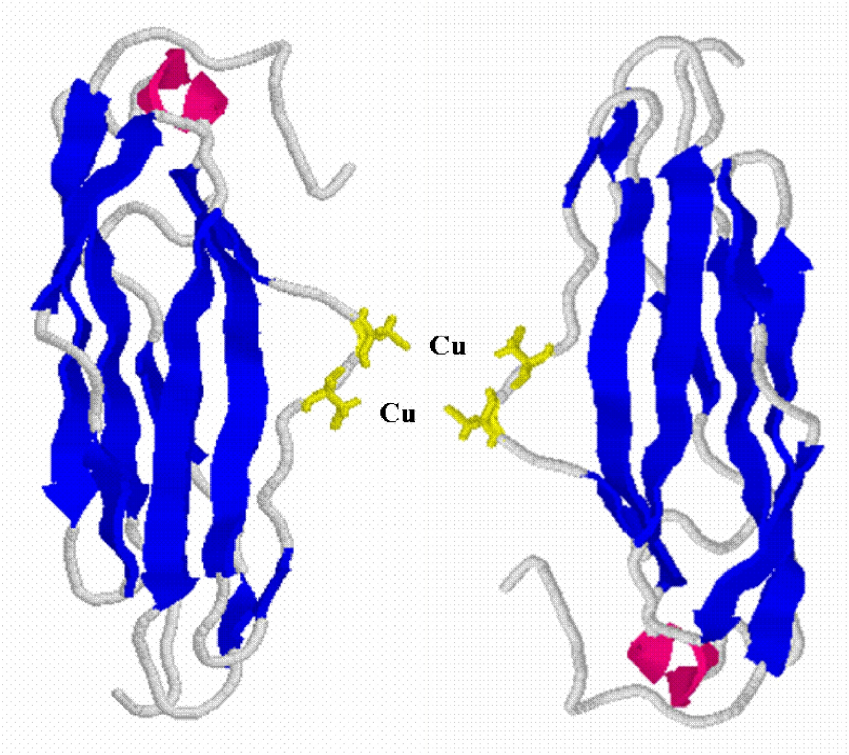

Figure 1.12: The solution structure of Cox11 with proposed copper binding site. The coordinates for this structure were taken from the protein data bank file 1SP0.

solution structure proposed that the cluster is formed between two Cox11 monomers (Figure 1.12) [Banci et al. 2004].

1.5 THE COPPER CHAPERONE TO SUPEROXIDE DISMUTASE

The copper chaperone to superoxide dismutase (CCS) was first discovered in yeast in 1997 when the LYS7 gene (previously known as a rescue gene for the production of lysine and methionine in the presence of oxygen) was shown to be phenotypically similar to null SOD strains [Culotta et al. 1997]. The homologous gene was identified in humans and the expressed protein was named CCS. Using a GST-hCCS fusion protein immobilized on agarose beads, it was shown the CCS could directly interact with SOD independent of copper status [Casareno et al. 1998]. Human Cu,Zn SOD is one of the only species of SOD known to be able to obtain copper without CCS.

This happens via copper-glutathione complexes, but this route of metalation is minimal and the main route of copper entry into SOD is via CCS [Carroll et al. 2004]. Metal binding studies of CCS in the presence of excess copper scavengers give results of one zinc and one copper atom per monomer [Torres et al. 2001]. One of the first structural studies that attempted to elucidate the copper binding geometry involved study of cobalt loaded CCS as a homolog of copper loaded CCS. The results suggested that copper would bind to CCS in a four coordinate sulfur site formed by the two metal binding motifs in domain I and domain III. [Zhu et al. 2000].

The levels of expressed CCS are inversely proportional to the levels of nutritional copper [Bertinato et al. 2003]. Using pulse and pulse-chase experiments with ^{64}Cu, Bartnikas and Gitlin showed that a large pool of SOD exists in the apo form without copper and that the abundance of this pool is also inversely proportional to intracellular copper levels. Under normal conditions, CCS loads newly formed SOD and SOD from the pool about equally, but under copper deficiency CCS preferentially loads SOD from the SOD pool. The authors of this paper suggest that this could be evidence of a CCS role in the activation of SOD beyond that of copper transfer and that CCS could be

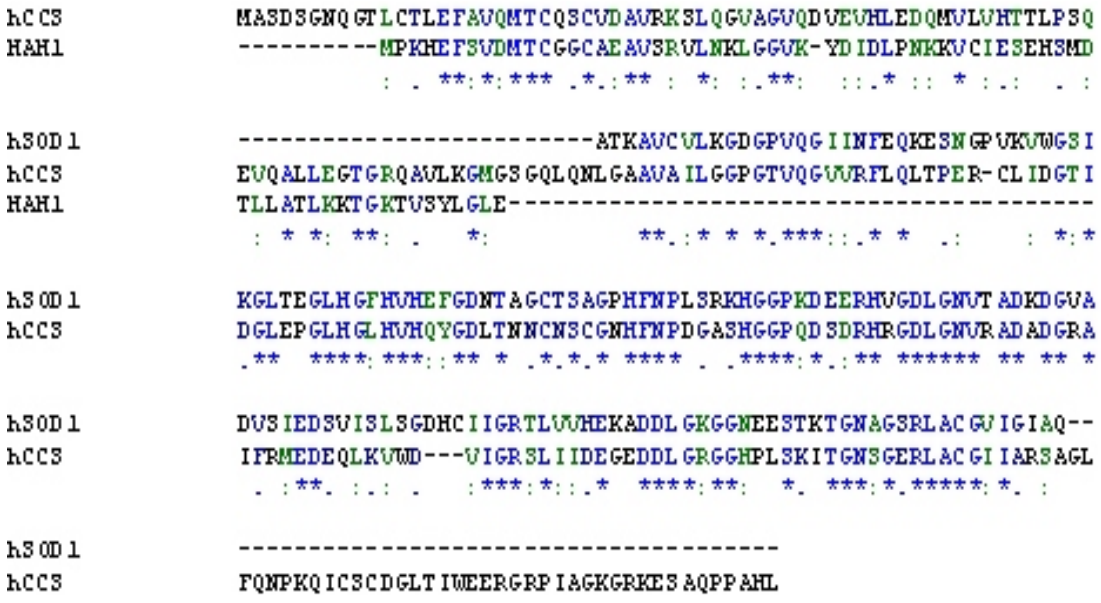

Figure 1.13: Comparison of hCCS, HAH1 and hSOD sequences.

responsible for the post-translational control [Bartnikas et al. 2003]. This view was furthered by work of Brown *et al* who showed that CCS and oxygen were needed to fully reconstitute denatured SOD [Brown et al. 2004]. Also the formation of a structurally important disulfide bond is slow in the presence of oxygen but is greatly accelerated with the addition of CCS. In fact formation of this bond in the copper free SOD can inhibit the transfer of copper by CCS [Furukawa et al. 2004].

CCS is a three domain protein containing an Atx-like domain (domain I), an SOD-like domain (domain II), and a C-terminal tail (domain III) (Figure 1.13). Domain I (residues 1 - 85) has sequence similarity to Atx1, Hah1 and the copper transporting ATPases. It contains the metal binding sequence MXCXXC (in hCCS MTCQSC). Domain II (residues 86 - 234) has 47% sequence identity with SOD. The SOD dimer interface is conserved in CCS, suggesting that CCS could dimerize in a similar fashion to SOD. CCS from most species does not have the metal-binding ligands of SOD conserved. However human CCS does have the SOD metal-binding ligands conserved, except His120 in SOD, a copper binding ligand, that has been changed to an aspartate (Asp201 in CCS). Domain III (residues 235 - 274) is a C-terminal tail that has no homology to any other known proteins. It does have a potential copper binding site of the CXC motif. Domain III is perhaps the most varied domain between species, rangeing from 13 AA to 35 AA in length from species to species, but all having the conserved CXC region (Figure 1.14). Studies on truncation mutants have assigned the roles of each

```
Mouse          IARSAGLFQNPKQICSCDGLTIWEERGRPIAGQGRKDSAQPPAHL
Human          IARSAGLFQNPKQICSCDGLTIWEERGRPIAGKGRKESAQPPAHL
Drosophilia    IARSAGILENFKRICACDGVTLWDERNKPLAGKDRSQKL------
Tomato         IARSAGVGENYKKLCTCDGTTIWEATSKI----------------
Yeast          IARSAGVWENMKQVCACTGKTVWEERKDALANNIK----------
               ******: :* *: :*:* * *:*:
```

Figure 1.14: Comparison of CCS domain III from several species.

domain. Domain I is thought to be responsible for copper sequestration at low copper levels. Domain II is thought to play a role in SOD recognition and Domain III is responsible for copper transport to SOD [Schmidt et al. 1999].

Cu,Zn SOD and CCS are generally cytosolic proteins, but have been found to also localize in the inner membrane space of the mitochondria [Weisiger et al. 1973; Sturtz et al. 2001]. The reason for this was debated, as the mitochondria already contains a form of SOD (MnSOD) which should be enough to scavenge any superoxide formed during respiration. Yet it has been shown that Δ*sod1* yeast cells show symptoms of mitochondrial oxidative stress, such as poor growth during respiration, rapid death in the stationary phase and a deficiency in mitochondrial aconitase, an iron-sulfur cluster containing protein known to be disrupted by superoxide [Longo et al. 1996; Jakubowski et al. 2000]. Neither Cu,Zn SOD or CCS have the putative mitochondrial targeting sequence, but it has been shown that levels of CCS expression regulate the amount of mitochondrial Cu,Zn SOD [Sturtz et al. 2001]. The authors suggest that apo-SOD is free to pass back and forth across the mitochondrial membrane, but once it interacts with CCS and receives copper this transport is inhibited. Still, the exact purpose of mitochondrial Cu,Zn SOD is unknown.

The first crystal structure of CCS that was published was done on the yeast form of the protein [Lamb et al. 1999]. It showed a homodimer of CCS with a dimer interface formed in domain II that was homologous to the SOD dimer interface (Figure 1.15). Domain I was also shown to have structural homology to Atx1. This crystal structure was on the apo form of the protein and the domain III tail was disordered. The crystal structure of a truncation mutant containing only the domain II region of human CCS showed that human CCS is also capable of forming a dimer interface similar to that of SOD. This structure also showed a zinc atom bound in the conserved zinc binding site of domain II [Lamb et al. 2000].

The most recent crystal structure published on CCS was done on yCCS complexed with H48F SOD, a mutant of SOD that is unable to bind copper (Figure 1.16) [Lamb et al. 2001]. Immunoprecipatation and gel electrophoresis studies showed that the mutant SOD and yCCS could form stable heterodimer intermediates. These dimers could form between H48F SOD and apo-yCCS but the interaction was strengthened by the addition of copper [Torres et al. 2001]. The protein was resolved as heterotetramers

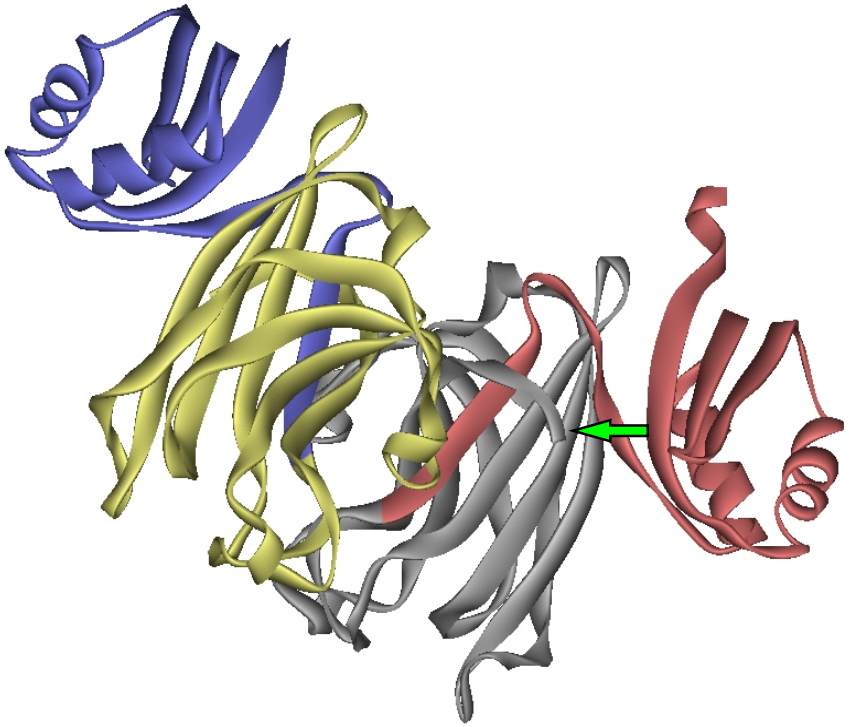

Figure 1.15: The crystal structure of the yCCS homodimer. Domains I are in blue and red, Domains II are in grey and yellow, Domain III was disordered and is not shown in the structure, but it location is marked by the green arrow. The coordinates for this structure were taken from the protein data bank file 1QUP.

formed from two monomers of CCS and two monomers of SOD, but the authors state that the tetramer is an artifact of crystal packing and that the asymetric unit is actually made of two heterodimers. The dimer interface of the heterodimer is similar to that of the homodimer except that the area of this heterodimer interface is larger than that of either of the homodimers. In this structure domain III was present, but there was still no copper bound to the CCS.

There are notable structural differences between the two monomers in the heterodimer and their original structure in the homodimers. Domain I in the heterodimer is rotated so that the copper binding site is further from the SOD metal sites than it would be in the homodimer. This shows that the linker region between domains I and II is flexible. In the structure of the homodimer, the MXCXXC site is free of copper and the two cysteine residues exist as a disulfide bond, whereas in the heterodimer there is still

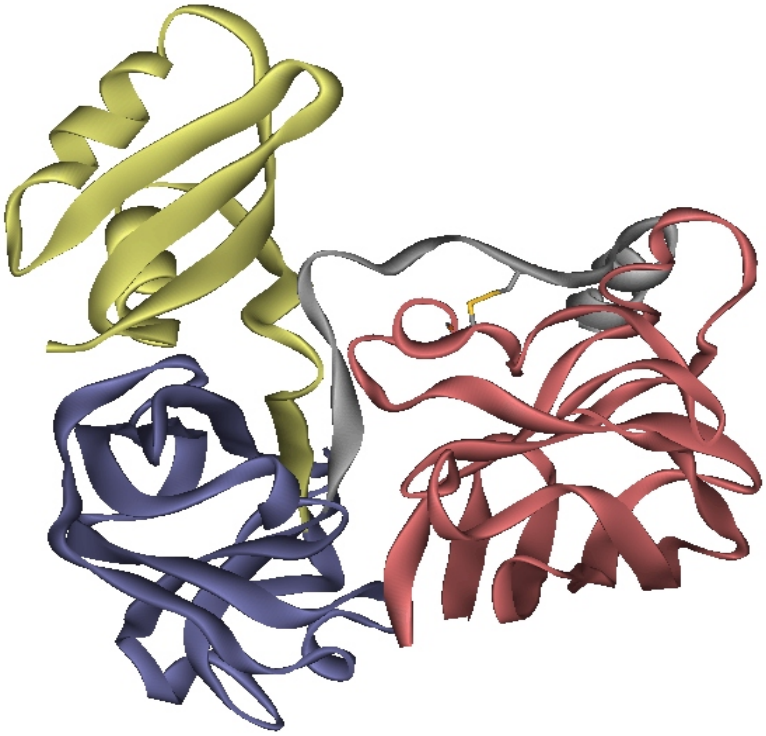

Figure 1.16: The yCCS - SOD heterodimer. SOD is in red, Domain I is in yellow, Domain II is in blue, Domain III is in grey. The disulfide bond between proteins is shown. The coordinates for this structure were taken from the protein data bank file 1JK9.

no copper bound, but the cysteines are free thiols. In the homodimer structure, domain III was unstructured and unresolved, but in the heterodimer structure domain III is present and ends in a 10-residue α-helix. The other major unexpected result in the heterodimer structure is the formation of a disulfide bond between Cys229 in CCS (of the CXC motif) and Cys57 of SOD (usually part of the disulfide bond in the metal binding loop). It is suggested that the disulfide bond is an artifact of crystallization, but the authors put forth that transitory interaction between the two cysteines might play a role in copper transfer to SOD.

It has been suggested that CCS might play more of a role than just copper transfer to SOD because of the disulfide linkage seen in the heterodimer crystal and because it was seen that denatured SOD could not be reconstituted by free copper ion. That taken with the conservation of the dimer interface and the ability of CCS and SOD to interact via the dimer interface has been used to construct the currently accepted

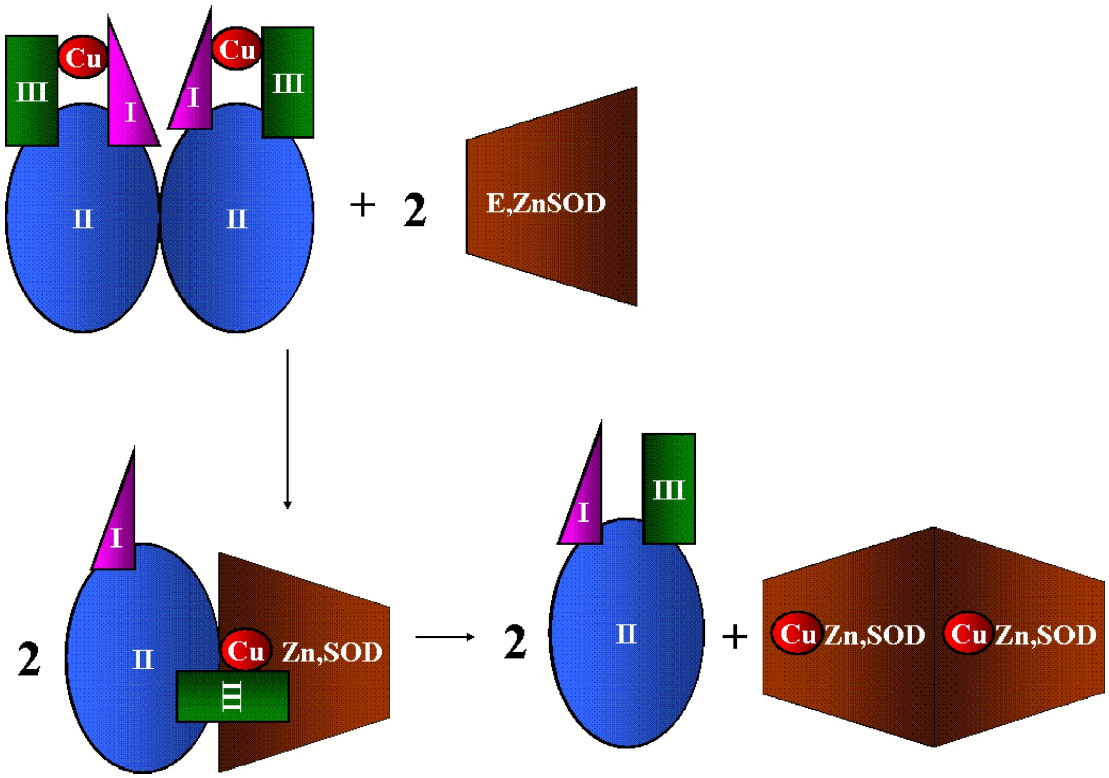

Figure 1.17: The heterodimer mechanism. CCS dimer, with a single copper ion per monomer bound between domain I and III, interacts with two SOD monomers to form two heterodimers. The heterodimer is the species in which copper transport between SOD and CCS happens. After transport, the heterodimer dissociates leaving two apo-CCS monomers and one copper loaded SOD dimer.

mechanism of CCS called the heterodimer mechanism (Figure 1.17). In the heterodimer mechanism, Cu-CCS exists as a free monomer with a single copper bound via bridging of domain I and domain III. The CCS monomer then forms a dimer with a disulfide free E,Zn SOD monomer. Copper transfer occurs with the interaction of domain III of CCS and the metal binding loop of SOD. After copper transfer the free thiols of the CXC motif of domain III then work as a disulfide isomerase to form the disulfide bond in the metal binding loop of SOD. The heterodimer then dissociates and the fully loaded SOD monomer interacts with another SOD monomer to form the stable dimer, while the apo-CCS monomer is free to pick up another copper atom. The exact role of oxygen in this mechanism is unknown but it is thought to play a role in either thiol or copper oxidation.

CHAPTER 2
METHODS AND MATERIALS

2.1 BIOLOGICAL METHODS

2.1.1 CLONING AND PURIFICATION OF MALTOSE BINDING PROTEIN - HUMAN COPPER CHAPERONE TO SUPEROXIDE DISMUTASE FUSION

2.1.1.1 Wildtype Human Copper Chaperone to Superoxide Dismutase. Cloning and transformation of the hCCS-MBP fusion as well as the mutagenesis (section 2.1.1.2) was done by John Eisses of Professor Jack Kaplan's lab in the department of Biochemistry at the Oregon Health and Science University. The hCCS cDNA was PCR-amplified from a human fetal brain cDNA library using primers at the 5' and 3' termini. The cDNA was cloned into the pMAL-c2X expression vector (New England Biolabs) using restriction sites EcoR I and Hind III introduced in the 5' and 3' PCR primers respectively. pMAL-c2X expression vector is used for the expression of a fusion of the target protein and the malE maltose binding protein (Figure 2.1) [di Guan et al. 1988; Maina et al. 1988]. The vector contains an ampicillin resistance gene and the $lacI^q$ promoter for control of expression.

The fusion protein contains a 48 kD N-terminal maltose binding protein tag (for purification on an amylose resin) connected to the 29 kD hCCS target protein by a 3 kD arginine-rich linker region with a Factor Xa protease cleavage site. The protease cleavage

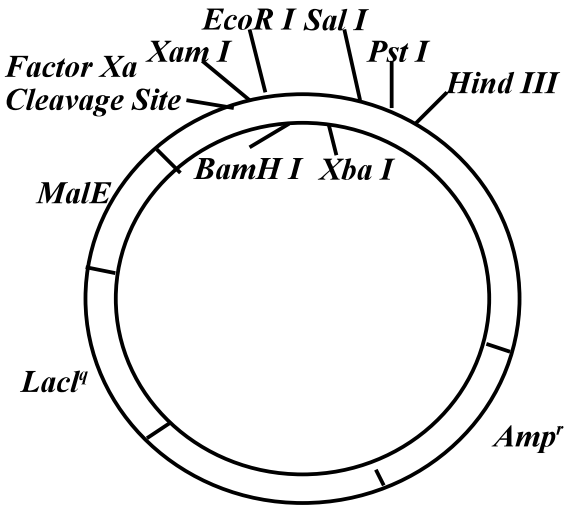

Figure 2.1: Map of the pMAL-c2X expression vector from New England Biolabs.

site is designed so that the target protein can be isolated from the protein tag but the cleavage reaction proved to have very low yield in our construct. Therefore, the protein used in these studies is the full-length expression without cleavage and the expressed protein contains 666 amino acids.

2.1.1.2 Mutants of the Human Copper Chaperone to Superoxide Dismutase. Mutagenesis was carried out using an overlap extension approach, in which four primers are used: two containing the mutations to be made (forward and reverse) and a forward and reverse primer for the full length gene. This allows for the gene to be copied from the point of mutation to the end (or beginning) of the gene. During the next cycle of PCR, these copies served as primers for the full length gene. Primers were designed to substitute a single cysteine with a serine, to the two mutants: C25S and C244S. Each single amino acid substitution was cloned into the pMAL-c2X vector and expressed as above. Additionally, two double serine mutants were also constructed and expressed, the C22/25S and C244/246S mutants. All expression constructs were confirmed by automated DNA sequence analysis.

```
1      MKIEEGKLVI  WINGDKGYNG  LAEVGKKFEK  DTGIKVTVEH  PDKLEEKFPQ
51     VAATGDGPDI  IFWAHDRFGG  YAQSGLLAEI  TPDKAFQDKL  YPFTWDAVRY
101    NGKLIAYPIA  VEALSLIYNK  DLLPNPPKTW  EEIPALDKEL  KAKGKSALMF
151    NLQEPYFTWP  LIAADGGYAF  KYENGKYDIK  DVGVDNAGAK  AGLTFLVDLI
201    KNKHMNADTD  YSIAEAAFNK  GETAMTINGP  WAWSNIDTSK  VNYGVTVLPT
251    FKGQPSKPFV  GVLSAGINAA  SPNKELAKEF  LENYLLTDEG  LEAVNKDKPL
301    GAVALKSYEE  ELAKDPRIAA  TMENAQKGEI  MPNIPQMSAF  WYAVRTAVIN
351    AASGRQTVDE  ALKDAQTNSS  SNNNNNNNNN  NLGIEGRISE  FRMASDSGNQ
401    GTLCTLEFAV  QMTCQSCVDA  VRKSLQGVAG  VQDVEVHLED  QMVLVHTTLP
                  *
451    SQEVQALLEG  TGRQAVLKGM  GSGQLQNLGA  AVAILGGPGT  VQGVVRFLQL
501    TPERCLIEGT  IDGLEPGLHG  LHVHQYGDLT  NNCNSCGNHF  NPDGASHGGP
551    QDSDRHRGDL  GNVRADADGR  AIFRMEDEQL  KVWDVIGRSL  IIDEGEDDLG
601    RGGHPLSKIT  GNSGERLACG  IIARSAGLFQ  NPKQICSCDG  LTIWEERGRP
                                                  *
651    IAGKGRKESA  QPPAHL
```

Figure 2.2: Amino acid sequence of the expressed maltose-binding protein - hCCS fusion protein. * denotes the cysteines mutated to serines in the single mutants.

2.1.1.3 Expression and Purification of the Maltose Binding Protein Fusion.

The pMAL-c2X vector containing the hCCS gene was transformed into the chemically competent *Escherichia coli* strain BL21 (DE3) (Novagen) by heat shock. The cells were then grown in LB-glucose medium (100 μg/ml Ampicillin) at 37°C until the OD_{600} was above 0.6. Expression of the target gene was then induced with the addition of 1 mM IPTG to the medium in the presence of 500 μM $CuSO_4$ and 500 μM $ZnSO_4$. Induction was carried out for 16 hours at 16°C. The cells were pelleted by centrifugation at 5000 rpm and resuspended in 50 mM potassium phosphate buffer (pH 7.5). The cells were lysed with a French Pressure Cell Press (SLM-Aminco). The maltose binding protein-CCS fusion protein was purified from the soluble portion on an amylose column. The amylose resin (New England Biolabs) was packed into a XK 16/20 column with an AK 16 adaptor (Amersham Pharmacia Biotech). Buffer flow into the column was controlled with a P-1 Peristaltic pump and the hCCS fraction leaving the column was monitored with a UV-1 single path monitor (Amersham Pharmacia Biotech). When necessary, the protein was concentrated with an Amicon centricon ultrafiltration cell.

2.1.2 CLONING AND PURIFICATION OF INTEIN -HUMAN COPPER CHAPERONE TO SUPEROXIDE DISMUTASE FUSION.

2.1.2.1 Wildtype Human Copper Chaperone to Superoxide Dismutase. Cloning and transformation of the intein-hCCS fusion plasmid was done by Dr. Michiko Nanako of the Department of Environmental and Biomolecular Systems of the Oregon Graduate Institute School of Science and Engineering at the Oregon Health and Science University. hCCS cDNA was PCR-amplified from the maltose binding protein cell line used in our previous studies using primers at the 5' and 3' terminus (5'-GAATTACCATGGCTTCGGATTCGGGGA-3', 5'-AATTTTAAGCTCTTCCGCACGCTGACTCCTTTCGGC-3') for the wild type protein, this expressed the full length protein minus the last five amino acids (AA1(Met) – AA269(Ala)). The amplified DNA was cloned into the pTXB3 expression vector (New England Biolabs) using restriction sites *Nco I* and *Sap I* introduced in the 5' and 3' PCR primers respectively. The pTXB3 vector contains an intein/chitin binding protein from the

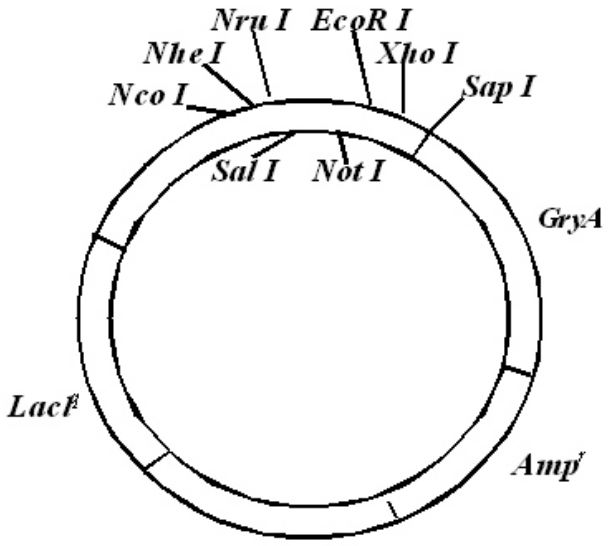

Figure 2.3 : Map of the pTXB3 expression vector from New England Biolabs.

gyrA gene of *Mycobacterium xenopi* which allows the fusion protein to be bound to a chitin bead column and the target protein to be cleaved from the fusion protein by thiol-induced cleavage [Chong et al. 1997; Telenti et al. 1997]. The truncated form of the protein was PCR-amplified from the same maltose binding protein cell line used in our previous studies using the same primer at the 5' and a new 3' terminal primer (5'-GAACTTAAGCTCTTCCGCAGATCTGCTTGGGGTTCT-3') to express a protein that terminates right before the CXC motif in domain III (AA1(Met) – AA243 (Ile)).

2.1.2.2 Mutants. Mutations to the wild type hCCS-intein fusion were done by Mary Mayfield-Gambill of the Department of Enivronmental and Biomolecular Systems at the Oregon Graduate Institute School of Science and Engineering at the Oregon Health and Science University. Mutagenesis was carried out using a site-directed technique. A Transformer Site-Directed Mutagenesis Kit (Clonetech) was used to create single mutations of Cys to Ala (C22A, C25A, C244A, and C246A) in the wild type expression system described above [Carter 1987]. Additionally, two double Ala mutants (C22/25A and C244/246A) were also constructed and expressed. All expression constructs were confirmed by automated DNA sequence analysis.

2.1.2.3 Expression and Purification. The intein-hCCS fusion protein was expressed in the *Escherichia coli* strain ER2566 (Novagen) after induction with IPTG with 500 μM $CuSO_4$ and 500 μM $ZnSO_4$, or with no metal added for the apo-protein. The cells

```
1      MASDSGNQGT  LCTLEFAVQM  TCQSCVDAVR  KSLQGVAGVQ  DVEVHLEDQM
                                 *   *
51     VLVHTTLPSQ  EVQALLEGTG  RQAVLKGMGS  GQLQNLGAAV  AILGGPGTVQ
101    GVVRFLQLTP  ERCLIEGTID  GLEPGLHGLH  VHQYGDLTNN  CNSCGNHFNP
151    DGASHGGPQD  SDRHRGDLGN  VRADADGRAI  FRMEDEQLKV  WDVIGRSLII
201    DEGEDDLGRG  GHPLSKITGN  SGERLACGII  ARSAGLFQNP  KQICSCDGLT
                                                       ↑*  *
251    IWEERGRPIA  GKGRKESA
```

Figure 2.4: Amino acid sequence of the expressed hCCS after cleavage from the chitin-binding intein fusion protein. * denotes the cysteines mutated to alanines in the mutants and ↑ indicates the final residue of the protein in the truncation mutant.

where lysed with a French Pressure Cell Press (SLM-Aminco). The intein-CCS fusion protein was purified from the soluble portion with a chitin bead column. The chitin beads (New England Biolabs) were packed into a XK 16/20 column with an AK 16 adaptor (Amersham Pharmacia Biotech) and washed with 10 column volumes of column buffer (50 mM sodium phosphate, 500 mM NaCl at pH 7.2). Buffer flow into the column was controlled by gravity. The soluble portion was then diluted three times with column buffer and added to the column. After the soluble portion was added, the column was again washed with 10 column volumes of column buffer. The column was then washed with three volumes of cleavage buffer (column buffer plus 5 mM 2-mercaptoethanesulfonate (MESNA)). The column was then left to incubate overnight at room temperature with one column volume of cleavage buffer. Next, the column was washed with four column volumes of column buffer. The hCCS fraction eluted from the column was monitored by Bradford assay, SDS-PAGE gel, and copper concentration of the different fractions. When necessary, the protein was concentrated with an Amicon centricon ultrafiltration cell.

2.1.3 CLONING AND PURIFICATION OF INTEIN - SUPEROXIDE DISMUTASE FUSION

Both cloning and purification of the hSOD used in these studies were done by Amanda Barry of the Department of Environmental and Biomolecular Systems of the Oregon Graduate Institute School of Science and Engineering at the Oregon Health and Science University. Recombinant human SOD (rSOD) was cloned as a *SapI-NdeI* fragment generated by PCR amplification of a cDNA clone obtained from Genome Systems (GB Accession # AA702004). PCR primers that contained the restriction sites *SapI* (5') and *NdeI* (3') were used to amplify SOD cDNA. This PCR fragment was cloned into the intein pTXB-1 vector from New England Biolabs (see section 2.1.2).

E,Zn-Recombinant human SOD was expressed in the *Escherichia coli* strain ER2566 (Novagen) after induction with IPTG in the presence of 500 μM $ZnSO_4$. The cells were lysed with a French Pressure Cell Press (SLM-Aminco). E,Zn-Recombinant human SOD

was purified from the soluble portion with a chitin bead column. The chitin beads (New England Biolabs) were packed into a XK 16/20 column with an AK 16 adaptor (Amersham Pharmacia Biotech) and washed with 10 volumes 50 mM sodium phosphate 500 mM NaCl pH 7.2 (column buffer). The soluble portion was diluted 3x with column buffer and run over the chitin column. The column was then washed with another 10 volumes of column buffer. The column was then washed with 3 volumes of cleavage buffer. One volume of cleavage buffer was then added to the column and allowed to sit overnight. The next morning, the cleavage buffer was removed from the column as the first fraction and another 3 volumes of cleavage buffer was added to the column. All of the fractions were saved and combined. When necessary the protein was concentrated with an Amicon centricon ultrafiltration cell. Fully loaded Cu,Zn-SOD was obtained by adding excess $CuSO_4$ to the E,Zn-SOD followed by dialysis against Cu-free column buffer.

2.2 PHYSICAL METHODS

2.2.1 EXAFS

X-rays are in the energy range (500 eV to 500 keV) required to eject an electron from a core orbital out of the atom into the continuum. This is known as the photo-electric effect, where an x-ray photon is absorbed and an electron is ejected from the atom. The energy at which this process occurs is element specific and each element can have multiple absorption edges resulting from excitation of 1s electrons (the K edge) or the 2s or 2p electrons (the L edge) to the continuum. When an X-ray with an energy of $h\nu$ is absorbed by an atom with an ionization energy of E_b, if $h\nu$ is greater than E_b the electron will be ejected with the energy:

$$E_f = h\nu - E_b$$

When hν is less than E_b no absorption occurs. However, when hν equals E_b absorption happens giving rise to a sharp jump in the XAS spectrum known as the absorption edge. X-ray absorption is also affected by Beer's law, which states:

$$I = I_o e^{-\mu t}$$

Where I_o is the intensity of the incident x-ray, I is the intensity transmitted through the sample, t is the thickness of the sample and μ is the absorption coefficient.

The energy of the excitation is specific for each element, though it is affected by the redox state of the metal ion. The higher the oxidation state, the higher the energy required to excite an inner core electron to the continuum because greater energy is needed to overcome the positive charge of the nucleus, therefore there is a higher X-ray absorption edge. After absorption and release of the core electron, the atom is in an excited state and must decay. This usually happens through x-ray fluorescence where an electron from a higher orbital fills the core hole and emits an x-ray. If an electron from the L shell fills a

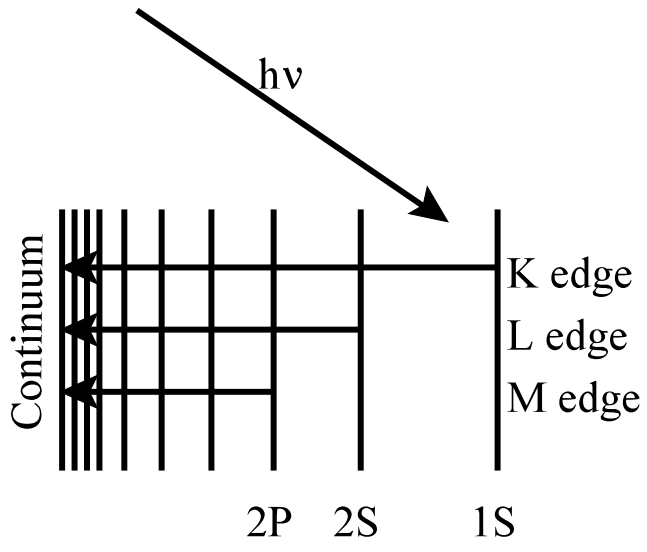

Figure 2.5: The excitation of a core electron to the continuum by an x-ray photon.

hole in the K shell, this is referred to as the K_α emission, while an electron moving from the M shell to the K shell is referred to a the K_β emission.

The EXAFS (Extended X-ray Absorption Fine Structure) region of the X-ray spectrum occurs at about 50 eV above the absorption edge. In this region there exist oscillatations in the spectrum that were first observed by Kronig in 1931 [Kronig 1931; Kronig 1932]. Eventually these oscillations were explained by the short range order theory [Sayers et al. 1971; Stern 1975]. This theory said that the oscillations were caused by the backscattering of the outgoing electron's wave by neighboring atoms causing interference in the absorption coefficient. The oscillations in the EXAFS spectrum are the modulations of the absorption probability of an atom brought on by the physical and chemical state of the atom. In EXAFS, these changes in the absorption coefficient are evaluated to determine the distance of the backscatterer from the central atom, the number of backscatterers around the central atom, and the type of backscattering atom present.

The equation used for analyzing EXAFS data is given below. It is a summation of

$$X(k) = k^{-1}\sum_{s} N_s \frac{|f_s(\pi,k)|}{R_{as}^2}\exp(-2\sigma_{as}^2 k^2)\sin\left[2kR_{as} + \alpha_{as}(k)\right]$$

the waves generated by the backscattering event at each shell (or layer of atoms around the central atom). Since EXAFS arises from the interaction of the wave of the outgoing and incoming photoelectron, it is common to convert the energy of the x-ray to the wave number (k) of the outgoing electron, where:

$$k = ((2m(E-E_o)/\hbar^2)^{1/2}$$

m is the mass of the electron, E_o is the energy of the absorption edge. The EXAFS equation is comprised of three main parts giving rise to the amplitude (the expression outside of the sine), the frequency ($2kR_{as}$) and the phase shift ($\Phi_{as}(k)$). The amplitude is given by the number of atoms in a shell (N_s), the electron scattering strength of the type of scattering atom (f_s), the distance between the central atom and the backscatter (R_{as}), and the Debye-Waller factor (σ^2), a measure of the disorder associated with the distance of the shell from

the central atom because of temperature, and static disorder effects. The frequency of the wave also is based on the distance between the central atom and the backscatter (R_{as}).

EXAFS elucidates three main traits about the atoms surrounding the absorbing atom: type of atom, number of atoms, and distance between absorber and scatterer. The distance is represented in the equation by R_{as} and is in both the frequency and the amplitude parts of the equation. As the distance decreases, the amplitude increases and the frequency increases. The number of atoms (N_s) relates to the amplitude of the wave which increases as the number of atoms increase. The type of atom is determined by the phase shift ($\Phi_{as}(k)$) and $f_s(\pi,k)$. Often to emphasize the later oscillations at higher k, the EXAFS will be presented as k-weighted where the equation is multiplied by the energy such as $k^3\chi(k)$.

The discussion so far has centered on the interactions between the absorbing atom and a single backscatterer in an event known as single scattering. However, it is possible to have multiple scattering events where the electron travels from the absorbing atom to a scattering atom then to additional scattering atoms before backscattering to the absorbing atom. The interactions of the outgoing wave and incoming wave are the same in multiple scattering as in single scattering and the EXAFS equation can be applied to deduce the same parameters. But in multiple scattering, the R_{as} is the distance of the complete path of the electron from the absorbing atom to the first scatterer to the second scatterer, etc. Also, the phase shift will differ from that of the single scattering event, as all of the atoms within the path will contribute.

2.2.1.1 EXAFS of Copper-Sulfur Systems. The copper K-edge - the maxima in the change of fluorescence over the change in energy, dF/dE - is at 8.979 keV for Cu(I), however for Cu(II), it shifts up to 8.983 keV. Cu(I) also can exhibit an intense edge feature at 8.984 keV which is not present in Cu(II) spectra. This feature has also been seen to change in intensity with respect to the number of coordinating ligands. Linear two coordinate copper-sulfur species show an extremely intense feature while three-coordinate species show a less intense feature. This feature represents the excitation of a 1s electron to the 4p orbital. In the linear system, the transition from 1s to 4p is allowed ($l \pm 1$) because the $4p_x$ and $4p_y$

orbitals are degenerate and non-bonding. However, when the coordination is increased the 4p orbital begins to take on some 4s character due to orbital mixing, therefore the transition from the 1s orbital becomes less allowed causing the absorption feature to be less intense. This loss of intensity can be exacerbated as the covalency of the metal-ligand bond increase and the metal 4p orbitals are mixed with the ligand sigma orbitals [Kau et al. 1987; Pickering et al. 1993].

Another notable change between lower and higher coordinate copper-sulfur species is the distance between the copper and sulfur atoms. This change is seen in the EXAFS of the species and not the edge feature. Typically, EXAFS has low accuracy in determining the coordination number of ligand to the metal ion but it has extreme accuracy in determining the bond distance. In copper-sulfur species it has been shown that the Cu-S distance can be a good indication of the coordination number of bound sulfur ligands. Two-coordinate Cu(I) complexes have been observed to show a distance of around 2.15 Å, while three coordinate complexes tend to have Cu-S distances closer to 2.25 Å [Blackburn et al. 1989; Ralle et al. 2004].

Other information that can be obtained from the EXAFS spectra of copper sulfur species is the presence of outer shell features. Copper sulfur species are often present in the form of copper clusters, formed from multiple copper ions connected by a bridging thiolate ligands. EXAFS of these species show an outer shell feature with intensity at around 2.7 Å brought on by non-bonded Cu-Cu scattering. Higher order complexes can also show a minor peak at 3.15 Å [Pickering et al. 1993].

2.2.1.2 EXAFS Experimental Conditions Cu K-edge (8.979 keV) and Zn K-edge (9.660 keV) extended X-ray absorption fine structure (EXAFS) data for the hCCS and the hCCS mutants was collected at the Stanford Synchrotron Radiation Laboratory operating at 3 GeV with currents between 100 and 50 mA. All samples were measured on BL 9-3 using a Si[220] monochromator and an Rh-coated mirror upstream of the monochromator with a 13 KeV energy cutoff to reject harmonics. The Si[220] monochromator is a double crystal

monochromator that uses Bragg's diffraction to produce monochromatic X-rays. Bragg's law is represented by the equation:

$$n\lambda = 2d \sin(\theta)$$

where d is the distance between the layers of atoms in a crystal, θ is the angle of diffraction and λ is the wavelength of the outgoing X-ray or particle. Therefore, in crystal monochromators the crystal can be rotated, changing the angle θ, to adjust the wavelength of the outgoing X-ray. The first crystal in the double crystal monochromator is tuned with a traditional motor, while the second crystal is controlled by a piezo-electric motor, whereby electricity applied to the crystal induces stress on the crystal and alters the distance between the crystal planes, and allows extremely accurate tuning of the X-ray wavelength. The intensity of the incoming x-ray (I_o) and the intensity of the x-ray after transmission through the sample (I, or I_1), is accomplished by a set of ion chambers before and after the cryostat holding the sample.

Data were collected in fluorescence mode using a high-count-rate Canberra 30-element Ge array detector with maximum count rates below 120 kHz (Figure 2.6). When collecting x-ray fluorescence the detector is placed at 90° to the that of the path of the incoming x-ray, this is because the synchrotron radiation is polarized and the majority of the scatter peak will be suppressed at an angle of 90° to that of the plane of the incident x-ray. A 6 μ Z-1 (Ni, Cu, oxide) filter and Soller slit assembly were placed in front of the detector to further reduce the elastic scatter peak. The Ni filter is used to absorb the elastic scatter peak and higher energy X-rays. The Ni K-edge is at 8331 eV, meaning any x-ray above that energy will be absorbed by the filter, however the K_α for copper is 8040 eV, therefore all of the x-rays generated by fluorescence from the sample should pass through the filter. There is the possibility of increased noise by the release of fluorescence from the Ni-filter after excitation by the higher energy X-rays and release of X-ray fluorescence, but this is reduced by the use of Soller slits which are metal plates aligned to deflect any x-ray not in the plane of the incident x-ray path from the detector.

Nine scans of a sample containing only sample buffer (20 mM $NaPO_4$, 500 mM NaCl, pH 7.0) were collected at each absorption edge, averaged and subtracted from the

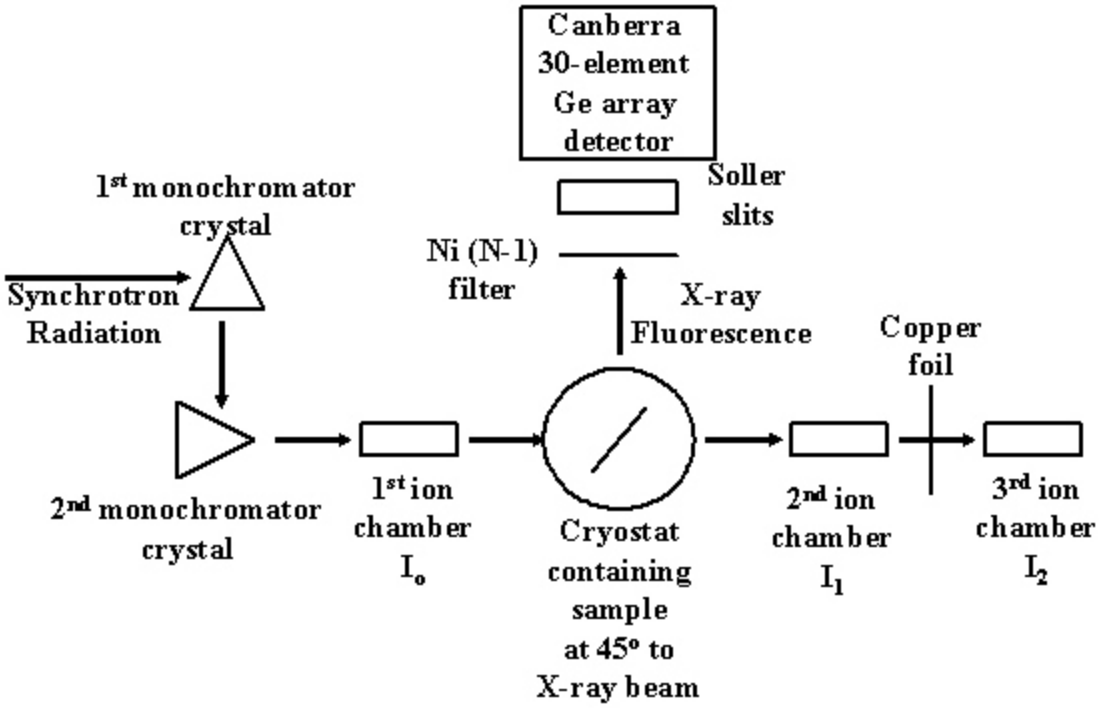

Figure 2.6: Schematic of the experimental set up of an X-ray beamline for collection of EXAFS data

averaged data for the protein samples to remove Z-1 K_β fluorescence and produce a flat pre-edge baseline. This procedure allowed data of an excellent signal-to-noise ratio to be collected down to 100 μM total copper in the sample. The samples (70 μL) were measured as aqueous glasses (>20% ethylene glycol) at 15 K. Energy calibration was achieved by reference to the first inflection point of a copper foil (8980.3 eV) for Cu K-edges and a zinc foil (9660.0 eV) for Zn K-edges, placed between the second (I_1) and third (I_2) ionization chamber. Data reduction and background subtraction were performed using the program modules of EXAFSPAK [George 1990]. Data from each detector channel were inspected for glitches or drop-outs before inclusion into the final average. Spectral Simulation was carried out using the program EXCURV98 [Gurman et al. 1984; Gurman et al. 1986; Binsted et al. 1996; Ralle et al. 1999] and the OPT module of EXAFSPAK with the theoretical phase shifts and amplitude functions calculated by FEFF 8.0 [Zabinsky et al. 1995]. Possible multiple scaterring paths and phased shifts where determined by FEFF 8.0 for use with

EXAFSPAK or they were determined by internal modules within EXCURV98. Both programs gave equivalent results.

Both EXAFSPAK and EXCURV98 fit the raw data to a set of variable parameters (usually N, R, E_0 and σ) using the least squares technique of curve fitting. This technique attempts to minimize the residual (or x,y ordinate differences) between the actual curve collected in the data and the theoretical curve derived from the parameters. The fit is judged by the sum of the squares of the residual, or the R^2, or R-value, not to be confused with the F-value, or the degrees of freedom of the fit. The R-value is used to determine the best values for a set of parameters, once determined, the F-value can be used to compare different sets of parameters, i.e.: the programs use the R-value to determine the appropriate values for a set of parameters and we use the F-value to determine the best set of parameters.

2.2.2 HPLC

HPLC was done with a Varian Prostar Solvent Delivery Module and a Varian Prostar UV/Vis detector set at 280 nm. The sample was run over a Bio-Rad Bio-Sil SEC-250 Gel Filtration Column in 500 mM NaCl, 50 mM Sodium Phosphate, 10 mM Sodium Azide, pH 6.8 buffer. The molecular weight was determined by comparison to Bio-Rad Gel Filtration Standard #151-1901 containing 10 mg/ml bovine Thyroglobulin (670 kD), 10 mg/ml bovine Gamma-globulin (158 kD), 10 mg/ml chicken Ovalbumin (44 kD), 5 mg/ml horse Myoglobin (17 kD), and 1 mg/ml Vitamin B_{12} (1.35 kD).

The calibration curve was then calculated using the equation:

$$K_{av} = \frac{V_e - V_o}{V_t - V_o}$$

V_e is the elution time of the sample or standard, V_o is the void volume and V_t is the total volume of the column. The K_{av} was then plotted against the log of the molecular weight to establish the calibration curve.

2.2.3 ACTIVITY

The assay for the determination of the activity of SOD is the xanthine oxidase assay originally developed by McCord and Fridovich [McCord et al. 1968; McCord et al. 1969]. Xanthine oxidase catalyzes the conversion of xanthine to urate. This reaction gives off high levels of superoxide anion as a by-product. The amount of superoxide released can be followed by its oxidation of cytochrome *c* which can be followed by an increase of absorption at 420 nm. The addition of SOD to the reaction mixture removes the superoxide and decreases the oxidation of cytochrome *c*. A unit of SOD is defined as the amount of SOD required to reduce the oxidation of cytochrome *c* by half under standard conditions.

The ability of CCS to transfer copper to SOD was measured by incubating apo-SOD with CCS for 15 minutes at 37^0C in a buffer of 50 mM sodium phosphate containing 10 μM bathrocuprine sulfonate and 10 μM EDTA at pH 7.8. The activity of CCS is defined as the amount of CCS required to activate one unit of activity of SOD.

2.2.4 METAL CONCENTRATION

Copper concentration was measured by three methods throughout these studies: bicinchoninic acid assay, flame atomic absorption spectroscopy (FAAS), and inductive coupled plasma optical emission spectroscopy (ICP-OES). The bicinchoninic acid (BCA) assay measures the complexing of BCA with copper(I) which forms a purple complex [Brenner et al. 1995]. Protein samples are first mixed with TCA to remove acid preciptable material such as proteins and other bioploymers and release all protein bound copper into the solution. The copper is then reduced by the addition of excess ascorbate and complexed with BCA. The amount of complex formed can be followed at 563 nm or 354 nm.

FAAS was done on a Varian-Techron AA-5 atomic absorption spectrophotometer to measure both copper and zinc concentration. Copper absorption was followed at 327 nm and compared to a calibration curve prepared from a copper concentration stock solution

purchased from Sigma. Zinc absorption was followed at 213 nm and compared to a calibration curve prepared from a zinc concentration stock solution purchased from Sigma

ICP-OES was run on a Perkin Elmer 2000 Optima DV spectrophotomer. Copper and zinc emission where followed simultaneously and compared to a calibration curve of a multi-element standard prepared from stock solutions purchased form Sigma.

CHAPTER 3

EXAFS AND COPPER-BINDING STUDIES OF THE HUMAN COPPER CHAPERONE TO SUPEROXIDE DISMUTASE - MALTOSE BINDING FUSION PROTEIN[1]

3.1 INITIAL STUDIES OF THE HUMAN COPPER CHAPERONE TO SUPEROXIDE DISMUTASE

The amino acid sequence of hCCS shows four possible metal binding motifs. First, in domain I, there is the conserved ATX1-like copper binding site MXCXXC (MTCQSC in hCCS)[Culotta et al. 1997]. Two potential binding sites exist in domain II, a SOD-like domain where both the zinc and copper sites of SOD are conserved or modified, with one of the histidine residues in the copper binding site replaced by an aspartate residue making it almost identical to the zinc binding site. The crystal structure of the truncated form of hCCS containing only domain II shows that the conserved zinc site does contain a zinc ion while the copper site remains empty[Lamb et al. 2000]. The last metal binding site is the CXC motif in domain III. Previous work on the yeast form of CCS showed that it may bind up to two coppers per protein, however the yeast form does not have the conserved metal

[1]The work described in this chapter was published in *Biochemistry* **2000**, 39(25), 7337-42, under the title "Domains I and III of the human copper chaperone to superoxide dismutase interact via a cysteine-bridged Dicopper(I) cluster".

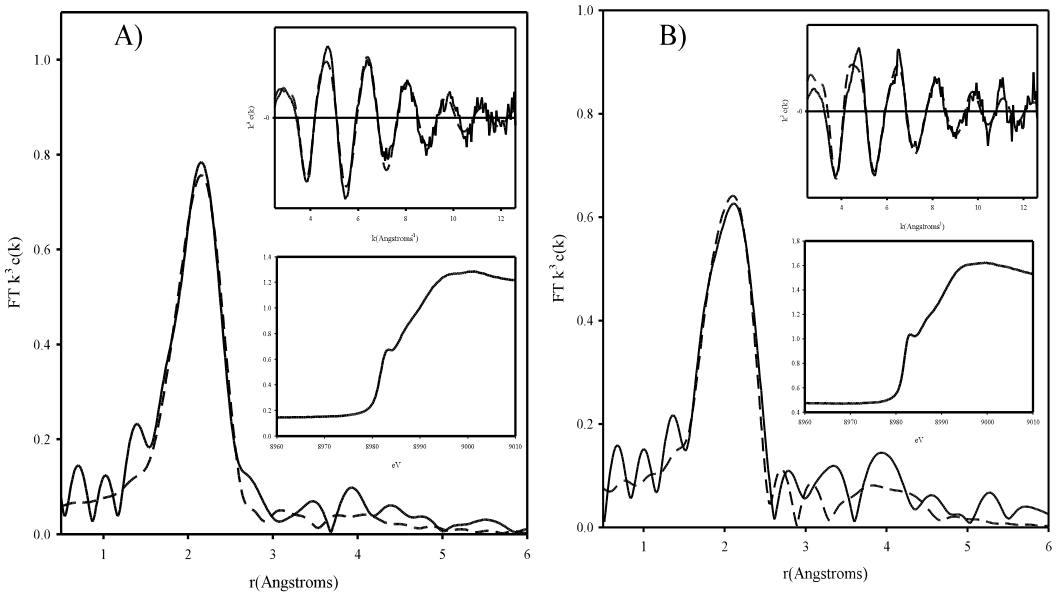

Figure 3.1: The edge, EXAFS, and Fourier Transform of the (A) hCCS-only and the (B) hCCS:hSOD samples

binding sites in domain II. The same study also showed that only domain III was needed for copper transfer to SOD and suggested that domain I was responsible for scavenging copper under low concentrations [Schmidt et al. 1999].

The crystal structure of yeast CCS suggests that copper would bind to CCS in a linear geometry [Lamb et al. 1999]. Although this crystal structure did not contain copper, this conclusion was reached because of the similarity between the disulfide formed in the MXCXXC region of the ATX-like domain I of CCS and that of the disulfide seen in the crystal structure of oxidized apo-ATX. In the crystal structure of the reduced Hg-ATX, the disulfide present in the oxidized ATX was reduced and the cysteine residues bound the metal ion in a linear geometry. It was therefore put forth that the same geometry would be found in CCS [Rosenzweig et al. 1999]. To elucidate what the actual coordination environment of copper in hCCS was, we have undertaken Cu-EXAFS studies.

John Eisses from Jack Kaplan's lab expressed and purified the two initial samples of hCCS we used for EXAFS. The samples consisted of an hCCS-only sample and a 1:1 mixture of Cu-hCCS and apo-hSOD. Both samples were mixed with 20% ethylene glycol as a glassing agent and concentrated for EXAFS data collection. The final copper

Table 3.1: Parameters for the Full Least-Squares Simulation of the EXAFS data of (A) hCCS and (B) hCC:hSOD

A) E_o = -3.92 F = 0.0041

First Shell			Outer Shells			
Shell (X)	R(Å)	δ^2 (Å^2)	Shell(Y)	R(Å)	∠Cu-X-Y (deg)	δ^2 (Å^2)
2 N/O	1.977	0.007	2 C_β	2.987	119.8	0.011
1.5 S	2.246	0.013	2 C_β	3.126	123.2	0.011
			2 N_γ	4.158	160.1	0.015
			2 C_γ	4.052	160.3	0.015

B) E_o = -5.21 F = 0.0006215

First Shell			Outer Shells			
Shell (X)	R(Å)	δ^2 (Å^2)	Shell(Y)	R(Å)	∠Cu-X-Y (deg)	δ^2 (Å^2)
2 N/O	1.991	0.001	2 C_β	2.766	121.1	0.010
1 S	2.252	0.011	2 C_β	2.991	123.8	0.010
			2 N_γ	4.215	159.9	0.015
			2 C_γ	4.070	159.4	0.015

*Errors in distance are ±0.002Å for the first shell and ±0.005Å for the outer shells. The given errors for the coordination numbers are ±25%

concentration of the hCCS-only sample was 1.6 mM, while the sample mixed 1:1 with apo-SOD had a final copper concentration of 0.4 mM. The EXAFS results for these samples are in Figure 3.1, and the fits used for this data are in Table 3.1. The first shell of the hCCS-only FT fits best with 1.5 Cu-S at 2.246 Å and 2 Cu-N at 1.977 Å. Our first interpretation of the

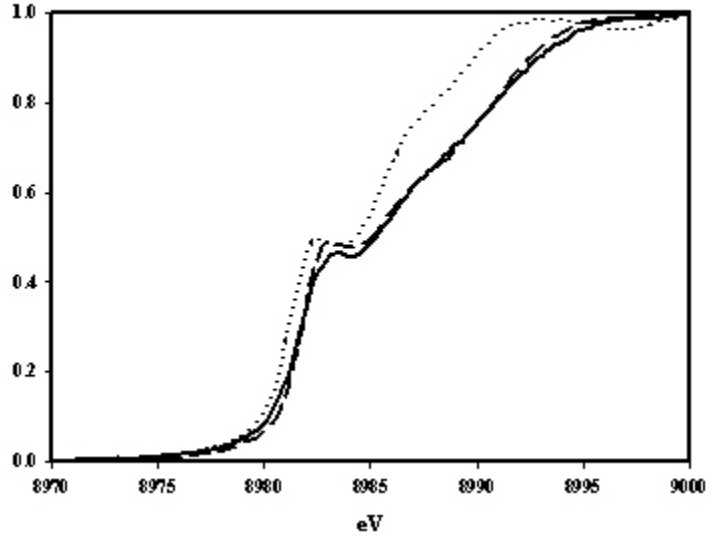

Figure 3.2: The edge spectra of hCCS(—), hCCS:hSOD (--) and a three coordianted copper(I)sulfur species(···)

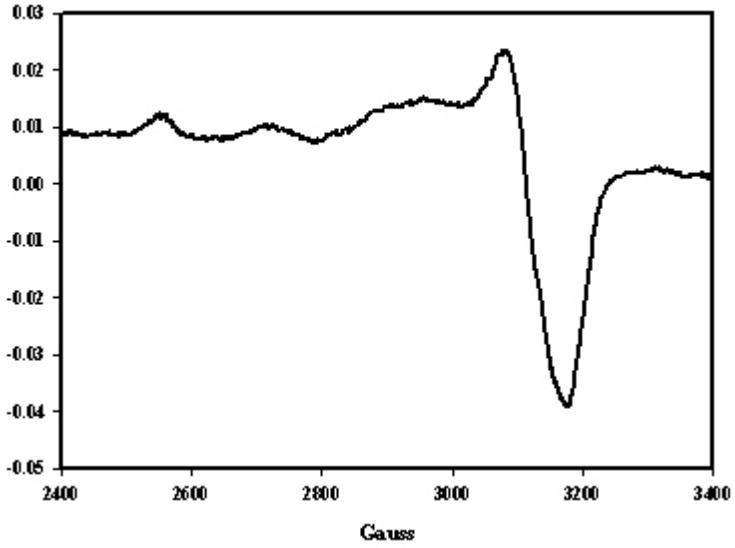

Figure 3.3: The EPR spectrum of the hCCS sample

data was that hCCS had a single three coordinate copper site containing cysteine and histidine residues. The hCCS:SOD mixed sample showed a decrease in the amount of sulfur contribution in the first shell (1 Cu-S at 2.252 Å) while the nitrogen contribution remained essentially the same. The decrease in the amount of sulfur in the mixed hCCS:SOD sample could be explained as copper transfer to the histidine-rich metal site in SOD. The edge for both samples appears at the appropriate energy for a Cu(I) species (8980.8 eV). Even though the EXAFS data fit to a three coordinate environment, the edge data does not exhibit as intense of an edge feature as would be expected in a three coordinate Cu(I) species (Figure 3.2) [Pickering et al. 1993]. One possible reason for this loss in intensity is a mix of oxidation states in the sample. The EPR spectrum of the hCCS-only sample showed that nearly 1/3 of the copper was in the Cu(II) state (Figure 3.3). Cu(II) would very likely bind to the conserved metal sites in the SOD-like domain and not to the sulfur rich sites in domains I and II. Therefore, one could surmise that the histidine seen in the Cu-EXAFS was binding Cu(II) in the SOD-like metal binding site and was not representative of the Cu(I) binding sites in hCCS.

3.2 COPPER BINDING PROPERTIES OF THE HUMAN COPPER CHAPERONE TO SUPEROXIDE DISMUTASE

To answer the questions: (1) how does copper bind to hCCS in the cell; (2) whether or not there is copper in the SOD-like domain; and (3) if so, is binding in the SOD-like domain advantageous, CCS was exposed to a variety of conditions to try and elucidate its copper binding properties. All of the hCCS protein used in these initial studies were expressed in *E. coli* in medium with 500 μM copper. After purification of the protein, dialysis was performed against copper-free buffer to determine if any of the bound copper was nonspecific. Then, a number of reductants were tried to ensure that all of the copper was in the +1 oxidation state. The reductants tried were DTT - a thiol containing reductant, and dithionite - a thiol-free reductant, and the biological reductant ascorbate because it has been shown to be able to reduce SOD [Banci et al. 2002]. Acetonitrile was also added to a sample to see if it would remove some of the Cu(I) bound to CCS. Copper concentrations where taken after each step and EPR was done to confirm the oxidation state of the copper.

Table 3.2 reviews a sampling of the copper binding data we collected on hCCS. Overall, the copper to protein ratio of the wildtype protein as expressed and purified ranged from 1.7 - 3.2 coppers per protein. Invariably, the amount of Cu(I) per protein was around 2:1 while the amount of Cu(II) was variable. Dialysis failed to remove any of the excess Cu(II) suggesting that this form of copper was not nonspecifically bound to the protein but actually resided in a metal binding site. Reduction with either DTT or dithionite, followed by dialysis against 50 mM potassium phosphate buffer, consistently left the copper to protein ratio at 2:1 and all of the copper was EPR undetectable. This finding was universal for samples of different concentrations of copper treated with the same procedures, i.e. there were no concentration effects. In fact, the nine-fold concentration sample D (Table 3.2) showed very little changes in copper to protein ratios and was still reduced to 2:1 Cu:protein after reduction. The reductant ascorbate was unable to reduce the Cu(II) in the protein and acetonitrile failed to remove any of the Cu(I).

Table 3.2: The copper binding properties of hCCS

Sample	Protien (P) (μM)	Cu_{total} (μM)	Cu/P	Cu(I) (μM)	Cu(I)/P	Cu(II) (μM)	Cu(II)/P
A As purified	776	1500	1.9				
B As purified	867	1677	1.9				
C First Dialysis	67	227	3.4				
Second Dialysis	48	152	3.2	92	1.9	60	1.3
+1 mM DTT	12	26	2.2	26	2.2	0	0
D As purified	41	100	2.5				
Dialysis	39	97	2.5				
Concentrated	275	699	2.4	494	1.8	175	0.6
+ 1 mM Dithionite	78	156	2.0	156	2.0	0	0
+ 1 mM DTT	75	158	2.1	158	2.1	0	0
+ Ascorbate	275	699	2.4				

3.3 Cu-EXAFS OF VARYING COPPER LOADED FORMS OF THE HUMAN COPPER CHAPERONE TO SUPEROXIDE DISMUTASE

To further understand the copper binding properties of hCCS, Cu-EXAFS was performed. The three as-purified undialyzed samples listed in Table 3.2 all showed EXAFS similar to that of the original EXAFS of the hCCS-only sample. The absorption edge of all three samples showed features and slight edge shifts that are indicative of mixed oxidation states. In fact, there is a correlation between copper per protein and the intensity of the edge feature. In Figure 3.4 the order of the edge feature intensity from bottom to top is D, C, A and B (A and B are essentially equal), this trend also follows the decrease in copper to protein ratios, therefore as the Cu to protein ratios decreased, the amount of Cu(II) per protein decreased.

Figure 3.5 shows the FTs of samples B,C and D: all had intense first shell peak at about 2.2 Å and the width of this peak suggests a mixed nitrogen sulfur ligand environment. All the spectra had peaks at around 4 Å which can come from the multiple scattering of the

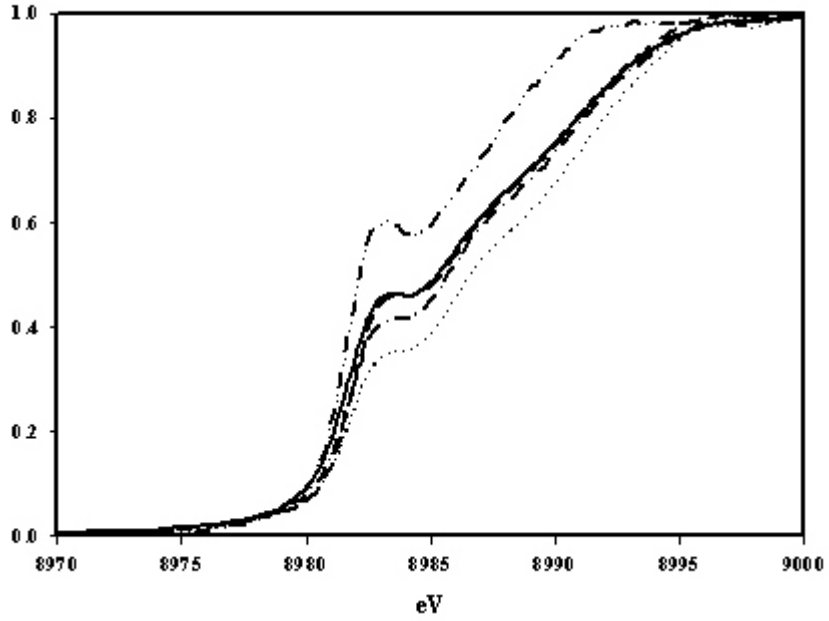

Figure 3.4: The edge features of the as-purified sample A(—), B (- -), C (-˙-), and D (¨) as compared to a three coordinate copper(I)sulfur species (-¨-)

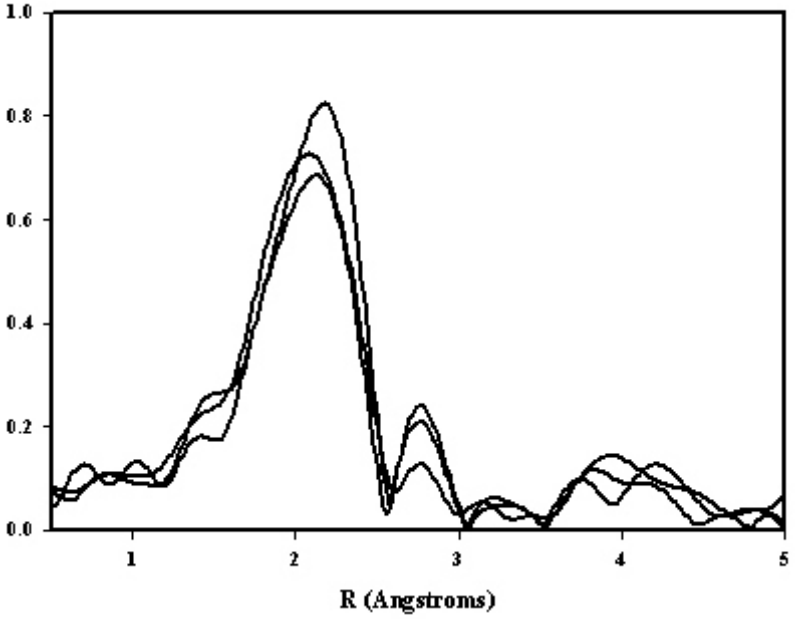

Figure 3.5: The first shell comparisons of the Fourier Transforms of samples B, C, and D

C_γ/N_γ of an imidazole ring. The second shell peak at 2.7 Å is too close for the C_β of histidine which is usually around 3 Å, suggesting that there must be another species present that is outweighing the histidine multiple scattering. This second shell peak also appears to increase as copper to protein ratios increase in the sample.

Table 3.3: Fits obtained from analysis of the first shell Fourier filtered data of hCCS sample D from Table 3.2

Fit no.	shell	distance	$2\sigma^2$	E_o	F
A	3 N	2.07	0.012	-8.90	0.944
B	3 S	2.20	0.022	5.05	0.120
C	2 S	2.23	0.010	5.16	0.063
	1 S	2.10	0.008		
D	1 S	2.27	0.007	5.45	0.068
	2 S	2.15	0.014		
E	1 S	2.25	0.008	-2.65	0.064
	2 N	2.01	0.010		
F	2 S	2.22	0.015	1.15	0.054
	1 N	1.96	0.009		

Analysis of the first shell filtered data (transform range 1.0 to 2.2 Å) of sample D is summarized in Table 3.3. The fits containing only a single shell (3N or 3S) both had very poor F values, meaning that the first shell in the FT is split. Having three sulfurs in a split shell with either two sulfurs at 2.15 Å and a single sulfur at 2.27 Å or two sulfurs at 2.23 Å and one at 2.10 Å, both give reasonable fits with F values of 0.068 or 0.063 compared to 0.120 when the three sulfur scatterers are kept together. However, both of the fits for the split sulfur shells had Cu-S distances of less than 2.2 Å which is unusually short for a three coordinated copper sulfur species, the only example in the literature that could be found of this short a distance were in the blue copper proteins [Adman 1991; Holm et al. 1996; Inoue et al. 1999]. The best fits came from the split shells of mixed sulfur and O/N scatters. The two sulfur - one O/N fit gave good distances of 2.22 Å and 1.96 Å, respectively, and the lowest F value of any of the fits at 0.054. While the one sulfur - two O/N fit gave distances of 2.25 Å for Cu-S distance and 2.01 Å for the Cu - O/N distance with an F value of 0.064.

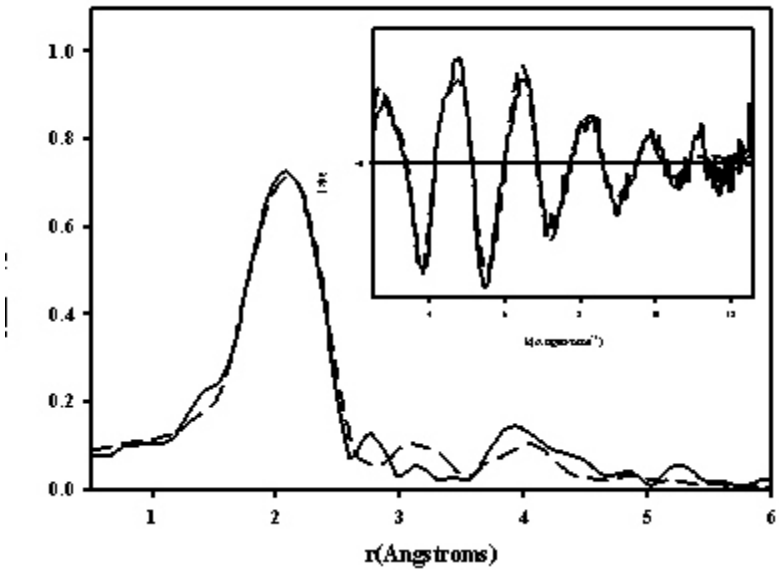

Figure 3.6: Experimental (—) and simulated (- -) Fourier transform and EXAFS (inset) of hCCS sample D. Parameters used in the fits are given in table 3.4

A search of the Cambridge Structural database showed that three coordinate copper model compounds with mixed sulfur and nitrogen ligand environments seem to favor the S_2N ligand donor set with distances of 2.25 Å for the Cu-S interactions and 1.98 Å for the Cu-N [Janssen et al. 1996; Blackburn et al. 1997; Garcia-Vasquez et al. 1997]. This made us favor the 2 S - 1 O/N fit which agreed well with the model compounds for the model of a single copper site in hCCS.

Further refinement of the model of two sulfur and 1 O/N ligands was done by using multiple scattering to simulate the O/N ligand as a histidine. The final spectra for sample D is in Figure 3.6 and the parameters used for the fit are in Table 3.4. The average ligand environment of two cysteine (Cu-S) and one histidine (Cu-N) can be explained two ways. First of all, it could represent a single trigonal site of copper bound to two cysteines and one histidine. Secondly, it could be a mixture of two copper sites; one in the SOD-like metal binding site in domain II which would be comprised entirely of histidine residues and one copper bound to the sulfur sites of domain I and/or domain III. The high copper content of the protein and the mixed oxidation states of the samples seem to favor the latter situation.

Table 3.4: Parameters for the Full Least-Squates simulation of the EXAFS data of hCCS sample D

A) E_0 = -4.03			F = 0.0040			
First Shell[a]			Outer Shells			
Shell (X)	R(Å)	δ^2 (Å^2)	Shell(Y)	R(Å)	∠ Cu-X-Y (deg)	δ^2 (Å^2)
2 N/O	1.980	0.010	2 C_β	2.981	122.7	0.011
1.5 S	2.246	0.011	2 C_β	3.126	123.5	0.011
			2 N_γ	4.207	160.6	0.015
			2 C_γ	4.122	160.3	0.015

[a]Errors in distance are ±0.002Å for the first shell and ±0.005Å for the outer shells. The given errors for the coordination numbers are ±25%.

Reduction by either dithionite or DTT consistently lowered the copper to protein ratio to two Cu(I) ions per protein. Figure 3.7 shows the effect of the reduction by dithionite to the x-ray absorption of sample D: the absorption energy decreased and the edge feature grew, which is to be expected for a change to a three-coordinate Cu(I) species. The EXAFS spectrum also noticeably changed: the first shell peak is narrower and more intense. The

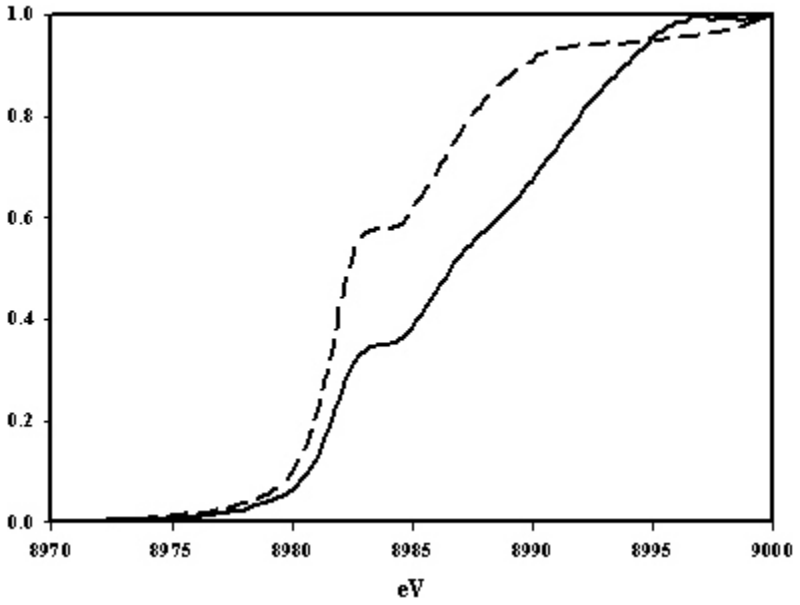

Figure 3.7: The X-ray absorption edge of hCCS sample (—) and the same sample reduced with dithionite (- -)

second shell peak also grew in intensity and there were no multiple scattering peaks. The intensities of the peaks remained consistent despite the overall copper concentrations, e.g. a 0.16 mM sample had the same intensity as a 1.6 mM sample, so the increase in the intensities of the EXAFS was not related to copper concentration but only to the Cu/protein ratio. Also, the loss of the histidine outer shells suggest that reduction removes copper solely from the SOD-like metal binding sites in domain II.

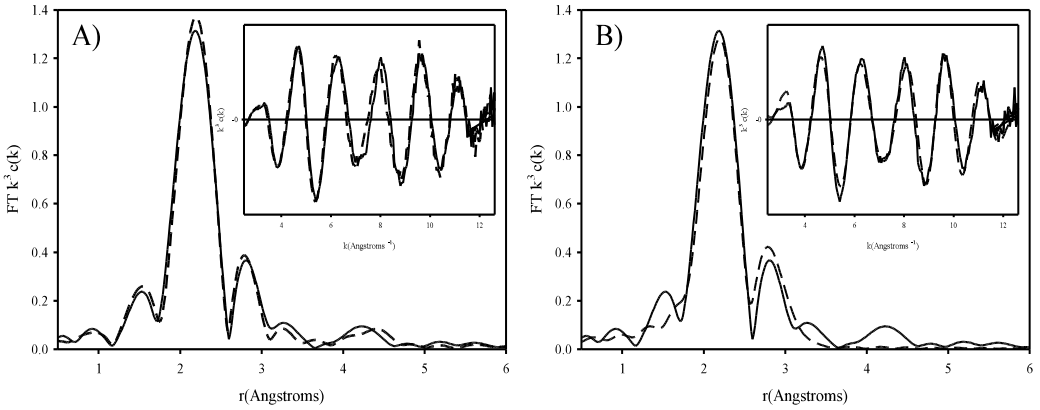

Figure 3.8: A) Comparison of the Fourier transform and EXAFS (inset) of the dithionite (—) and the DTT (- -) reduced hCCS. B) The experimental (—) and simulated (- -) Fourier transform and EXAFS (inset) of the dithionite reduced sample. Parameters used for the fit are in Table 3.5

The data for the hCSS samples reduced with DTT and with dithionite is shown in Figure 3.8, the results are comparable between the two reductants. The first shell fit best with 3 Cu-S at 2.25 Å, and this fit is not improved by splitting the first shell. No peaks indicative of histidine multiple scattering were present in these spectra and the second shell fit well as a single copper at 2.72 Å. With two coppers per protein and the distance of 2.72 Å, the data suggests that the copper site in hCCS exist in a multinuclear cluster. The distance of 2.25 Å is too long for the average bis-cysteine system which is usually closer, 2.15 Å, and it is more like the distances typically seen in three-coordinate systems [Ralle et al. 1998; Srinivasan et al. 1998; Ralle et al. 2003]. This data seems to be consistent with a cysteine-bridged dicopper(I) cluster with each copper being coordinated by three cysteines with at least one bridging cysteine (Figure 3.9). Srinivasan's work on the EXAFS of the

Table 3.5: Parameters used to simulate the EXAFS data of the Dithionite and DTT reduced samples of hCCS

	Cu-S[a]			Cu-Cu		
Sample	Shell	R(Å)	$2\sigma^2$(Å^2)	Shell	R(Å)	$2\sigma^2$(Å^2)
Dithionite reduced 1.6 mM, B[b]	3.0	2.25	0.009	1.0	2.74	0.013
Dithionite reduced 0.16 mM, D	3.0	2.25	0.010	1.0	2.71	0.009
DTT reduced 1.1 mM, B	3.0	2.26	0.009	1.0	2.72	0.014
Dithionite reduced 0.16, mM, D	3.0	2.27	0.011	1.0	2.72	0.009
COX17 [Sirinivasan et al. 1998]	3.0	2.26	0.009	1.0	2.72	0.012

[a]Errors in distance are ±0.002Å for the first shell and ±0.005Å for the outer shells. The given errors for the coordination numbers are ±25%. [b] denotes sample as indentified in Table 3.2

COX17 copper chaperone shows a cluster similar to ours [Srinivasan et al. 1998]. The authors of this work reached the conclusion that the cluster must be a doubly bridging μ_2 complex because the Cu-Cu distance of 2.7 Å is closer to that of other doubly bridged complexes (2.7 - 3.0 Å) than to that of singly bridged clusters (3.3 Å). To further validate the presence of a copper cluster in hCCS, the data from the unreduced samples of hCCS

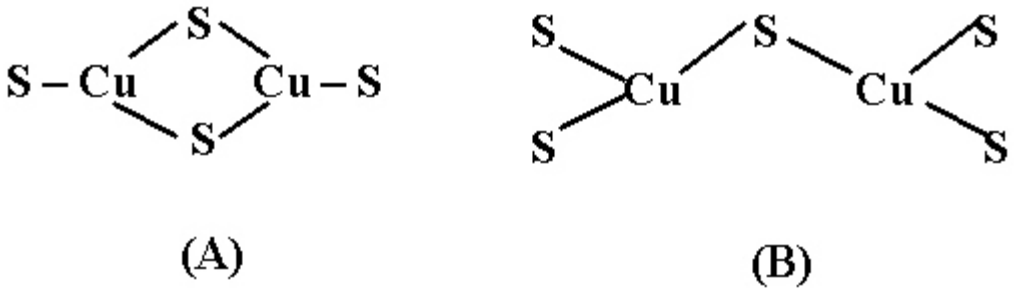

Figure 3.9: The two possible structures for the copper cluster simulated by the EXAFS data for hCCS. A) is the structure favored for COX17 which gives identical EXAFS results to that of hCCS

was reevaluated with the addition of a copper at 2.72 Å, so that the fit would represent a combination of the copper cluster and a copper in the histidine rich site of the SOD-like domain. The F value for this fit of the original data was an improvement over the fits without a copper present, suggesting that Cu(I) binds hCCS in a multiple copper cluster.

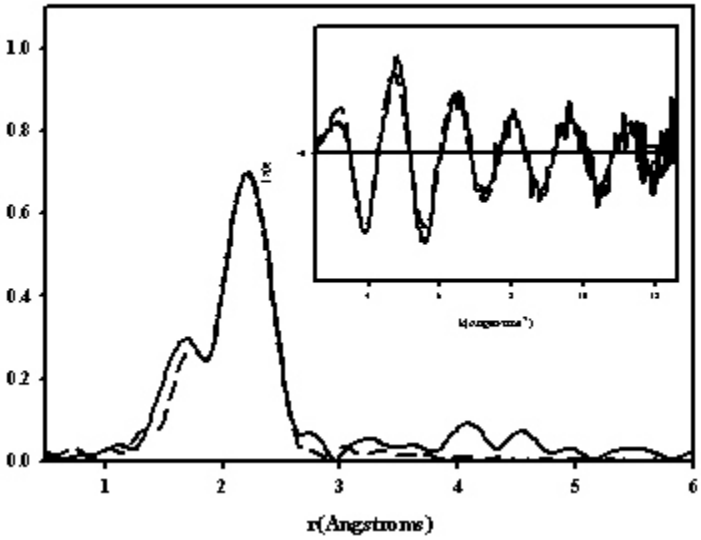

Figure 3.10: Experimental (—) and simulated (- -) Fourier transform and EXAFS (inset) of hCCS reduced by ascorbate. Parameters used for this fit are listed in Table 3.6

The acetonitrile samples were not examined by EXAFS, as the addition of acetonitrile had no effect on the copper to protein ratios or the oxidation state of the copper present. The Cu-EXAFS of the ascorbate reduced sample looked different compared to that of the DTT or dithionite reduced samples. The histidine multiple scattering appeared to be gone from the spectra but the copper peak at 2.72 Å was also missing. The best fit for the first shell peak is that of Cu-S at 2.24 Å and less than one Cu-O at 1.85 Å. It is possible that while ascorbate is able to reduce the copper ions in the protein, it is unable to reduce any disulfide bonds that might be present if the metal binding sites of domain I and domain III

Table 3.6: Parameters for the Full Least-Squares simulation of EXAFS data of hCCS reduced with ascorbate

Shell (X)[a]	R(Å)	$2\sigma^2$ (Å^2)	E_o	F
0.5 N/O	1.846	0.003	-4.21	0.0054
2.0 S	2.238	0.011		

[a]Errors in distance are ±0.002Å for the first shell and ±0.005Å for the outer shells. The given errors for the coordination numbers are ±25%.

were oxidized. It is, therefore, able to reduce the Cu(II) in the protein, but unable to free up the enough of the Cu(I) sites to form a significant amount of the cluster.

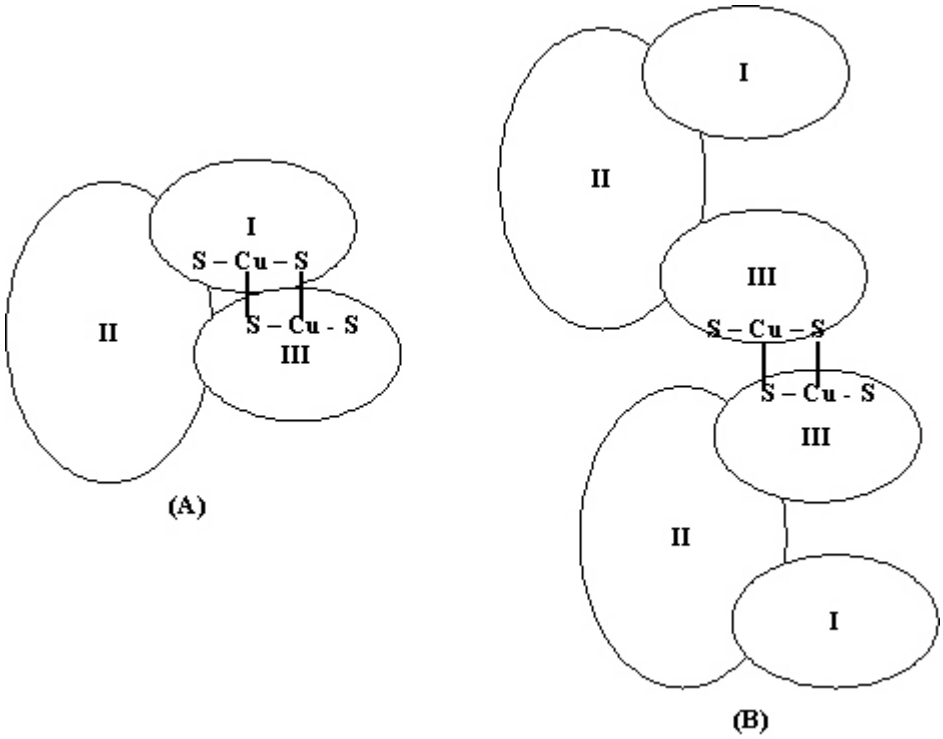

Figure 3.11: The two possible copper clusters that could be formed by hCCS, A) an intramolecular cluster and B) an intermolecular cluster

It is not possible to determine from the EXAFS data whether the cluster is formed from an intramolecular interaction of the two metal binding sites in domain I and domain III; involves other cysteine residues found in hCCS, or is formed by intermolecular interactions between two hCCS monomers. The option of another cysteine from hCCS in addition to the ones in the MXCXXC and the CXC motif is unlikely, there are four cysteine in hCCS not located in either of these motifs, but they are not conserved in other species of CCS, so their role in copper binding and transfer is questionable. The copper cluster seen in the copper chaperone COX17 was shown to be formed by a bridging of two COX17 monomers [Srinivasan et al. 1998]. COX17 is a small protein that shares little homology with hCCS [Glerum et al. 1996; Lamb et al. 1999]. COX17 has no motif similar to that of

the MXCXXC motif found in domain I of hCCS but does contain a CCXC motif similar to the site in hCCS domain III as well as three other conserved cysteines. Atox-1 which contains the MXCXXC from domain I but not the CXC motif found in domain III has not been seen to form clusters, nor has it been seen as a dimer, suggesting that the MXCXXC may not be suited for cluster formation [Ralle et al. 2003]. This evidence would suggest that a cluster is more likely to be formed as an intermolecular interaction between the CXC motif of two separate hCCS monomers. However, work done on cobalt binding to tomato CCS and truncation mutants of hCCS gives evidence for a single Co^{2+} being coordinated by all four cysteine of domains I and III, meaning that there is evidence that a cluster could be formed by the intramolecular interactions of domain I and domain III [Zhu et al. 2000]. There is no evidence in the literature of a cluster formed between dimerization of two MXCXXC motifs, the structures published of proteins containing this motif all appear to be single copper sites within a monomeric protein [Rosenzweig et al. 1999; Arnesano et al. 2001; Ralle et al. 2003]. Therefore, the most likely candidates for the cluster formation are the intramolecular domain I - domain III cluster or the intermolecular domain III - domain III cluster, but from the data collected in this study it would not be possible to distinguish between those two possible structures.

3.4 CONCLUSIONS

The work presented in this chapter shows that hCCS binds two copper ions per monomer of hCCS and that hCCS contains a binuclear copper cluster. Two possible structures are presented that would explain this data, an intramolecular cluster formed between the copper-binding motifs in the domain I and domain III of a single hCCS monomer, or an intermolecular cluster formed between two domain III copper-binding motifs of different hCCS monomers. Although it is impossible to distinguish between these two structures from the work done in the chapter, in either case, the evidence presented contradicts the heterodimer mechanism introduced in the first chapter (Figure 1.19). We see

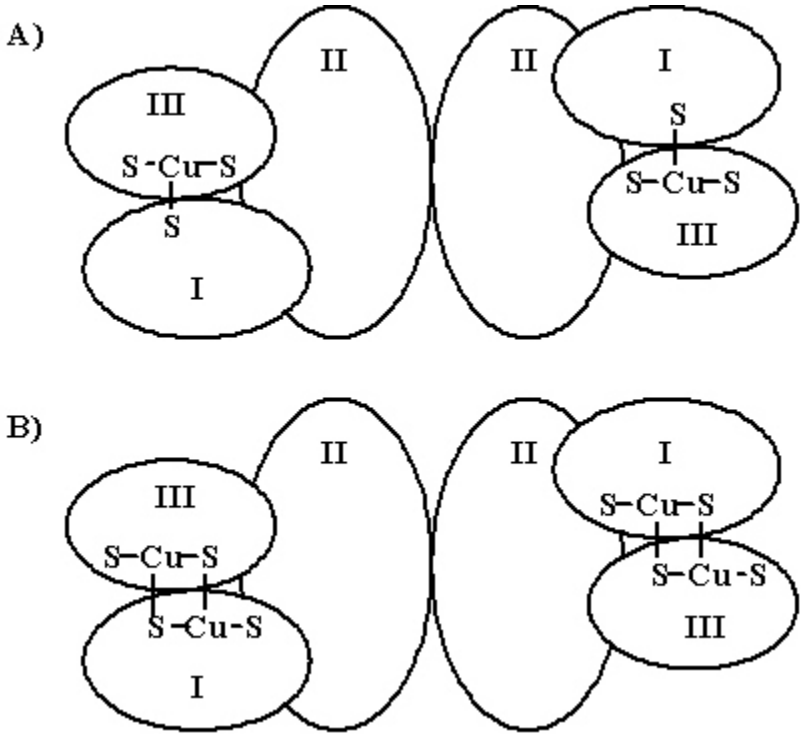

Figure 3.12: The structure hCCS proposed by the heterodimer mechanism (A) and the structure of hCCS proposed in this chapter (B).

that the starting form of hCCS put forth in the heterodimer mechanism, a dimer of hCCS with each monomer containing a single three-coordinated copper site formed between the domain I and domain III, must be changed to a dimer of hCCS with each monomer binding two copper ions in a copper cluster formed between the domain I and domain III (Figure 3.12).

CHAPTER 4
STUDIES ON MUTANTS OF THE HUMAN COPPER CHAPERONE TO SUPEROXIDE DISMUTASE - MALTOSE BINDING FUSION PROTEIN[1]

4.1 MUTANTS OF THE HUMAN COPPER CHAPERONE TO SUPEROXIDE DISMUTASE

Studies in the previous chapter showed that at least some of the copper bound to hCCS is in a copper sulfur cluster. This cluster could be formed by intramolecular interactions between the domain I motif, MCXXC, and the domain III motif, CXC; or it could be formed by intermolecular interactions between the motifs of different hCCS monomers. To further probe the role of the different motifs in cluster formation, we made various cysteine to serine mutations in both domain I (C22S and C22/25S) and domain III (C244S and C244/246S). It is expected that the mutation of a cysteine within the cluster to a serine would disrupt the cluster, therefore, the mutational studies should show whether one or both of the motifs play a role in cluster formation.

---

[1]The work described in this chapter was published in *Biochemistry* **2005**, 44(9), 3143-52, under the title "Cysteine-to-serine mutants of the human copper chaperone to superoxide dismutase reveal a copper cluster at a domain III dimer interface".

4.2 METAL BINDING STUDIES OF THE HUMAN COPPER CHAPERONE TO SUPEROXIDE DISMUTASE AND ITS MUTANTS

When expression of hCCS was induced in the presence of 500 μM copper sulfate, the purified protein bound copper in a ratio greater than 2:1, with some copper in the +2 oxidation state. To achieve solely Cu(I) containing protein, post-purification reduction had to be performed. The protein was reduced with either DTT or dithionite to achieve a final ratio of two Cu(I) per protein. It was later discovered, however, that the same copper to protein ratios could be obtained without reduction if hCCS was expressed in the presence of 500 μM copper sulfate and 500 μM zinc sulfate. Interestingly, the addition of zinc to the medium had no effect on the zinc concentrations in the protein, which was invariably about one zinc per monomer, but did result in a protein that had two Cu(I) per protein and no Cu(II). The simplest explanation for this is that excess Cu(II) in the media, with no zinc present, is able to be imported via divalent cation transporters and through other non-specific paths. The addition of Zn(II) to the media acts as a buffer to ensure that no Cu(II) is non-specifically transported and that all of the copper is brought into the cell as Cu(I) throught the normal copper transporting mechanisms.

WT hCCS was expressed in the presence of 500 μM $CuSO_4$ and 500 μM $ZnSO_4$ and purified with 1.85 Cu(I) and 0.91 Zn atom per protein (Table 4.1). The single mutants,

Table 4.1: The copper and zinc metal binding ratios for hCCS and its mutants, where Cu/P is the ratio of copper to protein, Zn/P is the ratio of zinc to protein and N is the number of data points collected for each metal concentration.

Protein	Cu/P	N	Zn/P	N
Wild Type	1.85 ± 0.105	12	0.91 ± 0.080	9
C22S	1.60 ± 0.277	5	0.72 ± 0.127	5
C244S	1.66 ± 0.100	5	0.87 ± 0.036	5
C2225S	0.91 ± 0.124	4	0.86 ± 0.065	4
C244246S	0.92 ± 0.102	5	0.95 ± 0.081	5

C22S and C244S, had similar metal binding properties as the wild type when expressed under the same conditions. C22S purified with 1.6 copper and 0.72 zinc, while C244S contained 1.7 copper and 0.87 zinc per protein. The most noticeable difference in metal binding was in the double mutants, C22/25S and C244/246S where zinc binding remained unchanged but the amount of copper bound dropped to one Cu(I) per protein. C22/25S had 0.91 atoms of copper and 0.86 atoms of zinc per molecule of protein, and C244/246S contained 0.92 atoms of copper and 0.95 atoms of zinc per molecule of protein. None of the constructs showed an EPR signal, meaning no Cu(II) was present in the wildtype or any of the mutant proteins. These results show that both domain I and domain III can each bind a single Cu(I) ion.

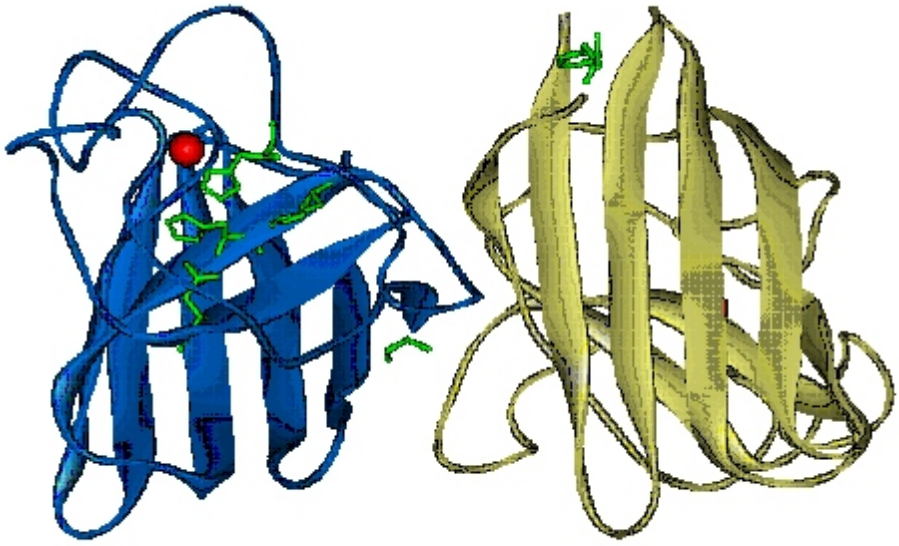

Figure 4.1: Structure of truncated Domain II-only hCCS showing bound Zn (red). Despite presence of conserved copper-binding ligands (green), no copper was present. The cooordinates for this structure were taken from the protein data bank file 1DO5

4.3 XAS STUDIES OF THE HUMAN COPPER CHAPERONE TO SUPEROXIDE DISMUTASE AND ITS MUTANTS

4.3.1 ZN-EXAFS

The Zn-EXAFS of the WT hCCS (Figure 4.2) has a first shell that fits best with 3 Cu-His and 2 O/N (non-His) around 2 Å. The outer shell peaks seen in the Fourier transform at about 3 Å and 4 Å are typical for histidine residues and arise from the multiple scattering contributions of δ- and γ-nitrogens and carbons. Simulations of these multiple scattering peaks in the Fourier transform fit best for 3 histidine residues at 1.98Å. The fit is further improved with the addition of two O/N single scatterers to the first shell. If the Zn is bound in the conserved SOD metal binding site in domain II, one of the extra O/N scatterers would most certainly be the aspartate residue seen in this site. This fit agrees with previously seen results for the Zn-EXAFS of SOD [Blackburn et al. 1983; Blackburn et al. 1984], and therefore suggests that hCCS binds a single zinc ion in one of the conserved metal binding sites of domain II. This would also agree with the crystal structure of the truncated domain II-only hCCS, which also saw a single zinc ion bound to domain II of hCCS (Figure 4.1) [Lamb et al. 2000].

The number of zinc ions bound changed very little between wild type hCCS and the mutant C22/25S, the only other sample Zn-EXAFS was performed on. Although, the signal to noise ratio on this sample was poor (Figure 4.3), it can still be fit as a three histidine and one O/N site. These results and the unaltered zinc binding ratios suggest that zinc binding is unchanged between the wildtype protein and the mutant. Zinc may play a role in the activity of CCS, most likely as a structural site, or the binding could be adventitious, but the role of zinc was not further explored in these studies.

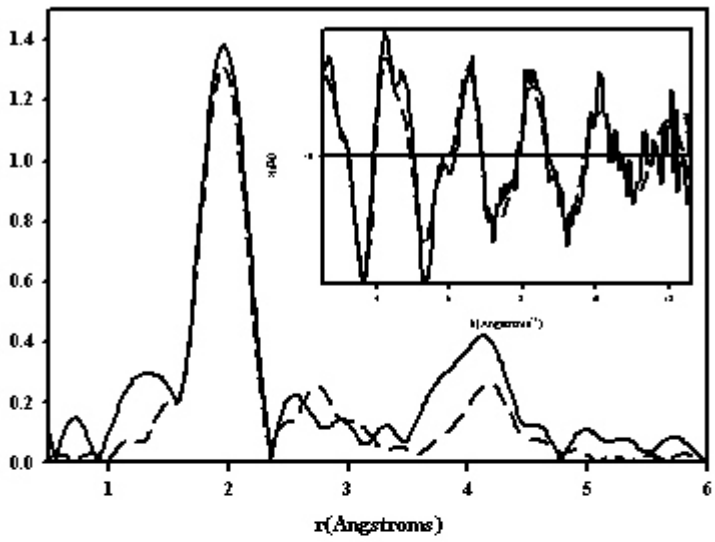

A) E_0 = -5.47 F = 0.00063

First Shell[a]				Outer Shells			
Shell (X)	R(Å)	δ^2 (Å^2)		Shell(Y)	R(Å)	∠Cu-X-Y (deg)	δ^2 (Å^2)
3 N/O	1.986	0.007		3 C_β	2.807	119.1	0.010
1 N/O	2.001	0.005		3 C_β	2.982	119.5	0.010
				3 N_γ	4.180	159.7	0.010
				3 C_γ	4.208	159.9	0.010

B) E_0 = -6.10 F = 0.00054

First Shell[a]				Outer Shells			
Shell (X)	R(Å)	δ^2 (Å^2)		Shell(Y)	R(Å)	∠Cu-X-Y (deg)	δ^2 (Å^2)
3 N/O	1.958	0.006		3 C_β	2.850	118.9	0.010
2 N/O	2.027	0.003		3 C_β	3.002	119.3	0.010
				3 N_γ	4.190	159.5	0.015
				3 C_γ	4.228	161.1	0.015

[a]Errors in distance are ±0.002Å for the first shell and ±0.005Å for the outer shells. The given errors for the coordination numbers are ±25 %.

Figure 4.2: The experimental (-) and theoretical (--) Fourier transform and Zn-EXAFS (inset) of the wildtype hCCS. The parameters for the fit are listed in the table, section A.

4.3.2 CU-EXAFS

The Fourier Transform of the Cu-EXAFS of the WT hCCS shows two shells, a large first shell at around 2.25 Å and a second outer shell at around 2.72 Å (Figure 4.4). The previous parameters used on the DTT reduced and the dithionite reduced samples from the

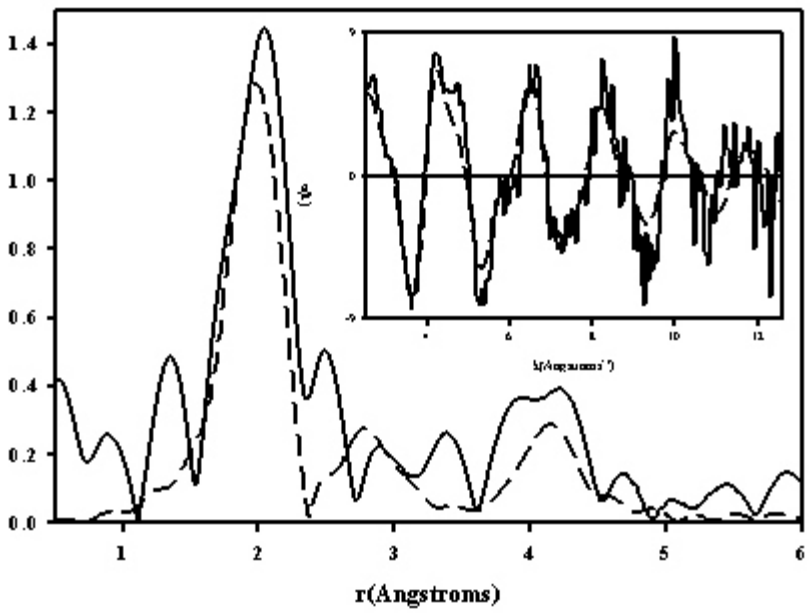

E_0 = -5.40 F = 0.00123

First Shell[a]			Outer Shells			
Shell (X)	R(Å)	δ^2 (Å^2)	Shell(Y)	R(Å)	∠Cu-X-Y (deg)	δ^2 (Å^2)
3 N/O	2.027	0.002	3 C_β	2.813	118.6	0.010
1 N/O	1.889	0.002	3 C_β	2.969	117.8	0.010
			3 N_γ	4.175	159.8	0.010
			3 C_γ	4.198	159.4	0.010

[a]Errors in distance are ±0.002Å for the first shell and ±0.005Å for the outer shells. The given errors for the coordination numbers are ± 25%.

Figure 4.3: The experimental (-) and theoretical (--) Fourier Transform and Zn-EXAFS (inset) of the C22/25S hCCS sample. The parameters used for the fit are listed in the table.

last study on hCCS gave a reasonable fit for this new data as well, with the first shell containing 3 Cu-S at 2.26 Å and the second shell consisting of a Cu-Cu at 2.71 Å. The Cu-EXAFS of the wild type hCCS showed the expected distances for both the Cu – S shell and the Cu –Cu shell that has been seen previously for trigonal copper thiolate clusters [Pickering et al. 1993]. A better fit for the data can be obtained when the number of coppers in the second shell is reduced from 1 to 0.5, however in this case even though the F-Value for the fit is better, the Debye-Waller factor is slightly lower than expected for the second shell feature.

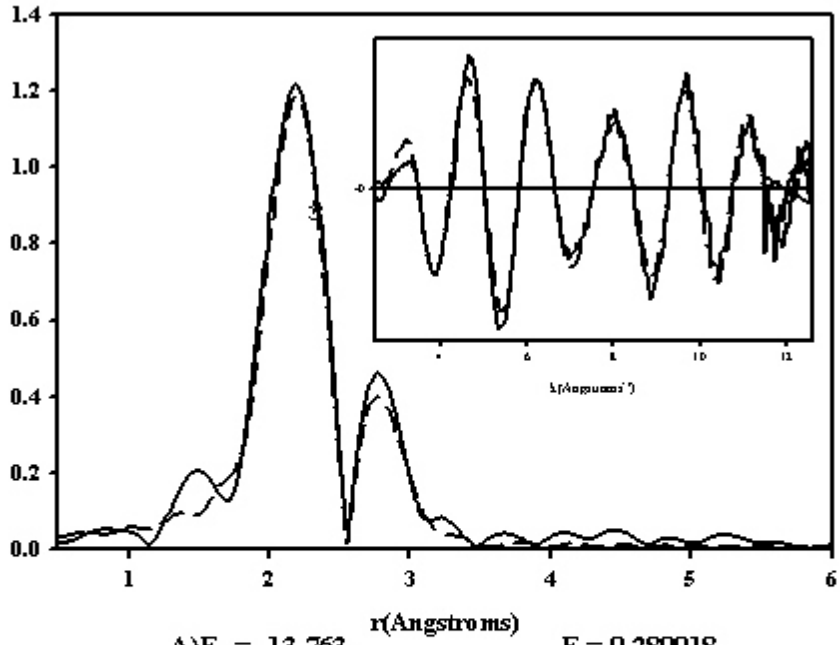

A) E_0 = -13.763 F = 0.280918

Shell(X)[a]	R(Å)	δ^2(Å^2)
3.1 S	2.245	0.0066
0.9 Cu	2.727	0.0051

B) E_0 = -14.630 F = 0.261524

Shell (X)[a]	R(Å)	δ^2(Å^2)
3.1 S	2.240	0.0067
0.5 Cu	2.723	0.0013

[a]Errors in distance are ±0.002Å for the first shell and ±0.005Å for the outer shells. The given errors for the coordination numbers are ±25%.

Figure 4.4: The experimental (-) and theoretical (--) Fourier Transform and Cu-EXAFS of the wildtype hCCS. The parameters used for the fit are listed in the table, section A.

The Cu-EXAFS of the single cysteine to serine mutants remains comparable to that of the wild type. In the C22S mutant, the parameters used for the best fit of the wild type data, a Cu-S shell (N=3) at 2.24 Å and a Cu-Cu shell (N=1) at 2.73 Å, give very good results for the mutant data as well (Figure 4.5). But it is also possible to achieve a reasonable fit by reducing the sulfur shell to N=2.5 and adding Cu-O (n=0.5) at 2.06 Å. The presence of the second shell in the single mutant shows that a single mutation of a cysteine to a serine is not enough to disrupt a binuclear copper cluster, as has been seen previously in studies of the COX17 copper chaperone [Heaton et al. 2001]. The improved fit with less sulfur in the

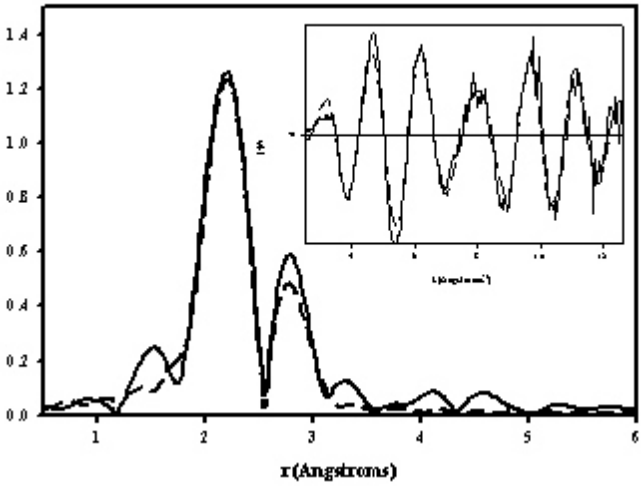

A) E_0 = -14.556 F = 0.307106

Shell(X)[a]	R(Å)	δ^2 (Å^2)
3.2 S	2.249	0.0065
0.9 Cu	2.720	0.0036

B) E_0 = -9.631 F = 0.293524

Shell(X)	R(Å)	δ^2 (Å^2)
2.0 S	2.279	0.0049
0.9 O	2.059	0.0008
1.0 Cu	2.736	0.0044

C) E0 = -12.263 F = 0.295205

Shell(X)	R(Å)	δ^2 (Å^2)
2.5 S	2.262	0.0055
0.6 O	2.05	0.0015
1.0 Cu	2.727	0.0045

[a]Errors in distance are ±0.002Å for the first shell and ±0.005Å for the outer shells. The give nerrors for the coordination numbers are ±25 %.

Figure 4.5: The experimental (-) and theoretical (--) Fourier Transform and Cu-EXAFS (inset) of the C22S mutant of hCCS. The parameters used for the fit are in the table, section A.

first shell and the addition of an oxygen scatterer could be explained by either serine replacing a cysteine residue within the cluster; or the omission of the mutated residue from the cluster and the introduction of a solvent molecule. The C244S mutant Cu-EXAFS is almost identical to that of the C22S mutant (Figure 4.6), and there is seemingly no change in the Cu environment from that of wild type, as the parameters for the best fit of the wild type Cu-EXAFS data work just as well on the C244S data. But again, a slightly better fit is obtained when half an oxygen is add at 2.06 Å and the Cu-S shell is reduced to 2.5.

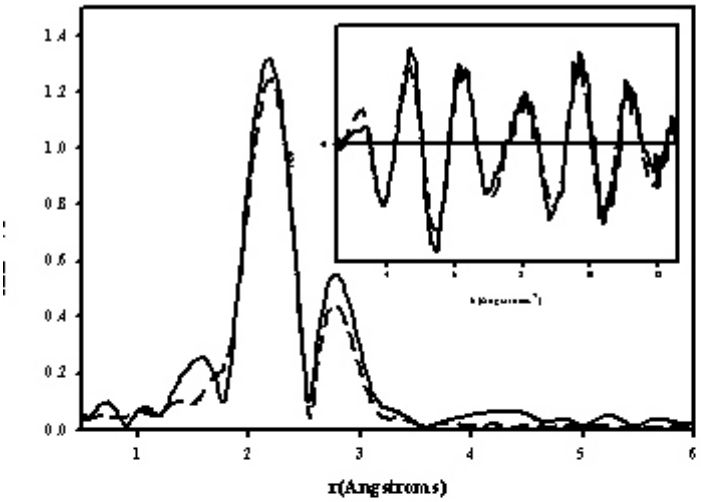

	A) E_0 = -3.91	F = 0.00055
Shell(X)[a]	R(Å)	δ^2 (Å^2)
3.0 S	2.251	0.0010
1.0 Cu	2.706	0.0010

	B) E_0 = -6.13	F = 0.00049
Shell(X)	R(Å)	δ^2 (Å^2)
2.5 S	2.262	0.0009
0.5 O	2.055	0.0001
1.0 Cu	2.715	0.0008

	C) E0= -8.51	F = 0.00053
Shell(X)	R(Å)	δ^2 (Å^2)
2.0 S	2.277	0.0008
1.0 O	2.057	0.0001
1.0 Cu	2.725	0.0009

[a]Errors in distance are ±0.002Å for the first shell and ±0.005Å for the outer shells. The given errors for the coordination numbers are ±25%.

Figure 4.6: The experimental (-) and theoretical (--) Fourier Transform and Cu-EXAFS (inset) of the C244S sample. The parameters used for the fit are listed in the table, section A.

The domain III double mutant, C244/246S, is the only mutant to show a loss of the second shell feature. The Fourier transform of C244/246S shows a single peak centered around 2.20 Å. The best fit for the EXAFS spectrum is a split first shell of Cu-S (n=2) at 2.24 Å and Cu-O (n=1) at 2.04 Å (Figure 4.7). This shows that the copper cluster is located exclusively in the domain III region of hCCS and, although an intramolecular cluster between domain I and domain III may be possible, the intermolecular cluster between two domain III motifs from different hCCS monomers is the dominate form of the cluster.

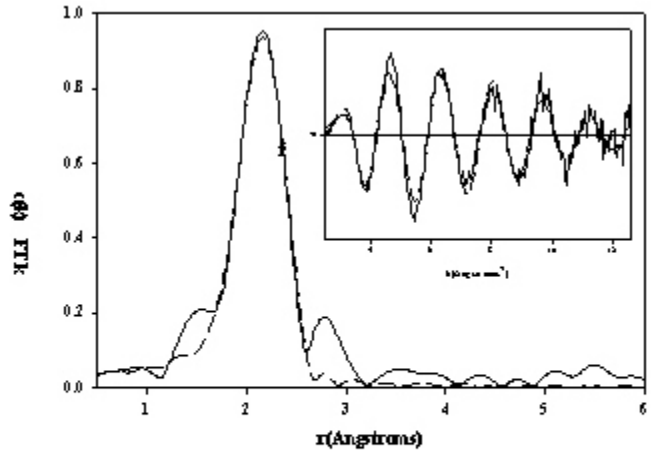

E_0 = -10.093 F = 0.394284

Shell(X)[a]	R(Å)	δ^2 (Å^2)
1.9 S	2.244	0.0072
1.0 O	2.043	0.0061

[a]Errors in distance are ±0.002Å for the first shell and ±0.005Å for the outer shells. The given errors for the coordination numbers are ±25 %.

Figure 4.7: The experimental (-) and theoretical (--) Fourier Transform and Cu-EXAFS (inset) of the C244/246S sample. The parameters used for the fit are listed in the table, section A.

The domain I double mutant (C22/25S) also has a large second shell feature showing that the copper cluster is still present in this mutant. The best fit obtained for its Cu-EXAFS was a first shell of Cu-S (n=3) at 2.24 Å and a second shell of Cu-Cu at 2.72 Å (Figure 4.8). The largest difference between Cu-EXAFS of the wild type hCCS and C22/25S is a drop in the Debye-Waller factor of the second shell copper in the C22/25S mutant. The Debye-Waller factor for the wild type fit with one Cu-Cu at 2.72 for the second shell is 0.0051, however in C22/25S this factor drops to 0.0013. When the amount of Cu-Cu scatter in the wild type fit is reduced to an n=0.5, the Debye-Waller factors of the wild type drops to 0.0013 Å^2, the value seen in the double mutant.

The better fit resulting from a lower amount of copper in the second shell of the wild type hCCS could be explained as the EXAFS data being an average of two sites: an intermolecular complex between two domain III metal binding regions of two separate hCCS monomers and a second copper site in domain I existing as a single trigonal copper site (Figure 4.9). With three sulfur atoms and one copper from the domain III site, and two

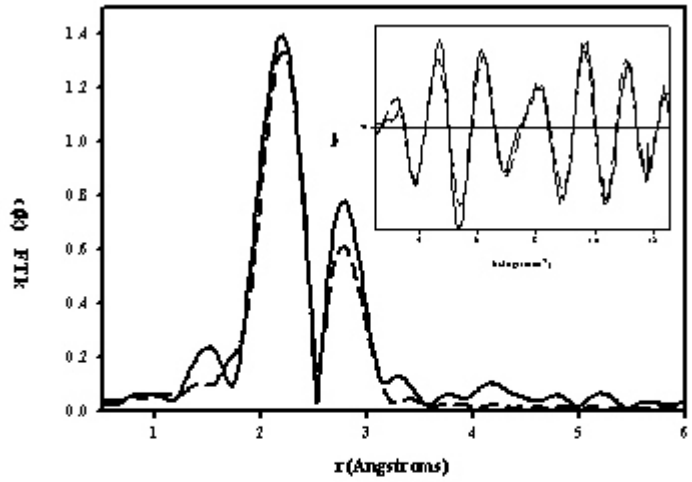

E_0 = -15.481 F = 0.282147

Shell (X)[a]	R(Å)	δ^2 (Å^2)
3.3 S	2.244	0.0061
0.9 Cu	2.722	0.0013

[a]Errors in distance are ±0.002Å for the first shell and ±0.005Å for the outer shells. The given errors for the coordination numbers are ±25 %.

Figure 4.8: The experimental (-) and theoretical (--) Fourier Transform and Cu-EXAFS (inset) of the C22/25S samples. The parameters used for the fit are listed in the table.

sulfur atoms and one oxygen from the domain I site, this would give an average ligand environment for copper as 2.5 sulfur, 0.5 oxygen and 0.5 copper scatterers. This is a valid model as the double mutants studied show that domain III seems to be the center for the copper cluster while domain I is a single three coordinate copper site. Attempts to model this scenario show that dropping the amount of copper in the second shell of the wildtype EXAFS results in a better fit, but adding a small amount of oxygen to the first shell did not produce as good of a fit as leaving the shell comprised solely of sulfur. The reduced amount of copper in the second shell does give a lower Debye-Waller factor than would be expected for a high Z scatterer in the second shell, but this could be explained by increased rigidity of the complex, i.e. very little variance between the Cu-Cu distance between clusters. But it could be argued that one would expect to see the same drop in the Debye-Waller factors for the sulfur shell as well. However, the sulfur shell is comprised of both bridging and terminal ligands which could have different distances and therefore show a higher Debye

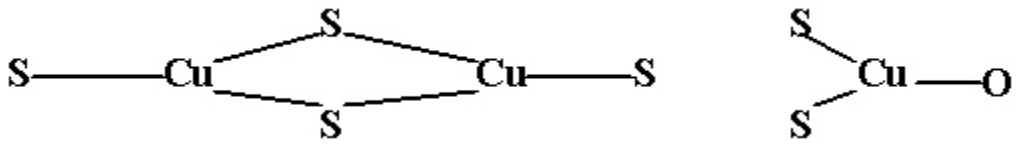

Figure 4.9: The two copper sites possible in hCCS. The binuclear copper sulfur cluster and the single trigonal site seen the in the C22/25S and C244/246S mutants, respectively.

Waller factor. Three-coordinate binuclear copper-sulfur clusters are rare and there are no examples of models of them in the Cambridge structural database, therefore it is difficult to cite the expected parameters for such a cluster. But in this case given the extensive data we have collected on the copper to protein ratios and the Cu-EXAFS data on the mutants, the model of a single copper site in domain I and dinuclear μ_2-cysteinyl-bridged copper cluster in domain III is the best model for all of the data collected[2].

4.3.3 COPPER X-RAY ABSORPTION EDGE

The edge data of all of the mutants and the wild type hCCS appears as a typical edge spectrum for trigonal copper-thiolate species [Pickering et al. 1993; Ralle et al. 2003]. There is no 8978 eV feature, which is seen in Cu(II) spectra due to the 1s → 3d transition. The edge is at 8980 eV which is the expected edge energy for Cu(I) species and slightly lower than what would be expected for Cu(II). All of the spectra show an edge feature at 8983 eV which is characteristic of Cu(I) species and has been assigned to the 1s → 4p transitions [Kau et al. 1987]. The most noticeable difference between the edge spectra of

---

[2] The Cu-EXAFS data could also be fit with the addition of multiple coppers to the second shell, increasing the Cu-Cu N>1. This would increase the Debye-Waller factor to a higher value which would be expected for a high Z scatterer in the second shell. Also multi-nuclear copper sulfur clusters containing more than two copper ions are far more common in the literature as model compounds. Therefore, the argument could be made for modeling the copper cluster in hCCS with more than two coppers. However, it was felt that this model did not sufficiently explain the copper to protein ratios seen with hCCS taking into account that there is a copper present in domain I, which the EXAFS data confirms.

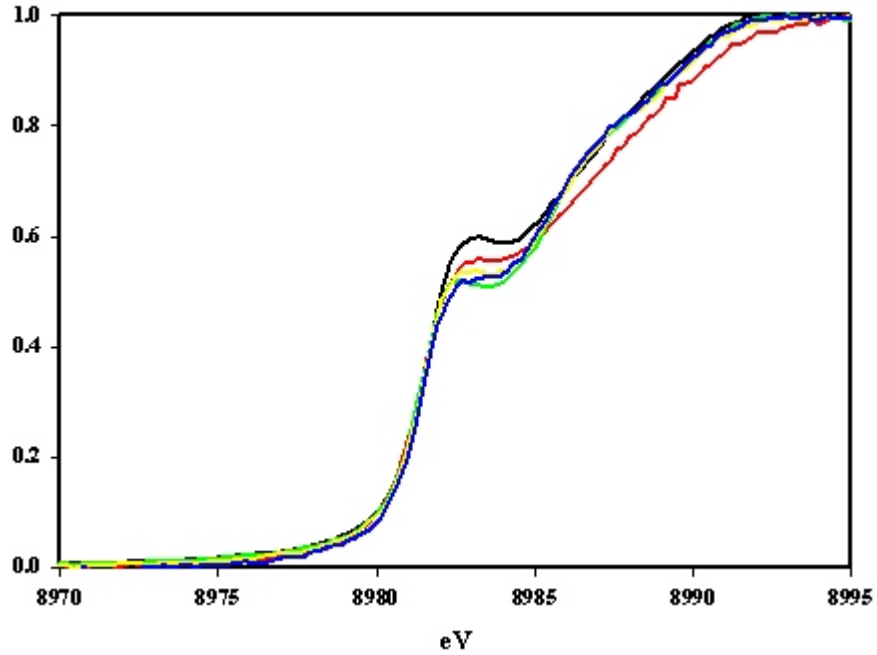

Figure 4.10: The edge data comparison of the wildtype hCCS (black), with the mutants: C22/25S (red), C244S (yellow), C22S (blue) and C244/246S (green).

all of the hCCS constructs is that the C22S, C244S and C244/246S variants have a slightly reduced edge feature when compared to the wild type or the C22/25S mutant (Figure 4.10). This could be explained by the fact that C22S, C244S and C244/246S all fit better with the oxygen scatterer present in the first shell. The fact that oxygen as a ligand reduces the edge feature in comparison to sulfur has been seen previously, because the copper-oxygen bond is less covalent than a copper sulfur bond [Pickering et al. 1993].

4.4 ACTIVITIES OF WILD TYPE AND MUTANT HUMAN COPPER CHAPERONE TO SUPEROXIDE DISMUTASE TRANSFER OF COPPER TO HUMAN SUPEROXIDE DISMUTASE

The activity of CCS is expressed as the SOD activity (in units per mg) that is obtained for a sample of apo-SOD after incubation with CCS, where a unit of SOD activity is defined as the amount of SOD needed to reduce by half, the oxidation of cytochrome *c*

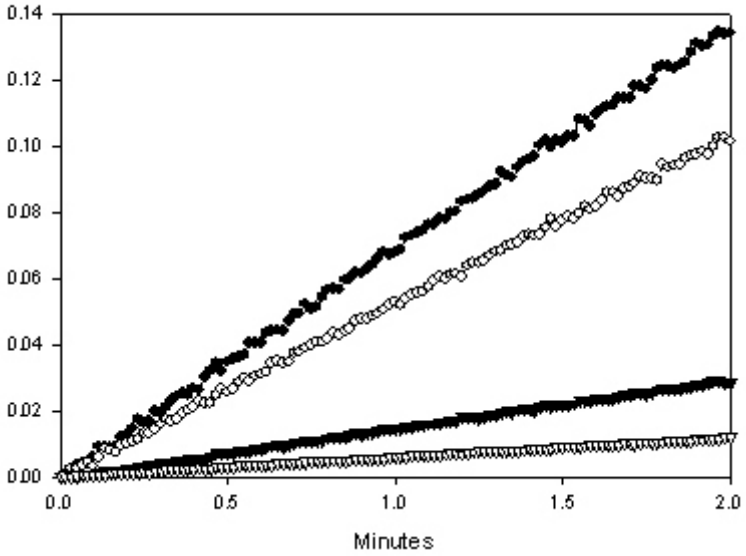

Figure 4.11: The ΔABS at 419 nm for the xanthine oxidase assay containing cytochrome *c* (●) with the addition of apo-SOD (○), SOD reconsitituted by incubation with CCS (▽), or SOD reconstituted by dialysis agianst copper containing buffer (▼).

by superoxide anion generated by the conversion of xanthine to urate by xanthine oxidase, under given conditions [McCord et al. 1969]. Figure 4.11 shows an example of the change at OD_{419}, following the conversion of reduced to oxidized cytochrome *c*, in a typical activity assay. When the ratio of hCCS to SOD in the incubation mixture was increased from 0.25 CCS:SOD to 3 CCS:SOD, the activity maximum was reached at a equimolar ratio of 1 hCCS molecule and 1 SOD molecule. If both coppers from CCS were transferring to SOD, the expected ratio would be 1 hCCS to 2 hSOD since there are two coppers per hCCS monomer but only one copper per SOD monomer. Therefore, although CCS can bind two coppers, it only transfers one of those coppers to SOD.

The wild type CCS when incubated 1:1 CCS to SOD was able to restore 1276 units of activity per mg to apo-SOD (Table 4.2), 91% of the activity of SOD after dialysis against aqueous copper (1400 units/mg). When the time of incubation of hCCS with SOD was varied, it was seen that SOD reached its maximum activity before 5 minutes. Incubation with the domain I double mutant, C22/25S, reduced the SOD activity to 76% of wild type

Table 4.2: The activities of wildtype hCCS and its mutants.

Protein	Units/mg of SOD[a]	N	%Activity[b]
Wild Type	1276 ± 74	12	100
C22S	1056 ± 47	5	83
C244S	1110 ± 86	4	87
C222S	964 ± 61	4	76
C244246S	223 ± 56	2	17

[a]Units/mg of hSOD activated after incubation with hCCS above that measured in an apo-SOD control. [b]% Activity assuming that wild type CCS is 100% active.

CCS with an activity of 964 mg/units. Both increasing the incubation time and concentration of the mutant incubated with SOD had little effect on the activity of this mutant. It is possible that the reduced activity shows that domain I, while not directly involved in transfer of copper to SOD, could play some important structural or regulatory role. Therefore, the inability of this mutant to bind copper in domain I causes a reduced activity compared to wildtype. The only mutant with greatly reduced activity was the domain III double mutant, C244/246S. It was only able to restore 17 percent of the activity to SOD. This shows that domain III is the site of copper transfer to SOD consistent with the previous work [Lamb et al. 2001; Rae et al. 2001; Furukawa et al. 2004].

The activity of SOD incubated with the C22S CCS mutant is about 33 percent that of wild type, at a concentration ratio of 1 CCS: 1 SOD and an incubation time of 15 minutes. Increasing the concentration of C22S CCS that was incubated with apo-SOD increased the activity until a maximum was reached at an 8:1 ratio of C22S CCS to apo-SOD. Under these conditions incubation at 15 mins gave an SOD activity of 1056 units/mg, about 83% of wild type activity. Keeping the ratio of C22S CCS and apo-SOD at 1:1 and increasing the incubation time had no effect on maximum activity. Since concentration changes effect the activity while changes in incubation time do not, this suggests that the decreased activity seen in this mutant is an equilibrium effect rather than a kinetic one.

When the other single mutant, C244S, was incubated with apo-SOD under standard conditions, it showed an activity of about 31% wild type, thus behaving similarly to the C22S mutant. Increased incubation time had little effect on C244S CCS, but again increasing the concentration of the C244S mutant eight times in the incubation mixture

increased the activity of SOD to about 87% that of wild type (1110 units/mg). The results of the single mutants are puzzling: the C25S and C244S mutants seem to show a very similar activity profile, even though they contain mutations in different domains. This result could be explained if hCCS is able to form two types of copper clusters: an intramolecular cluster, between domain I and domain III, and an intermolecular cluster, between two domain III metal binding regions. If the mutation of a cysteine in the cluster to serine did not disrupt the copper complex, but did inhibit the ability of hCCS to interconvert between these two complexes, then only the percentage of the population of hCCS that was in the domain III – domain III complex form would be active, as the C244/246S mutant suggests that this is the active species. Therefore, the only way to rescue the activity would be to increase the concentration of hCCS until the concentration of the hCCS, in the domain III – domain III form was equal to that of the concentration of SOD. Therefore, it appears that hCCS in its native form is in equilibrium between two states; one involves a copper cluster formed between domain I and domain III, the other has a single copper site in domain I and a copper cluster formed between two domain III from two different CCS proteins.

4.5 CONCLUSIONS

The most relevant data in these studies are those pertaining to the double mutants, C244/246S and C22/25S. In these variants we see that the formation of the cluster appears to be confined to the domain III copper-binding motif. Removal of the metal binding site in domain I, by mutation, has no effect upon the formation of copper cluster or upon the activity of hCCS. However, removal of the domain III binding site, by mutation, does disrupt the formation of copper cluster and severely reduces the activity of hCCS. These results implicate the domain III copper-binding motif as the focal point of the copper cluster and suggest that formation of the copper cluster is important for the activity of hCCS.

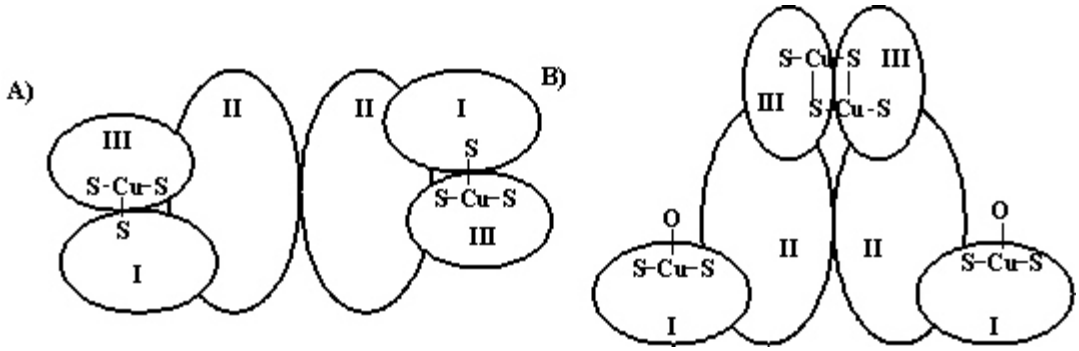

Figure 4.12: Comparison of the proposed form of hCCS that transfer copper to hSOD in the heterodimer mechanism (A) and the form of hCCS that transfer copper to hSOD proposed by the results of this chapter (B).

In the last chapter we elucidated the heterodimer mechanism introduced in section 1.4 of this thesis, by changing the perception that the active form in hCCS is copper bound in a single three-coordinate copper site formed between the copper-binding motifs of domain I and domain III, to an active form of hCCS that contains a binuclear copper cluster formed between the copper-binding motifs of domain I and domain III. The results from this current chapter suggest that we must again change this view, so that the current hypothesis of the active form of hCCS that transfers copper to hSOD is a dimer that forms a copper cluster between the two domain III copper binding motifs of different hCCS monomers.

CHAPTER 5
OLIGOMERIZATION STATES AND COPPER-SULFUR CLUSTER FORMATION IN THE HUMAN COPPER CHAPERONE FOR SUPEROXIDE DISMUTASE

5.1 INTRODUCTION

The previous studies on hCCS where done on the hCCS-maltose binding protein fusion construct. Although these studies on this expression system began to give us insight into the copper binding sites and activity of the protein, this expression system was limited by the large affinity tag attached to the expressed protein. This tag hindered our ability to perform gel filtration studies and assess the oligomerization states of the protein. Also, the mutation of cysteine to serine did not fully knock out activity of the protein or the formation of the copper cluster in most of the mutants studied. We decided to try a new expression system for hCCS that would eliminate the tag attached to the target protein and also to construct cysteine to alanine mutations which should serve better to elucidate the important residues for copper binding.

The intein expression system from New England Biolabs was chosen because it is designed to leave no affinity tag on the target protein [Chong et al. 1997]. Constructs for the wild type and the 243I truncation mutant were made by Dr. Michiko Nanako of the Department of Environmental and Biomolecular Systems of the Oregon Graduate Institute School of Science and Engineering at the Oregon Health and Science

University. This truncation mutant contains only domains I and II of hCCS and terminates right before the CXC motif of domain III. Cysteine to alanine mutants were made by Mary Mayfeild-Gambill of the Blackburn laboratory of the Department of Environmental and Biomolecular Systems of the Oregon Graduate Institute School of Science and Engineering at the Oregon Health and Science University. These mutants include the single mutants, C22A, C25A, C244A and C246A as well as the double mutants, C22/25A and C244/246A.

5.2 WILD TYPE HUMAN COPPER CHAPERONE FOR SUPEROXIDE DISMUTASE AND ITS CYSTEINE TO ALANINE MUTANTS

5.2.1 ACTIVITY AND METAL BINDING

The hCCS-intein construct purified with roughly 2 copper and one zinc ions per protein molecule (ratios of 1.81 and 1.02, respectively, Table 5.1). This behavior is similar to the wild type-hCCS/MBP construct which purified with 1.85 coppers and 0.95 zincs per protein molecule. With respect to copper binding, all of the cysteine to alanine mutants (single and double) behaved uniformly, binding one copper to protein (Table 5.1). The mutants can be separated by their interactions with zinc. Both of the double mutants (C22/25A and C244/246A) show no change in zinc binding with respect to that of wild type, retaining a ratio of one zinc ion per protein molecule. However, the single mutants did show altered zinc binding characteristics. The C22A and C246A mutants show reduced zinc occupancy with about 0.5 zinc ions per protein, while the C244A and C25A mutants show increased zinc occupancy with binding at 1.5 zinc ions per protein molecule.

It is interesting that this effect on zinc binding is not contained within a single domain of the protein: mutation of one of the cysteines from each of the binding sites yields a protein with increased affinity for zinc, while mutating the other cysteine results in a protein with reduced affinity for zinc. In both domain I and III, it is the mutation of the cysteine closest to domain II that shows increased affinity, while mutation of the

Table 5.1: The metal binding ratios of hCCS and its cysteine to alanine mutants

Protein	Cu/P	95%Con	N	Zn/P	95%Con	N
Wild Type	1.81	0.132	10	1.02	0.057	8
C22A	0.95	0.023	5	0.43	0.051	5
C25A	1.08	0.145	5	1.54	0.289	5
C244A	0.95	0.148	5	1.63	0.330	5
C246A	0.76	0.113	6	0.45	0.051	5
C2225A	0.99	0.057	3	0.89	0.116	3
C244246A	0.87	0.123	3	0.95	0.129	3

cysteine furthest from domain II shows decreased affinity. It is possible that the altered zinc binding is a sign of interdomain communication such that the changes in domain I and III brought on by the mutation to alanine are affecting the metal binding abilities of domain II. It is unknown whether these changes are due to the presence of a free thiol in domain I and III or if they are brought on by structural changes to the protein caused by the mutations. It is also not known whether or not these findings are artifactual or if they have any biological relevance.

The activity of the wild type hCCS-intein construct is slightly higher than the hCCS-MBP construct (1800 units/mg compared to 1300 units per mg). This could be explained by the loss of the affinity tag on domain I, which is present in the MBP constructs but not the hCCS/intein construct. Unlike the MBP constructs in which the single mutants still showed activity and only the C244/246S double mutant lost activity, all the hCCS domain III alanine mutants, single and double, lost activity. The domain I mutants suffer a minimal loss of activity, which is in agreement with the previous work with the MBP constructs (Table 5.2).

Table 5.2 The activities of hCCS and its cysteine to alanine mutants

Protein	Units/mg of SOD[a]	N	%Activity[b]
Wild Type	1865 ± 74	10	100
C22A	1585 ± 110	4	85
C25A	1764 ± 68	4	95
C224A	134 ± 29	4	8
C246A	172 ± 42	4	9
C22/25A	1657 ± 64	3	89
C244/246A	153 ± 25	3	8

[a]Units/mg of hSOD activated after incubation with hCCS above that measured in an apo-SOD control. [b]% Activity assuming that wild type CCS is 100% active.

The results of the metal binding studies and activity measurement seem to support the hypothesis that the domain III metal binding site is the site of metal transfer to SOD [Schmidt et al. 1999]. It also shows that copper binding to domain I is not necessary for transfer to SOD.

5.2.2 OLIGOMERIZATION STATES

The SDS-PAGE gels of wild type hCCS and its alanine mutants all show a single band at 36 kD, whether or not β-mercaptoethanol was added to the loading buffer. This indicates that the higher oligomerization states of hCCS are not cross-linked by disulfide bonds. In some more concentrated samples a second band is seen at around 72 kD. It is possible that this band is a dimer of hCCS as dimers of SOD are known to be resistant to many forms of denaturation [Lepock et al. 1985], but assignment to a contaminant or low levels of the full length CCS-intein construct could not be ruled out.

Further studies were done using gel filtration HPLC to determine the oligomerization states of hCCS. The first samples compared were the apoprotein and metal loaded wild type hCCS. The metal loaded hCCS sample elutes as both dimer and

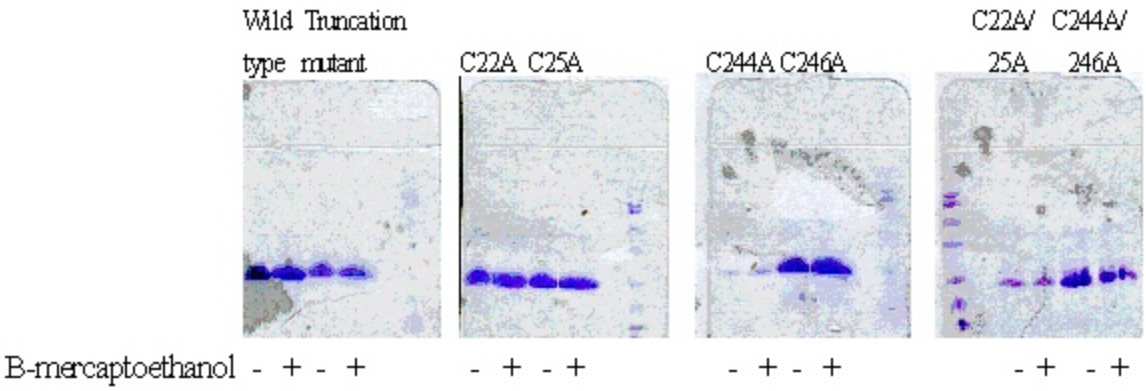

Figure 5.1: SDS-PAGE of hCCS, the 243I truncation mutant and the cysteine to alanine mutants with and without mercaptoethanol

tetramer; however the apo form of the protein elutes only as a dimer (Figure 5.2). The presence of a tetramer in the metal loaded form of the protein means that there must be two possible oligomerization interfaces in hCCS. It is assumed that one of the oligomerization interfaces is the conserved SOD-like dimer interface. If this interface behaves the same as the interface in SOD the formation of an oligomer through this interface would be independent of metal binding in the protein. The presence of tetramer in the metal loaded form of the protein but not in the apo form suggests that there is a second oligomerization interface that is dependent on metal binding. Whether the interface contains the copper cluster seen in our previous studies or an interface that is exposed after copper binding is unknown.

All of the domain III mutants (C244A, C246A, and C244/246A) exhibit a gel filtration profile similar to that of apo protein, i.e. they elute only as dimers. The domain I mutants (C22A, C25A and C22/25A) show a gel filtration elution profile similar to the metal loaded form of the wild type protein, but with more intensity in the tetramer peak. Assuming the oligomerization site in hCCS is in domain III, it is likely that the copper cluster is involved, but other residues may play a role in the interaction.

A comparison of the sequence of hCCS and extracellular SOD (EC-SOD) - a known tetrameric form of SOD - shows some sequence similarity. Although there is no crystal structure of EC-SOD, mutation studies have identified residues important for tetramer formation in EC-SOD [Stenlund et al. 1997]. At the N-terminus of EC-SOD,

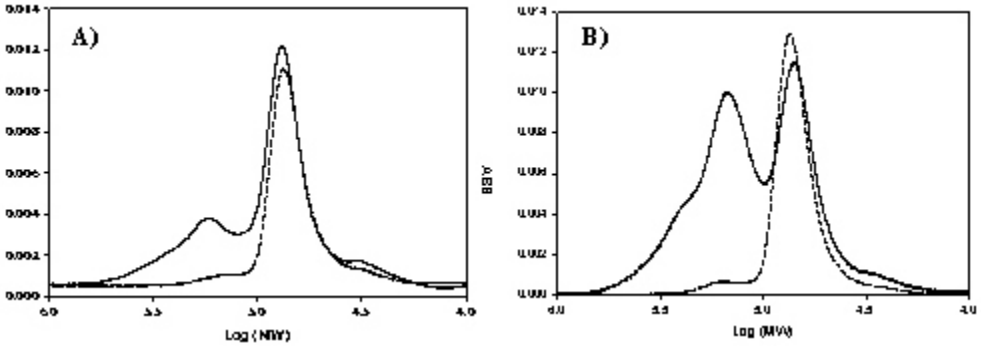

Figure 5.2: Gel filtration HPLC of apo-hCCS (–) and copper loaded hCCS (-) (A) and gel filtration HPLC of a copper loaded domain I mutant, C22/25A (-) and a copper loaded domain III mutant, C244/246A (--) (B).

there is a hydrophobic α-helix and in the C-terminal region of the protein there is a cysteine residue that is known to form a disulfide bond between two EC-SOD subunits [Oury et al. 1996; Stenlund et al. 1999]. Five residues upstream from the cysteine residue is a tryptophan residue that, when mutated, causes EC-SOD to lose the ability to form tetramers. Although the exact interactions are unknown, it is thought that in EC-SOD a dimer is formed through the conserved SOD dimer interface; and the tetramer is formed by a disulfide bond between the cysteine in C-terminal tail, and this interaction is further stabilized by hydrophobic interactions between the tryptophan and the hydrophobic α-helix. The regions important for tetramer formation in EC-SOD are conserved in hCCS: there is a hydrophobic α-helix in domain I just prior to domain II. Also in domain III, four residues downstream of the CXC motif is a tryptophan in an IWEERG motif compared to EC-SOD where the tryptophan is in a LWERQA motif. If the interaction of the two CCS monomers is evaluated in what has been termed the hCCS/hSOD heterodimer crystal structure (Section 1.4) [Lamb et al. 2001], but which is actually a heterotetramer, it is seen that the WEER motif of one monomer is lined up with the hydrophobic α-helix of the domain I of the other CCS monomer. Therefore, it is possible that while the copper cluster forms part of the interface, this interaction is

strengthened by the interactions between the WEER motif and the hydrophobic α-helix. From the initial gel filtration studies we conclude that both the conserved SOD dimer interface and the copper cluster region are capable of creating higher oligomerization interactions. However, it has not been determined which is the site of dimer formation and which is the site of tetramer formation nor whether the dimer or the tetramer are the biologically relevant species that transfer copper to SOD.

5.2.3 COPPER CLUSTER FORMATION

Copper EXAFS and x-ray edge studies were carried out to determine the copper binding environment in wild type hCCS and its alanine mutants as well as to determine the amount of copper cluster formation. Initial EXAFS studies where carried out on the wild type hCCS as well as the 243I truncation mutant that ends just before the CXC motif in domain III. The wild type hCCS gave an EXAFS spectrum almost identical to that of the wild type hCCS-MBP construct reported in Chapter 4, even though the current construct is cleaved from its protein tag (Figure 5.3). The wild type protein showed 3 Cu-S at 2.25 Å and one Cu-Cu at 2.72 Å. Just like the MBP constructs, an equally good

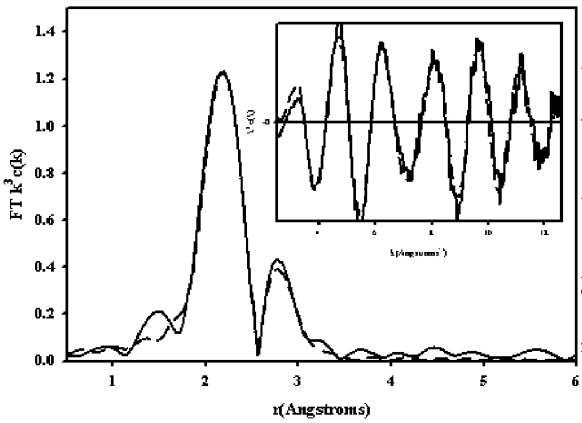

A) E_0 = -14.556 F = 0.307106

Shell (X)[a]	R(Å)	δ² (Å²)
3 S	2.248	0.010
1 Cu	2.719	0.011

B) E_0 = -9.631 F = 0.293524

Shell (X)	R(Å)	δ² (Å²)
2.5 S	2.258	0.010
0.5 O	2.035	0.001
0.5 Cu	2.720	0.004

[a]Errors in distance are ±0.002Å for the first shell and ±0.005Å for the outer shells. The given errors for the coordination numbers are ±25%.

Figure 5.3: The experimental (-) and theoretical (--) Fourier Transform and Cu-EXAFS (inset) of wildtype hCCS. The parameters used for the fit are listed in the table, section A

fit can be obtained by adding some oxygen into the first shell and reducing the amount of copper in the second shell. Therefore, the intein-hCCS, like the MBP-hCCS fusion, give results that are a combination of the two sites: the trigonal single copper site in domain I and the trigonal copper sulfur cluster in domain III.

The truncated form of CCS does not show a second shell feature in its Fourier Transform, meaning that the cluster is not present in this form of the protein. The Fourier Transform shows a single shell at around 2.2 Å (Figure 5.4). The best fit for this spectrum has three sulfurs at 2.24 Å; the second best fit has two sulfurs at 2.26 Å and one oxygen at 2.04 Å. The two sulfurs certainly come from the CXXC metal binding site in domain I, as the cysteine in domain III are not present, and the third ligand is most probably exogenous, water, if it is an oxygen molecule or if a sulfur molecule, some of the excess thiol left over from the intein purification.

The domain III mutants all behave slightly differently from the truncation mutant. Initially, the mutants purified with one copper per protein with similar metal binding behavior as the truncation mutant, but the edge data of the mutants suggest that they were not fully reduced. Cu-EXAFS of the single mutant C244A shows an EXAFS spectrum that fits well as a 3 histidine, one oxygen environment, similar to the fit one would expect for a copper bound to the conserved SOD metal binding sites in domain II. Data

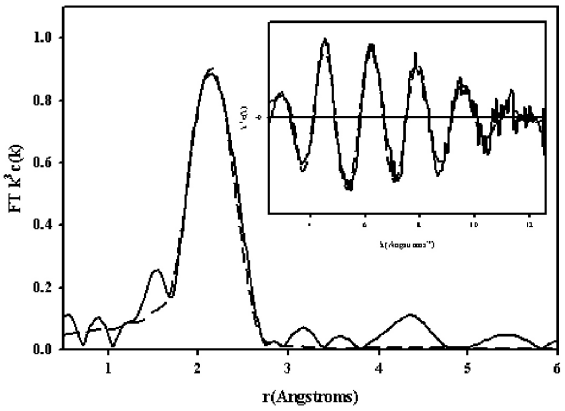

A) E_0 = -10.3		F = 0.00063
Shell (X)[a]	R(Å)	δ^2 (Å^2)
2 S	2.282	0.013
1 O	2.034	0.003

B) E_0 = -4.51		F = 0.00058
Shell (X)	R(Å)	δ^2 (Å^2)
3 S	2.242	0.015

[a]Errors in distance are ±0.002Å for the first shell and ±0.005Å for the outer shells. The given errors for the coordination numbers are ±25%.

Figure 5.4: The experimental (-) and theoretical (--) Fourier Transforms and Cu-EXAFS (inset) of the 243I truncation mutant of hCCS. The parameters used for the fit are listed in the table, section A

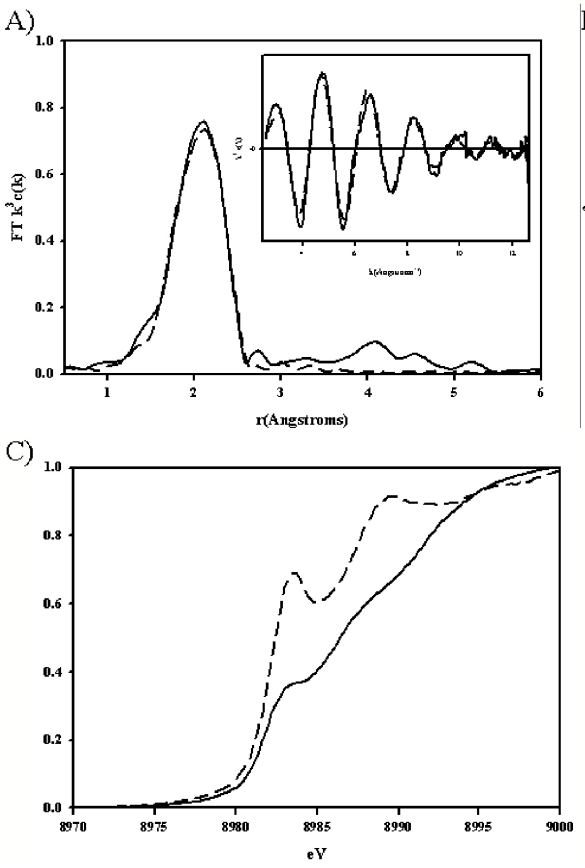

A) E_0 = -0.8 F = 0.00028

Shell (X)[a]	R(Å)	δ^2 (Å^2)
2 S	2.211	0.014
1 N	1.926	0.004

B) E_0 = -9.65 F = 0.00035

Shell (X)	R(Å)	δ^2 (Å^2)
2 S	2.253	0.004
1 O	2.025	0.001

[a]Errors in distance are ±0.002Å for the first shell and ±0.005Å for the outer shells. The given errors for the coordination numbers are ±25%.

Figure 5.5: A) The experimental (-) and theoretical (--) Fourier Transform and Cu-EXAFS (inset) of the as-purified C246A. The parameters for this fit are listed in the table, section B. B) The experimental (-) and theoretical (--) Fourier Transform and Cu-EXAFS (inset) of the reduced C246A hCCS. The parameters for this fit are listed in the table, section B. C) The edge comparison of the as-purified C246A (-) and the reduced C246A (--)

collected on the non-reduced, as-purified C246A fit best as a single mixed sulfur-nitrogen shell with either two sulfurs at 2.21 Å and one nitrogen at 1.93 Å, or 1 sulfur at 2.24 Å and 2 nitrogens 1.97 Å. Finally, the double mutant (C244/246A) yielded very poor data that, despite reasonable copper concentrations, fit best as a first shell of 2 oxygen at 2.08 Å, a sulfur at 2.33 Å, and a sulfur at 2.71 Å. This implies that there are mixed, multiple copper sites in the sample. Since we can infer from the edge data of three samples that all of the bound copper is not fully reduced, we reduced the samples both (1) at the beam line - by adding dithionite to the original samples and (2) before the EXAFS samples were made - by incorporating an additional step in the purification of

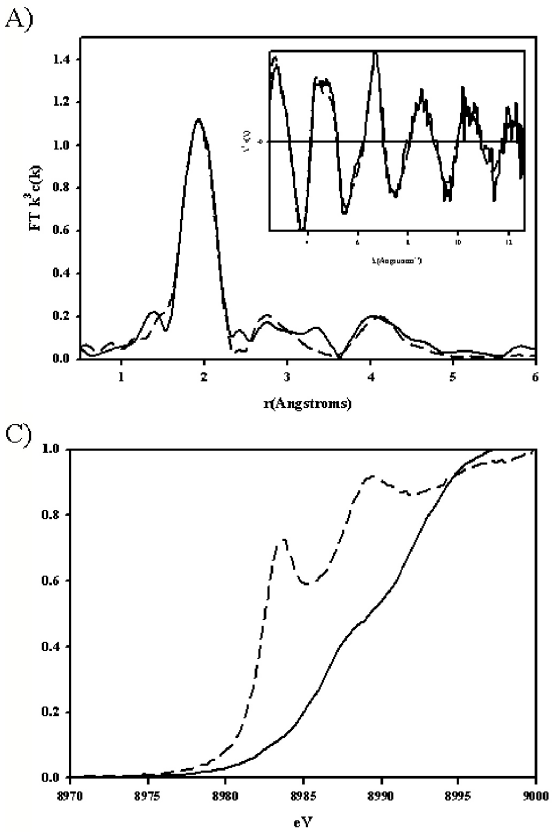

A) E_0 = -4.31 F = 0.00038

Shell (X)[a]	R(Å)	δ^2 (Å^2)
3 N (His)	1.977	0.007
1 O	1.922	0.014

B) E_0 = -9.19 F = 0.00068

Shell (X)	R(Å)	δ^2 (Å^2)
2 S	2.242	0.004
1 O	2.085	0.001

[a]Errors in distance are ±0.002Å for the first shell and ±0.005Å for the outer shells. The given errors for the coordination numbers are ±25%.

Figure 5.6: A) the experimental (-) and theoretical (--) Fourier Transform and Cu-EXAFS (inset) of the as-purified C244A. The parameters for this fit are listed in the table, section A. B) The experimental (-) and theoretical (--) Fourier Transform and Cu-EXAFS (inset) of the reduced C244A hCCS. The parameters for this fit are listed in the table, section B. C) the edge comparison of the as-purified C244A (-) and the reduced C244A (--)

the protein, reducing and dialyzing the samples before performing metal concentration analysis, activities, and EXAFS.

The reduced samples of the domain III mutants had EXAFS spectra that were similar to the truncated CCS sample. The edge data contained a large edge feature that would be expected for a fully reduced trigonal copper site and the EXAFS data fit well with the parameters for a single trigonal copper site. The data for the C244A mutant had two equally good fits; one for a two Cu-S at 2.24 Å and Cu-O at 2.09 Å and the other with three Cu-S at 2.22 Å (Figure 5.5). The reduced C246A sample had a slightly better fit of two Cu-S at 2.25 Å and one Cu-O at 2.03 Å than the fit with three Cu-S at 2.23 Å but both fits give reasonable results (Figure 5.6).

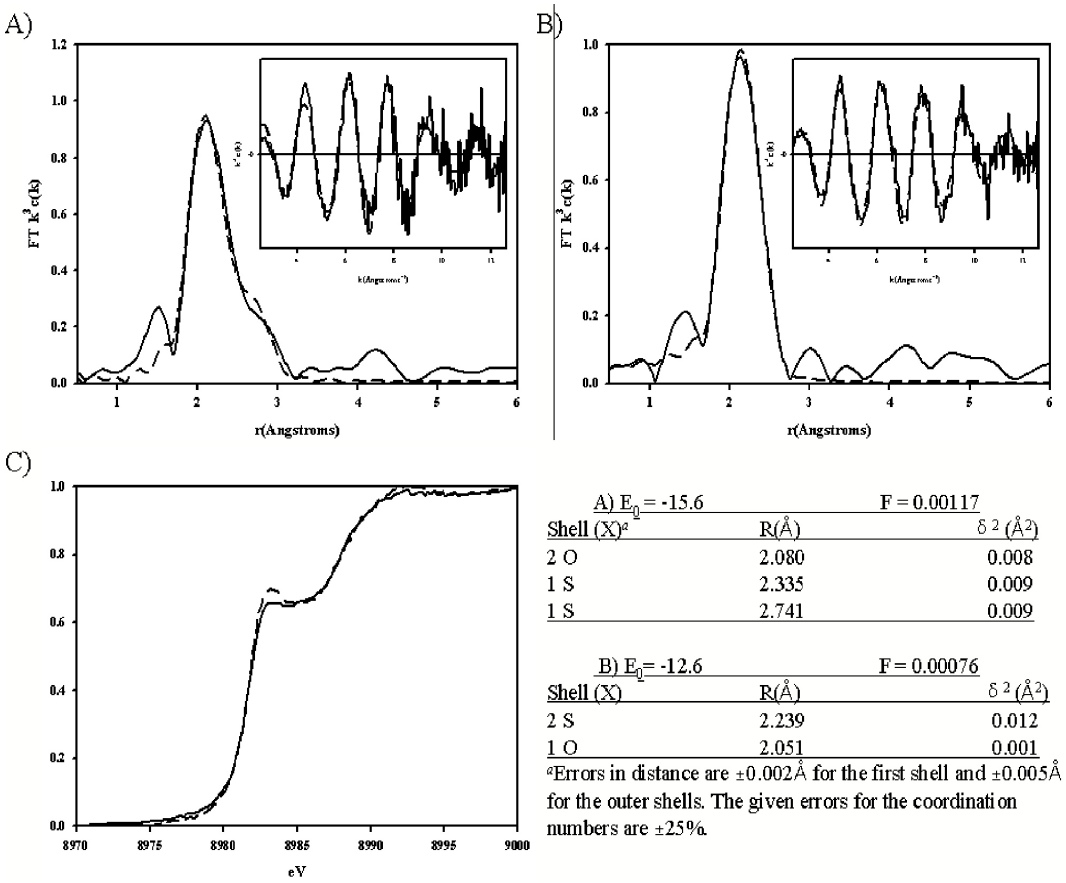

A) E_0 = -15.6 F = 0.00117

Shell (X)[a]	R(Å)	δ^2 (Å^2)
2 O	2.080	0.008
1 S	2.335	0.009
1 S	2.741	0.009

B) E_0 = -12.6 F = 0.00076

Shell (X)	R(Å)	δ^2 (Å^2)
2 S	2.239	0.012
1 O	2.051	0.001

[a]Errors in distance are ±0.002Å for the first shell and ±0.005Å for the outer shells. The given errors for the coordination numbers are ±25%.

Figure 5.7: A) The experimental (-) and theoretical (--) Fourier Transform and Cu-EXAFS (inset) of the as-purified C244/246A. The parameters for this fit are listed in the table, section A. B) The experimental (-) and theoretical (--) Fourier Transform and Cu-EXAFS (inset) of the reduced C244/246A hCCS. The parameters for this fit are listed in the table, section B. C) The edge comparison of the as-purified C244/246A (-) and the reduced C244/246A (--)

Finally, the reduced C244/246A sample also gives equally good results for a fit with two Cu-S at 2.29 Å and one Cu-O at 2.05 Å and one fit with three sulfurs at 2.24 Å (Figure 5.7). It is hard to say which of these fits for the domain III mutants is better since the third ligand is almost certainly exogenous. Both fits are reasonable because there is plenty of water around to provide a water ligand, and since the method of cleavage of the protein from the intein-chitin binding protein tag involves the addition of high levels of MESNA, which could provide an exogenous thiol ligand. However, the width of the first shell peak in the Fourier Transform does suggest a mixed shell favoring the 2S - 1O fit. Also, the sulfur distances are slightly longer in the mixed shells fit which agrees more

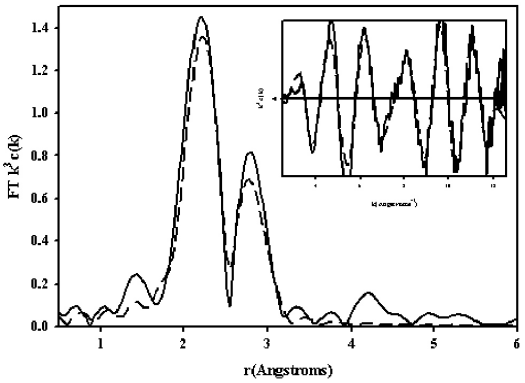

E_0 = -10.3		F = 0.00063
Shell (X)[a]	R(Å)	δ^2 (Å^2)
3 S	2.262	0.009
1 Cu	2.712	0.004

[a]Errors in distance are ±0.002Å for the first shell and ±0.005Å for the outer shells. The given errors for the coordination numbers are ±25%.

Figure 5.8: The experimental (-) and theoretical (--) Fourier Transform and Cu-EXAFS (inset) of C22A hCCS. The parameters used for the fit are listed in the table.

with the distances seen in models of trigonal sulfur containing copper sites than do the shorter distances of the 3 Cu-S fits[Pickering et al. 1993].

The domain I mutants did not exhibit the same oddity in metal binding as the domain III mutants, all of these mutants purified with one Cu(I) ion per protein molecule. These mutants gave two shells in the Fourier transforms of the EXAFS data like the wild type protein, but with a more intense second shell feature, similar to the data for the C22/25S hCCS-MBP fusion protein. The C22A mutant fits well with a first shell of three Cu-S at 2.26 Å and a second shell of one Cu-Cu at 2.71 Å. Unlike the wild type protein, here the fit is not improved by the reduction of the amount of copper in the second shell. This is to be expected since the metal binding site in domain I, the single copper site, has been mutated. Unlike the single cysteine to serine mutation, a single mutation of cysteine to alanine knocks out metal binding in domain I. The C25A mutant showed results similar to that of the C22A mutant with three sulfurs at 2.27Å and one copper at 2.71Å. The C22/25A mutant showed similar results with three sulfurs at 2.26Å and one copper at 2.72Å[1].

The initial studies of wild type hCCS and its cysteine to alanine mutants seem to support the hypothesis suggested earlier by the cysteine to serine mutant studies: that

[1]As discussed in section 4.3.2, it is also possible to fit the data as a higher order copper cluster. However, for the same reasons discussed earlier, mainly the copper to protein ratios, we feel that the binuclear cluster is the best model for this data.

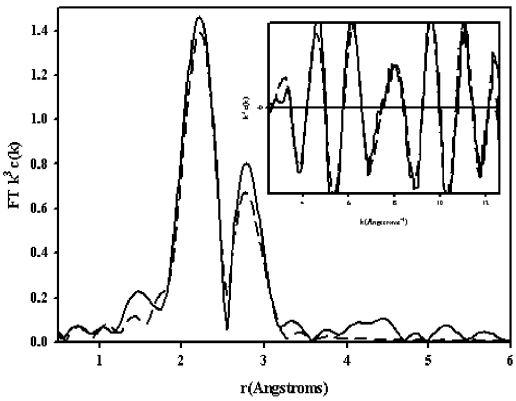

E_0 = -5.73 F = 0.00045

Shell (X)[a]	R(Å)	δ^2 (Å^2)
3 S	2.269	0.008
1 Cu	2.709	0.004

[a]Errors in distance are ±0.002Å for the first shell and ±0.005Å for the outer shells. The given errors for the coordination numbers are ±25%.

Figure 5.9: The experimental (-) and theoretical (--) Fourier Transform and Cu-EXAFS of C25A hCCS. The parameters used for the fit are listed in the table.

domain III is the site of metal transfer to SOD and that it is also the site of the copper cluster. We were also able to determine that the cluster is involved in the formation of higher oligomeric states of hCCS. It is still unclear if the cluster itself is needed for the activity of hCCS. It has also not been determined whether the dimeric or the tetrameric form, or possibly both, is the active form of hCCS.

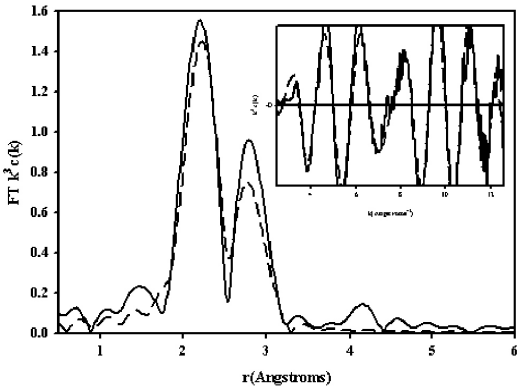

E_0 = -5.04 F = 0.00067

Shell (X)[a]	R(Å)	δ^2 (Å^2)
3 S	2.259	0.008
1 Cu	2.715	0.002

[a]Errors in distance are ±0.002Å for the first shell and ±0.005Å for the outer shells. The given errors for the coordination numbers are ±25%.

Figure 5.10: The experimental (-) and theoretical (--) Fourier Transform and Cu-EXAFS of C22/25A hCCS. The parameters used for the fit are listed in the table.

5.3 RECONSTITUTION STUDIES

To relate cluster formation with the activity of hCCS, we undertook reconstitution studies so that we could compare fully copper loaded hCCS with hCCS containing substoichiometric amounts of copper. hCCS was expressed and purified as apoprotein without any copper added to the growth medium. The protein was then reconstituted anaerobically using Cu(I)-acetonitrile. The expressed protein was dialyzed into buffer containing 10% acetonitrile. Cu(I) stock was made by dissolving tetrakis(acetonitrile)copper(I) hexafluorophosphate in acetonitrile. This stock was then diluted in buffer to achieve a 10% acetonitrile solution. Stoichiometric amounts of copper were then added to the apoprotein slowly over an hour. Any excess copper was then removed by dialysis against copper-free 10% acetonitrile buffer overnight. Acetonitrile was then removed from the buffer stepwise by first dialyzing overnight against 5% acetonitrile and then finally by overnight dialysis against acetonitrile-free buffer. Following this method we were able to prepare fully copper loaded hCCS (2 Cu: 1 protein) as well as the substoichiometric samples containing 1.5 Cu, 1 Cu and 0.5 Cu per protein. After reconstitution, copper concentration was confirmed by ICP-AES and protein concentration was confirmed by Bradford analysis, to assure that the appropriate copper to protein ratios were obtained.

5.3.1 CLUSTER FORMATION AS A FUNCTION OF COPPER RATIOS

To elucidate which site might be binding copper first and begin to correlate the Cu:protein ratio versus cluster formation, we began Cu-EXAFS studies of hCCS samples reconstituted anaerobically with Cu(I). The 0.5 Cu: protein sample gave a Fourier Transform of the EXAFS data with a single shell that fits as a two sulfur, one oxygen single copper site. Like the domain III mutants, the EXAFS data for this sample also fit a 3 sulfur single shell well. However again the longer distances in the mixed shell fit make that fit preferable. In the 1 Cu to protein sample, there is the beginning of a second shell feature at 2.72 Å suggesting that cluster formation has begun. The percentage cluster

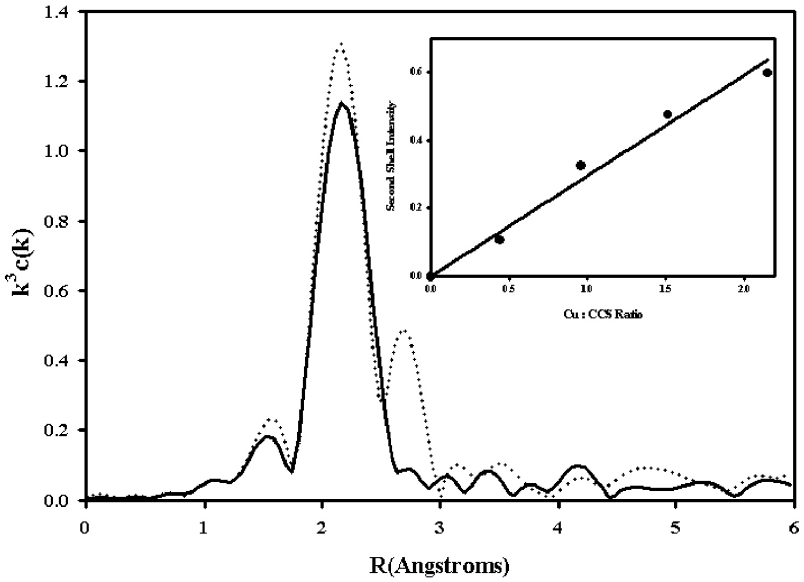

Figure 5.11: Comparison of the Fourier Transform of the 0.5 Cu:protien sample (-) and the 2 Cu:protien sample (--). The inset shows the relationship between Cu ratio and second shell intensity.

formed in this sample is hard to quantify but the high Debye Waller factor of 0.014 when the number of coppers at 2.72 Å is set to one, suggests that the complex is not fully formed.

The 1.5 Cu:protein sample begins to look more like the EXAFS for the wild type sample. The second shell is not yet as intense as the feature in the wild type sample but it is higher than that of the 1 Cu to protein sample. Again the Debye Waller factor, at 0.012, is a little higher than would be expected for the copper sulfur cluster. Finally the 2 Cu:protein sample gives an EXAFS spectrum identical to that of the wild type sample.

These results show that first a single trigonal copper site is formed and then the cluster is formed. The formation of the two sites does not seem to happen sequentially, i.e. full formation of one site followed by formation of the second site, as there is no cluster in the 0.5 Cu: protein sample but in the 1 Cu: protein sample there is a quantity of cluster formed. If the single copper site loaded first then the cluster formed, one would expect little or no cluster in the 1 Cu:protein sample. It cannot be determined from this

data whether or not the single copper site that loads first is the single site in domain I or if it is loading in domain III prior to cluster formation.

To determine whether the cluster formation is based on the copper to protein ratio and is independent of overall copper concentration, EXAFS was performed on a dilute sample of 1 Cu:protein and the sample was then concentrated and the EXAFS was performed again (Figure 5.12). The concentrated sample is the sample reported above, while the dilute sample gives identical results, with the exception of a slightly worse fit index but this is to be expected with a more dilute sample and lower signal to noise ratio.

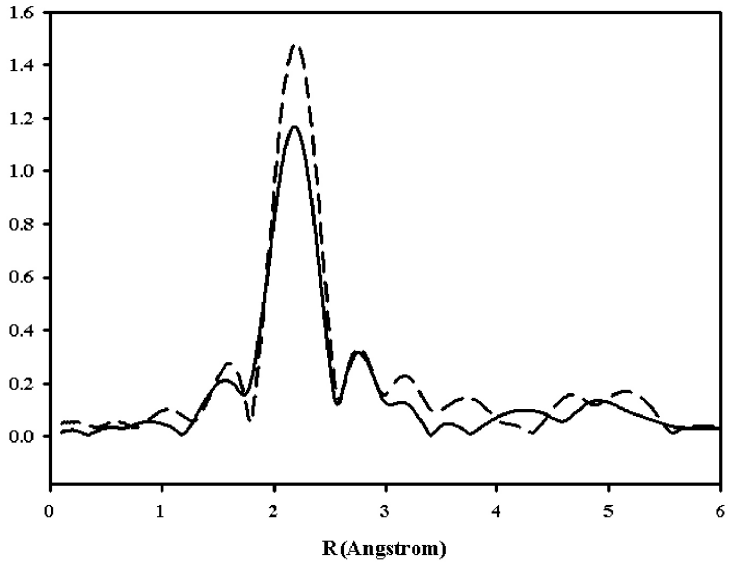

Figure 5.12 Comparison of the Fourier Transform of the dilute (-) and concentrated (--) 1 Cu:protien sample.

5.3.2 CLUSTER FORMATION VERSUS ACTIVITY

Once the amount of cluster formed in the reconstituted samples was determined, we tested the activity of the samples to relate cluster formation with activity. Activity assays where performed as previously described by incubation of hCCS with apoSOD, then the activity of SOD was tested by the xanthine oxidase cytochrome *c* assay[McCord

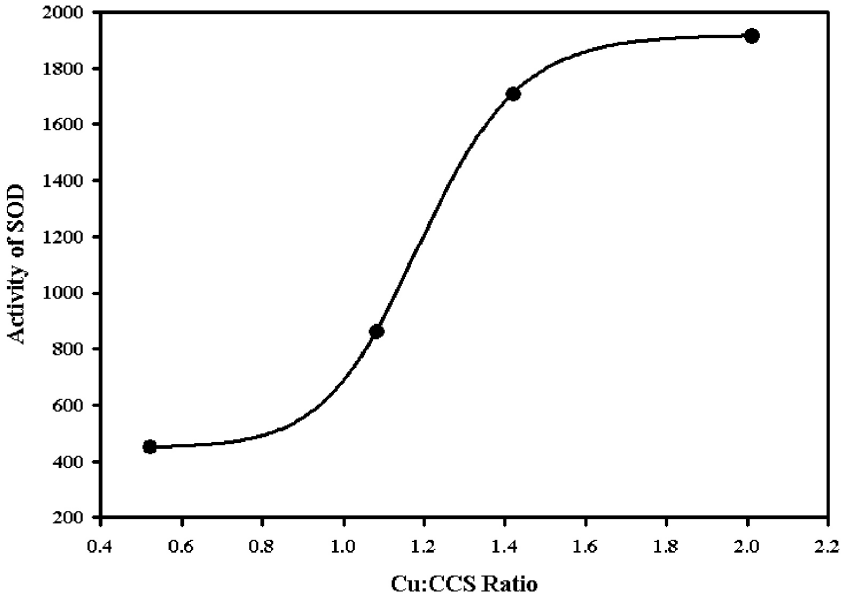

Figure 5.13: Activity of SOD after incubation with hCCS versus the Cu:protein ratio of the hCCS in the incubation mixture.

et al. 1968; McCord et al. 1969]. Previously, the amount of hCCS protein incubated with SOD was at a ratio of 1:1, and since there are two coppers in hCCS this means that the copper to SOD ratio was 2:1. To insure that the activity seen was based on the ability of the different copper loaded forms of hCCS to transfer copper to SOD and not overall concentration, in these studies the amount of hCCS added was enough to maintain the Cu:SOD ratio of 2:1. Therefore, with the 0.5Cu:hCCS sample, four times the amount of hCCS was incubated with SOD to keep the 2:1 ratio of Cu to SOD and with the 1 Cu:hCCS sample two times the amount of hCCS was incubated with SOD, etc.

Under these conditions, the 0.5 Cu:protein sample gave an activity of around 450 units/mg, greatly reduced from the wild type protein. The 1 Cu:protein sample had an activity of 860 units/mg, while the activity of the 1.5 Cu:protein sample was almost double at 1700 units/ mg. Finally, the 2 Cu:protien sample was comparable to the wild type protein with an activity of 1900 units/mg.

These results show that there is a relationship between the amount of copper loaded into hCCS and its ability to transfer copper to SOD that goes beyond simple

copper concentration and is directly related to the Cu:protein ratio of hCCS. Whether it is directly related to cluster formation is not clear. In the EXAFS studies, the cluster formation had not begun in the 0.5 sample, but it rapidly increased as the ratio approached 1 Cu:protein and it was almost complete at 1.5 Cu:protien. The activities approximately parallel this trend suggesting there are relationships between cluster formation and activity. It is interesting that the amount of activity remaining in the 0.5 Cu:protein sample is comparable to the activity of the domain III alanine mutants when one considers that there is four times the amount protein in the incubation mixture. This suggests that even though there is excess copper chelator present in the incubation mixture, there is some leakage between hCCS and SOD that might not be protein mediated transfer, or that domain I might be able to transfer a minimal amount of copper to SOD.

5.3.3 CLUSTER FORMATION VERSUS OLIGOMERIZATION STATES

To determine what effect cluster formation might have on the formation of higher oligomeric states of hCCS, we undertook HPLC gel filtration studies on the reconstituted samples (Figure 5.14). The 2 Cu:protein sample is identical to that of the wild type HPLC with the dominant species being the dimeric form, but with about 1/3 of the protein existing in the tetrameric form. The HPLC experiments unexpectedly show that the remaining reconstitution samples all appear to have a population of monomer present, that was not seen in the apoprotein HPLC. If the oligomerization states are followed from the apo form to the fully loaded protein, it is seen that in the apoprotein there exists only dimer. In the 0.5 Cu:protein sample the dominant species is dimer but there is a population of monomer present. In the 1 Cu:protein the monomer and dimer populations are almost equal, while in the 1.5 Cu:protein the monomer has begun to decrease and a population of tetramer has begun to form and again dimer is the dominant species.

These data can be interpreted to suggest that the difference between the metal loaded protein and the apoprotein is not the ability to form tetramer but that instead the dimer in the apo protein and the dimer in the metal loaded protein are two different

species, where the dimer in the metal loaded form is able to further interact to form tetramer. Our interpretation is that apoprotein exists as a dimer formed via the conserved SOD dimer interface. Binding of a single copper to the protein interferes with this dimer interaction forming hCCS monomers. As more copper is bound to domain III and the cluster begins to form, dimerization becomes possible through the domain III interaction. Finally, once the domain III domain III dimers are formed the domain II dimer interface can interact again and tetramer can be formed via the interaction of two dimers through the conserved SOD dimer interface.

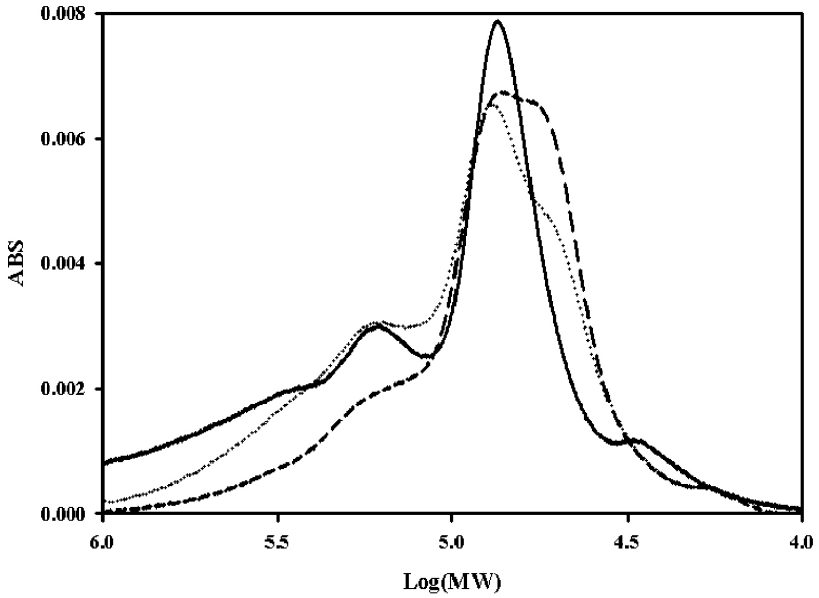

Figure 5.14: Comparisons of the HPLC gel Filtration of the 1Cu:protein (--), 1.5 Cu:protien (...) and the 2 Cu:protein (-) samples.

5.4 CONCLUSIONS

The reconstitution studies in this chapter tie the formation of the copper cluster to the ability of hCCS to transfer copper to hSOD. By comparing the EXAFS data with the activity studies, we see that only after a population of cluster containing protein is established does hCCS show significant activity, and that it is not copper concentration

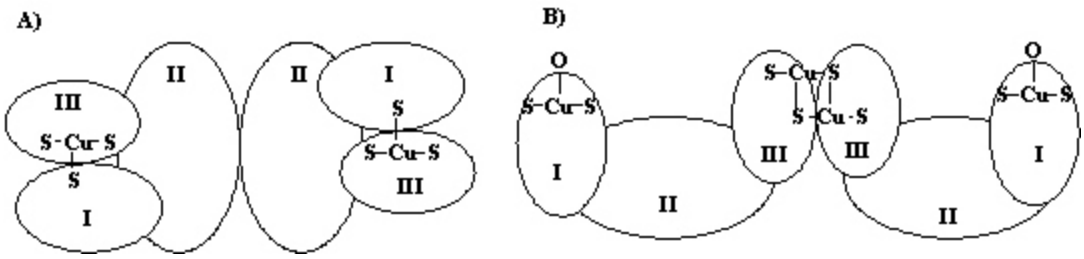

Figure 5.15: Comparison of the active form of hCCS proposed in the heterodimer mechanism (A) and the active form of hCCS proposed by this thesis (B).

but the amount of copper contained in the cluster that correlates with the activity of hCCS. Therefore, we see that the formation of the binuclear copper cluster is essential for the activity of hCCS. Also, the gel filtration studies show that increasing the copper bound to the protein appears to cause a structural change in the protein, shifting it from a dimer formed via the domain II SOD-like interface to a dimer formed through the copper cluster in domain III. And again, comparing this to the activity profile of the copper titration, it shows that it is the dimer formed through the domain III interface, and not through the domain II interface, that is the active species.

Taking the conclusions of this chapter into consideration we must again refine the proposed mechanism of copper transfer. To review, the heterodimer mechanism suggested that the active form of hCCS is a dimer formed through the domain II interface with a single three-coordinate copper site per hCCS monomer formed by the copper-binding motifs of domain I and domain II. The results of Chapter 3 led us to propose that the active form of hCCS was in fact a dimer formed through the domain II dimer interface with a binuclear copper cluster per hCCS monomer formed by the copper binding motifs of domain I and domain III. In Chapter 4, the structure of the copper-binding site in hCCS was further elucidated and the mechanism was changed to reflect the data that the active form of hCCS must be a dimer of hCCS formed through the domain II dimer interface with an additional interaction between the domain III metal binding motifs from the different hCCS monomers to form an intermolecular binuclear copper cluster. In this chapter we conclude that the interaction between two domain III

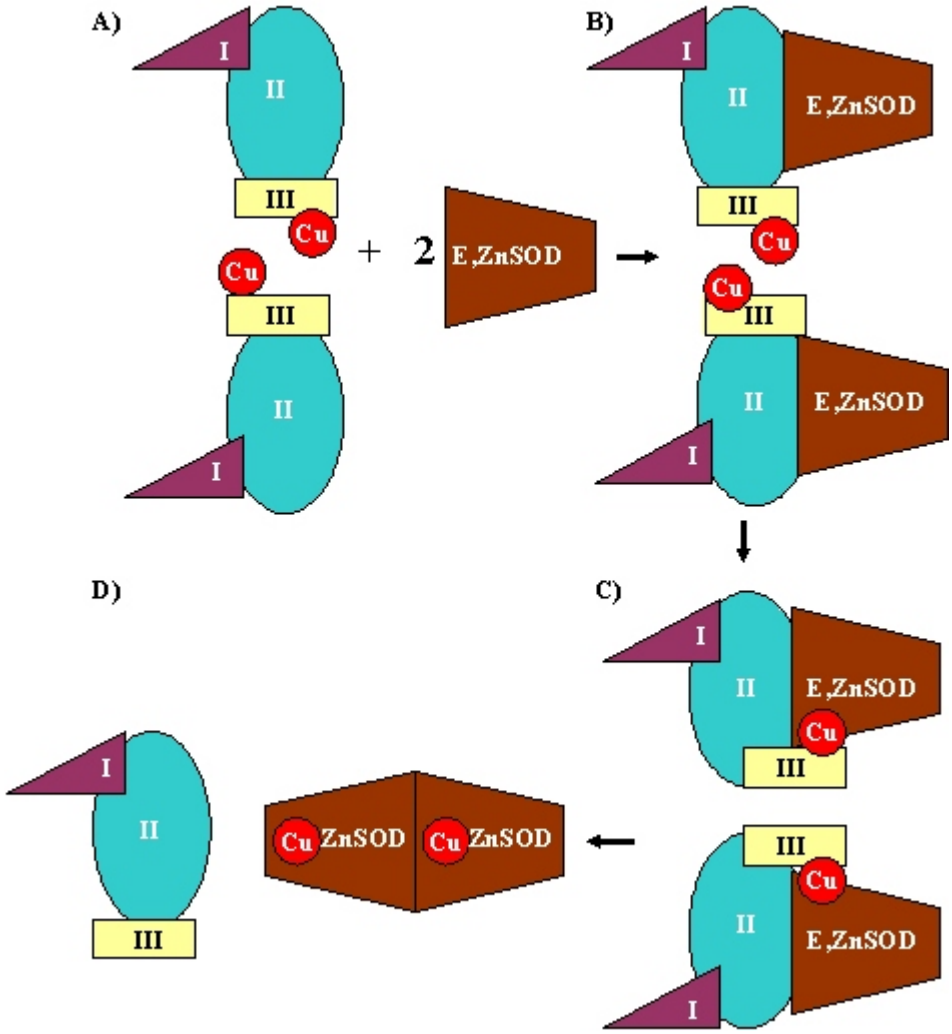

Figure 5.16: Altered heterodimer mechanism using the active form of hCCS proposed in this thesis. Compare to Figure 1.19

copper binding motifs, from the two hCCS monomers in the dimer, to form the intermolecular binuclear copper cluster is the only site of dimerization in the active form of hCSS (Figure 5.15). In this conclusion, the conserved dimer interface region in the SOD-like domain II is not interacting between the two hCCS monomers. This view of the active form of hCCS works well as the starting form for the heterodimer mechanism since in this structure the conserved SOD-like dimer interface would be exposed and free to interact with apo-SOD monomers (Figure 5.16).

CHAPTER 6
CONCLUSIONS AND FUTURE STUDIES

6.1 CONCLUSIONS

The view of CCS before we undertook these studies was that, in both the apo and metal loaded forms, it exists as a dimer formed through the conserved SOD-like domain II dimer interface. Upon interaction with apo-SOD, the CCS dimer dissociated and formed two heterodimers with apo-SOD monomers and this species was the form that facilitated copper transfer. This mechanism was termed the heterodimer mechanism[Lamb et al. 2000]; however our studies suggest a different mechanism for hCCS.

The crystal structure of the yeast apoprotein and the human domain II only truncation mutant, both show dimerization via the domain II interface [Lamb et al. 1999; Lamb et al. 2000]. Our data, too, show that apo-hCCS is a dimer, and as there are no disulfide linkages, as shown by the SDS-PAGE gels, and no metal present, (ruling out the domain III – domain III cluster as a site of interaction), the most likely candidate for dimerization being through the domain II dimer interface. But, our data shows that there must be a change in the structure of this dimer upon copper binding. The initial shift from dimer to monomer shows that copper binding initiates a structural rearrangement of the protein. The addition of more copper to the protein pushes the equilibrium away from monomer back to dimer, and also, a population of

tetramer is introduced. The introduction of tetramer suggests that there is a difference between the original apo-dimer and the newly formed copper-loaded dimer. The obvious difference between the apo and the metal loaded forms of the protein is the formation of the copper cluster. Another difference between the apo-dimer and the copper-loaded dimer is the ability of the copper loaded dimer to further interact to form tetramers. We know that the copper cluster must be one site of oligomerization, because the mutant studies showed that the cluster was formed between two domain III binding sites from two different hCCS monomers Therefore it might be reasonable to assume that dimer is formed through the domain II dimer interface, as in the apoprotein, and the tetramer is being formed through the copper

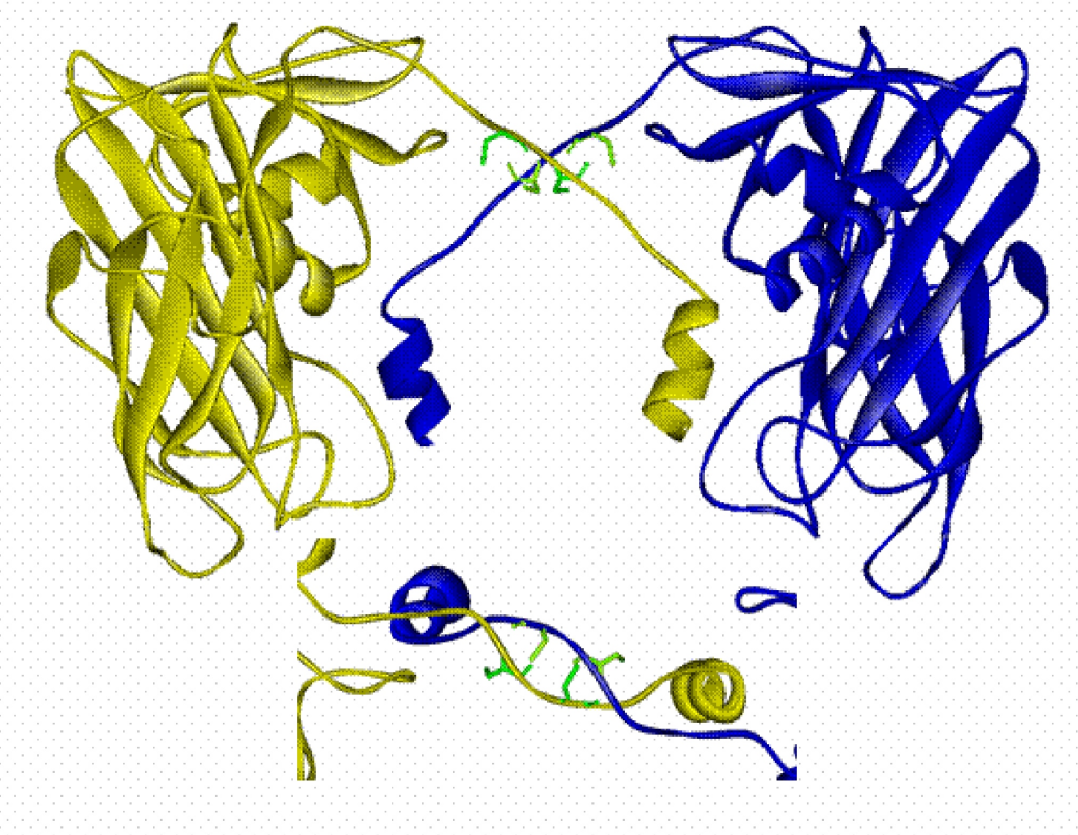

Figure 6.1: Proposed structure taken from the crystal structure of the heterodimer with the SOD subunits removed. The inset shows the proximity of the CXC motifs of the two domain III. The cooridnates for this structure were downloaded from the protein databank file 1JK9.

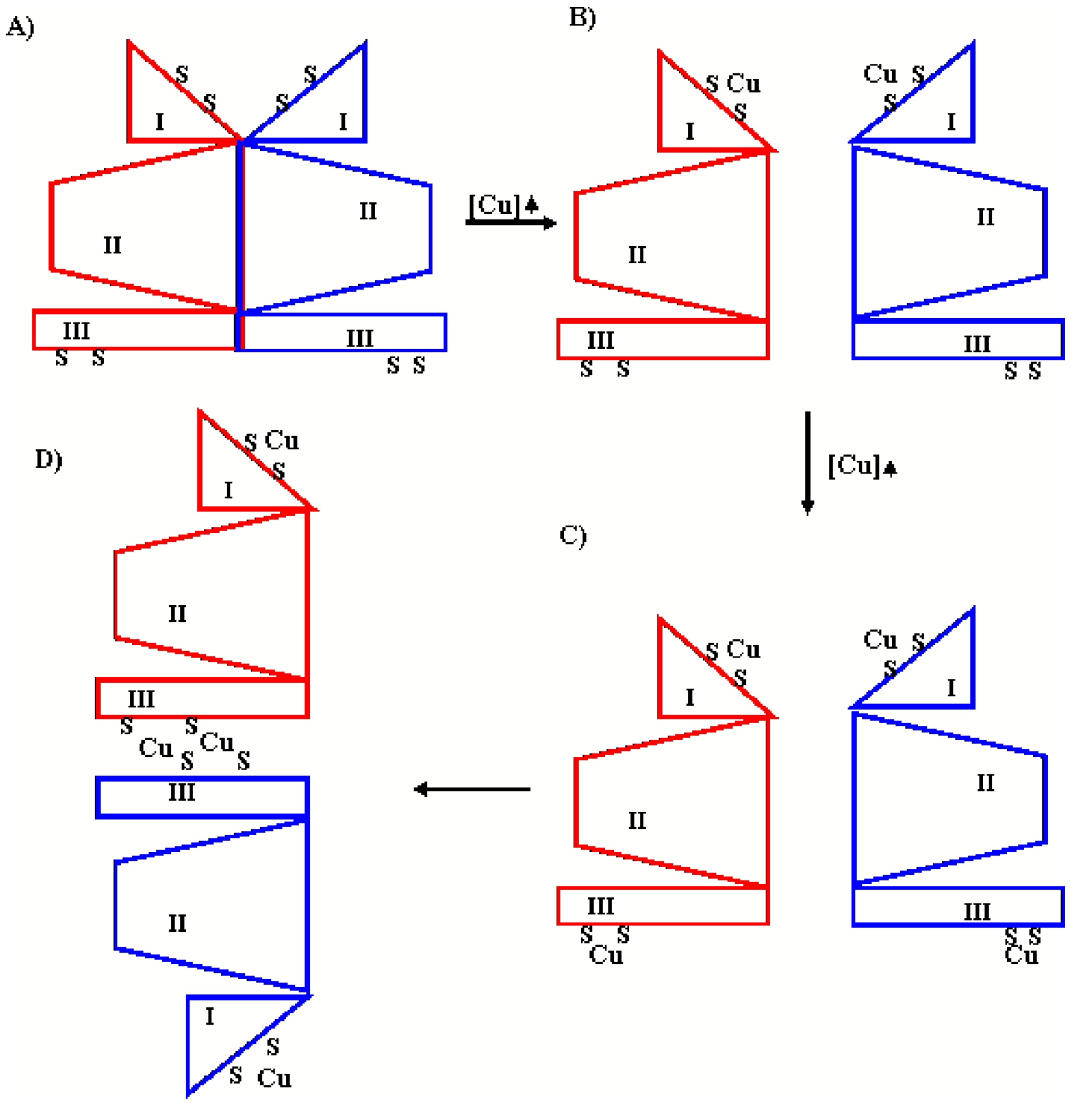

Figure 6.2: Proposed mechanism of hCCS. A) apo-dimer formed through the domain II interface, B) binding of copper dissociates the dimer, C) binding of copper at domain III, D) formation of the cluster and the dimer through domain III leaving the domain II interface open for interaction with COD or another hCCS dimer

cluster, since the copper loaded form can interact to form tetramers. However, the data from the domain I mutants shows that this cannot be the case. The EXAFS spectra of the domain I mutants with the intense second shell peak show that most or all of the copper must be in the domain III copper cluster, while the gel filtration data shows that the protein is in a mixed dimer/tetramer equilibrium with dimer being the main species. Since the EXAFS data show no mononuclear copper sites, the cluster

between two domain III binding sites must be present in both the dimer and the tetramer. This means that in the copper loaded form of the protein, the dimer is formed through the domain III-domain III copper complex and that tetramerization is most likely occurring through the domain II dimer interface. The structure of a possible domain III – domain III dimer can be observed in the crystal structure of the heterodimer form of hCCS-SOD if the SOD subunits are removed.

This model of the resting state of hCCS suggests a mechanism for transfer of copper to SOD that is more consistent with the interaction of a heterotetramer, rather than heterodimer. Apo-hCCS exists as a dimer formed between the conserved SOD dimer interface. As copper levels increase, copper is bound to domain I. The binding of copper to domain I causes structural changes that lead to the dissociation of the dimer. As copper levels increase and binding occurs at domain III, dimer is reformed through the domain III-domain III copper complex. This dimer formation now allows tetramer (homotetramer with another hCCS dimer or heterotetramer with SOD monomers for copper transfer) to form through the exposed domain II interface.

6.2 FUTURE STUDIES

More work to characterize hCCS's metal-binding sites and oligomerization states needs to be done, expecially the reconstitution titration of the mutants. We showed that the amount of copper bound to the wildtype protein had a great effect on its oligomerization state, and the next step is to see what effect copper loading has on the mutants. Are the apo-forms of the domain I and domain III mutants solely dimers, as the wildtype? And do they show the same shift to monomer and then back to dimer as bound copper increases? Also, an attempt to isolate the monomeric, dimeric, and tetrameric forms of the protein should be under taken to further study the different oligomerization states of hCCS. Cu-EXAFS and activities done on the different forms of hCCS should help to elucidate which of the forms is the active form of hCCS and what changes hCCS is undergoing as copper levels increase.

To see if the copper cluster is the site of transfer to hSOD, studies should be done to see if the cluster is lost after incubation with hSOD. Apo-hSOD could be immobilized on a column and copper loaded hCCS could be passed over the column. After hCCS has eluted from the column, Cu-EXAFS could be performed to see if the cluster was indeed lost. Also, gel filtration HPLC could be performed to see if the protein elutes at the same time as the copper-loaded hCCS or the apo-form of the protein.

Also, we barely began to study the zinc binding properties of hCCS in these studies, and more could be done in this area to see if the zinc site in hCCS actually plays a role in the activity of the protein. Zn-EXAFS needs to be performed on all of the cysteine to alanine mutants of hCCS, since we have seen that these mutants have altered zinc binding capacities, but we did not do EXAFS to see if the zinc binding sites were altered in anyway. Also, hCCS could be made zinc-free by chelation and use of Chelex-treated buffer, then the copper could be added back to the protein using the reconstitution method previously described in this thesis in chapter 5. Cu-EXAFS, gel filtration HPLC, and activities could be done to see if the zinc-free copper-loaded hCCS behaved the same as the Cu, Zn hCCS.

6.2.1 FLUORESENCE

One of the questions to be resolved about hCCS is the role of domain I. It contains the CXXC motif that is characteristic of copper chaperones but it does not appear to take part in copper transfer. It has previously been hypothesized that domain I plays a role in copper scavenging at low copper concentrations, but at this point no interactions between the sites in domain I and domain II has been shown. CXXC motifs also play an alternate role in biology. They are often used as redox regulators in proteins than can be inhibited or activated as a disulfide bond between the two cysteines that are broken or formed [Barford 2004; Farrell et al. 2005]. It is not hard to imagine that the same structural regulation could be imposed not by the formation of a disulfide at the site but by metal binding at the site. Therefore, it is

possible that domain I could function as a regulator of hCCS activity, turning on the ability of domain III to bind copper when excess copper is present. If one considers the three main roles of copper in the eukaryotic cell; respiration (COX), iron transport (ceruloplasmin) and anti-oxidation (SOD), it is clear that the first two functions, respiration and iron transport, should have priority over anti-oxidation. Therefore, it is possible that domain I could be a copper sensor, turning on the activity of hCCS in the presence of free copper, delegating hCCS to the end of the line in priority for copper. We were hampered in our ability to study the effects domain I may have on the activity and kinetics of copper transfer to SOD, because the current assay for hCCS is not a direct assay of hCCS activity but instead an assay of the activity of SOD after incubation with hCCS.

Previous work has shown that copper sulfur clusters exhibit fluorescence [Byrd et al. 1988]. Preliminary work in our lab suggests that hCCS may show this fluorescence, but instrument failure and technical problems prevented us from successfully exploring this possibility. If hCCS does show the fluorescence typical of a copper sulfur cluster, this would open up some interesting possibilities. Since copper loaded hCCS (before transfer to SOD) is expected to have a copper cluster and therefore exhibits fluorescence, and hCCS without copper in domain III (after transfer to SOD) should have no copper cluster and no fluorescence, then the activity of hCCS could be measured by following the change in fluorescence. So an assay that directly measures the activity of hCCS could be developed using fluorescence. This would be a great advantage over the current assay because now kinetic studies could be performed on hCCS. This could be used to shed light on the effects of domain I on the activity of the protein and to further study the effects of the single cysteine to serine mutants to decide if these mutations had a kinetic or thermodynamic effect.

6.2.2 PROTEIN LIGATION AND SELENIUM EXAFS

Further studies need to be performed on the metal binding site in domain III to determine the local structure of the site, which of the cysteine residues is the terminal ligand and which is the bridging ligand, as well as to determine the mechanism of transfer of copper from the complex to SOD. One way to get information on the environment of a specific cysteine residue within the complex is by mutating the cysteine to a selenocysteine (Sec, U), thereby creating the mutants CXU and UXC. Se-EXAFS could then be performed on the protein to elucidate the environment of a specific cysteine residue. When combined with freeze quench, the environment of a specific cysteine residue could be followed through the transfer of copper to SOD.

Selenocysteine is a naturally occurring amino-acid that has its own codon and tRNA, separate and distinct from that of cysteine. However, mutating a cysteine residue to a selenocystiene has its own set of problems. Selenocysteine is encoded by the codon UGA which also serves a stop codon. The cell differentiates between the selenocysteine and the stop codon by use of secondary structures in mRNA called selenocysteine insertion sequences (SECIS) [Lescure et al. 2002]. These SECIS introduce their own problems in overexpressing selenocysteine mutants. In higher eukaryotes, SECIS lie outside of the open reading frame and the information in them is not translated, but in prokaryotes, the SECIS lie within the open reading frame and the information within them is translated [Engelberg-Kulka et al. 2001]. Therefore, to make a mutation to a selenocysteine and overexpress it in *E. coli*, one must not only insert the UGA codon but also a SECIS that can be translated. Work has been done with mild success on making selenocysteine mutants but it is still a difficult process [Arner 2002].

One way around the difficulties of overexpressing a selenocysteine mutant is a process known as intein mediated protein ligation [Evans et al. 1999]. Expression vectors using an intein sequence for cleavage of the target protein from an affinity tag can have the intein site on the N-terminus or the C-terminus of the target protein.

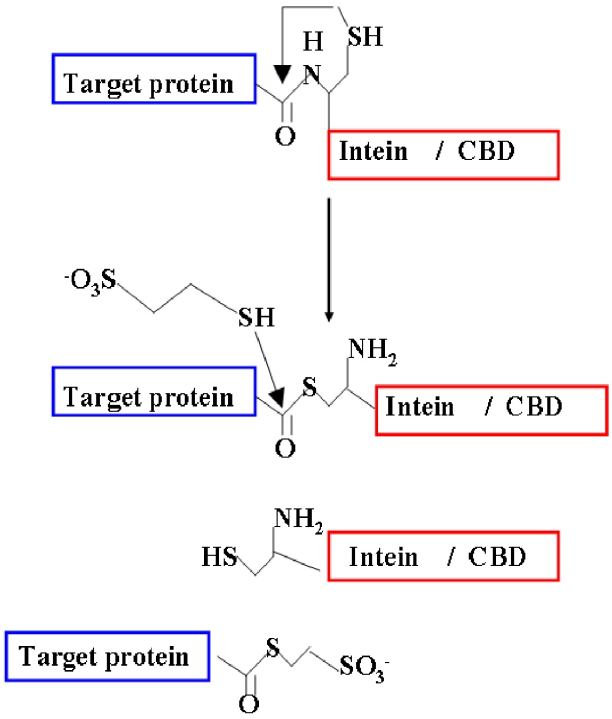

Figure 6.3: Mechaninsm of cleavage of the C-terminal intein construct for protein purification

When it is attached to the C-terminus of the target protein, as it is in our case, the mechanism of intein cleavage of the target protein from the affinity tag is through an active cysteine residue [Chong et al. 1997]. This cysteine residue is located at the beginning of the intein sequence and is the residue just after the final residue of the target protein. This cysteine is able to spontaneously attack the peptide bond causing N-S shift in the peptide bond and the formation of a thioester. Exogenous thiol, such as 2-mercaptoethanesulfonate, DTT, or free cysteine, can perform a nucleophillic attack on this thioester and form a new thioester between the peptide bond and the free thiol, causing cleavage of the target protein from the intein linked affinity tag. The C-terminus of the target protein can remain as a modified thioester or it can spontaneously hydrolyze to reform a native carboxyl C-terminus. The rate at which this happens is variable and changes from protein to protein. If the protein keeps the

modified thioester C-terminus, a peptide containing a N-terminal cysteine can attack and ligate itself to the target protein; this process is called intein mediated protein ligation (IPL). It has been shown that this procedure can be carried out using selenocysteine as the attacking group in place of cysteine; therefore, this method can be used to introduce selenocystiene into a protein sequence [Berry et al. 2002].

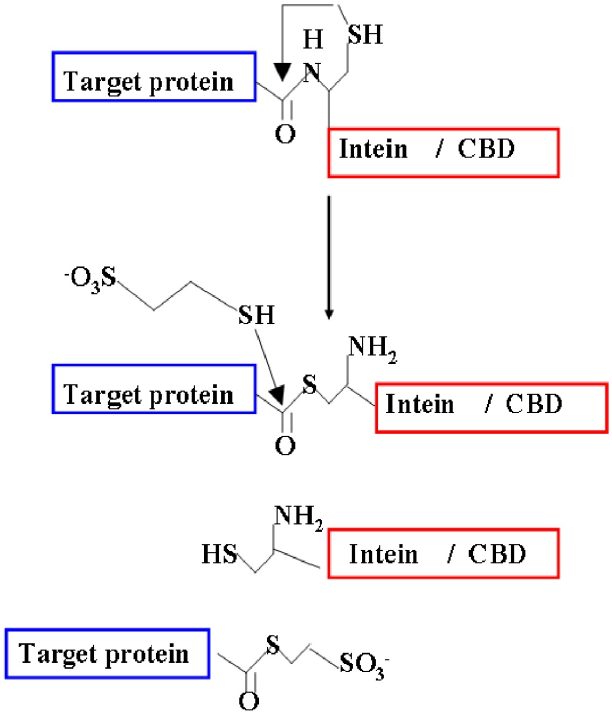

Figure 6.4: Mechanism of Intein mediated protein ligation

Our initial attempts with this procedure met with mild success. We were able to ligate single cysteine residues to the C-terminus of the truncation mutant; however, we were unable to perform the ligation using free selenocystiene. Se-EXAFS on the sample and on the reduced selenocystiene we were using to facilitate the ligation showed that we were not properly reducing the selenocysteine and that all of the

sample existed in a di-selenide bond and was therefore unable to carry out the intein mediated protein ligation.

6.2.3 MUTATIONAL STUDIES

In previous chapters, comparisons have been made between hCCS and EC-SOD; these comparisons introduce new residues of interest for mutational studies. Specifically mutants of the residues in the WEER motif of domain III would be of great interest. There is great variety in the sequence of the domain III tails between species of CCS but the WEER motif is highly conserved, this suggests that it plays a

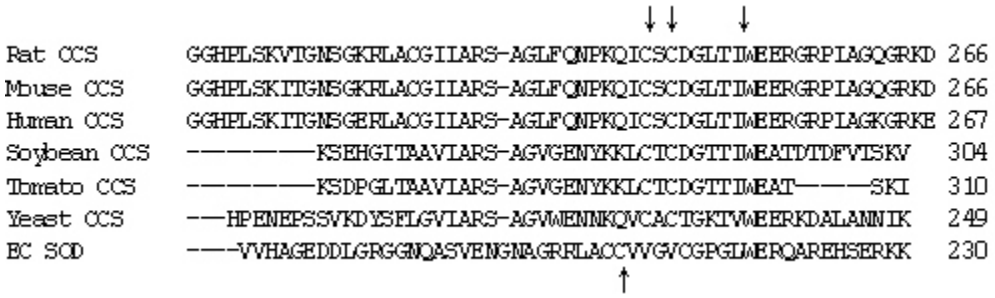

Figure 6.5: Alignment of various species of CCS with ECSOD using CLUSTALW. The CXC motif and the WE motif are marked with ↓ and the C residue of ECSOD involved in the intermolecular disulfide bond is marked with ↑

very important role. Activity and oligomerization studies of mutants of these residues would confirm whether copper loaded dimer of hCCS forms solely through the domain III-domain III complex and would further map this dimerization site.

BIBLIOGRAPHY

CHAPTER 1

Abernethy, J. L., H. M. Steinman and R. L. Hill (1974). Bovine erythrocyte superoxide dismutase. Subunit structure and sequence location of the intrasubunit disulfide bond. *J Biol Chem* **249**(22): 7339-47.

Adman, E. T. (1991). Copper protein structures. *Adv Protein Chem* **42**: 145-97.

Aldred, A. R., A. Grimes, G. Schreiber and J. F. Mercer (1987). Rat ceruloplasmin. Molecular cloning and gene expression in liver, choroid plexus, yolk sac, placenta, and testis. *J Biol Chem* **262**(6): 2875-8.

Arner, E. S. (2002). Recombinant expression of mammalian selenocysteine-containing thioredoxin reductase and other selenoproteins in *Escherichia coli*. *Methods Enzymol* **347**: 226-35

Arnesano, F., L. Banci, I. Bertini, F. Cantini, S. Ciofi-Baffoni, D. L. Huffman and T. V. O'Halloran (2001). Characterization of the binding interface between the copper chaperone Atx1 and the first cytosolic domain of CCC2 ATPase. *J Biol Chem* **276**(44): 41365-76.

Arnesano, F., L. Banci, I. Bertini, D. L. Huffman and T. V. O'Halloran (2001). Solution structure of the Cu(I) and apo forms of the yeast metallochaperone, Atx1. *Biochemistry* **40**(6): 1528-39.

Arseniev, A., P. Schultze, E. Worgotter, W. Braun, G. Wagner, M. Vasak, J. H. Kagi and K. Wuthrich (1988). Three-dimensional structure of rabbit liver [cd7]metallothionein-2a in aqueous solution determined by nuclear magnetic resonance. *J Mol Biol* **201**(3): 637-57.

Banci, L., I. Bertini, B. Bruni, P. Carloni, C. Luchinat, S. Mangani, P. L. Orioli, M. Piccioli, W. Ripniewski and K. S. Wilson (1994). X-ray, NMR and molecular dynamics studies on reduced bovine superoxide dismutase: Implications for the mechanism. *Biochem Biophys Res Commun* **202**(2): 1088-95.

Banci, L., I. Bertini, F. Cantini, S. Ciofi-Baffoni, L. Gonnelli and S. Mangani (2004). Solution structure of Cox11, a novel type of beta-immunoglobulin-like fold involved in Cu_B site formation of cytochrome *c* oxidase. *J Biol Chem* **279**(33): 34833-9.

Banci, L., I. Bertini, F. Cramaro, R. Del Conte and M. S. Viezzoli (2002). The solution structure of reduced dimeric Copper, Zinc superoxide dismutase. The structural effects of dimerization. *Eur J Biochem* **269**(7): 1905-15.

Barceloux, D. G. (1999). Copper. *Clin. Toxicol.* **37**(2): 217 - 230.

Barford, D. (2004). The role of cysteine residues as redox-sensitive regulatory switches. *Curr Opin Struct Biol* **14**(6): 679-86.

Bartnikas, T. B. and J. D. Gitlin (2003). Mechanisms of biosynthesis of mammalian copper, zinc superoxide dismutase. *J Biol Chem* **278**(35): 33602-8.

Beers, J., D. M. Glerum and A. Tzagoloff (1997). Purification, characterization, and localization of yeast Cox17p, a mitochondrial copper shuttle. *J Biol Chem* **272**(52): 33191-6.

Beinert, H. (1995). Crystals and structures of cytochrome *c* oxidases--the end of an arduous road. *Chem Biol* **2**(12): 781-5.

Berry, S. M., M. D. Gieselman, M. J. Nilges, W. A. van Der Donk and Y. Lu (2002). An engineered azurin variant containing a selenocysteine copper ligand. *J Am Chem Soc* **124**(10): 2084-5.

Bertinato, J., M. Iskandar and M. R. L'Abbe (2003). Copper deficiency induces the upregulation of the copper chaperone for Cu,Zn superoxide dismutase in weanling male rats. *J Nutr* **133**(1): 28-31.

Binsted, N. and S. S. Hasnain (1996). State of the art analysis of whole X-ray absorption spectra. *J. Synchrotron Radiat.* **3**: 185 - 196.

Blackburn, N. J., M. E. Barr, W. H. Woodruff, J. van der Oost and S. de Vries (1994). Metal-metal bonding in biology: EXAFS evidence for a 2.5 Å copper-copper bond in the Cu_A center of cytochrome oxidase. *Biochemistry* **33**(34): 10401-7.

Blackburn, N. J., S. de Vries, M. E. Barr, R. P. Houser, W. B. Tolman, D. Sanders and J. A. Fee (1997). X-ray absorption studies on the mixed-valence and fully reduced of the soluble Cu_A domains of cytochrome *c* oxidase. *J. Am. Chem. Soc* **119**: 6135-6143.

Blackburn, N. J., S. S. Hasnain, N. Binsted, G. P. Diakun, C. D. Garner and P. F. Knowles (1984). An Extended X-ray Absorption Fine Structure study of bovine erythrocyte superoxide dismutase in aqueous solution. Direct evidence for three coordinate Cu(I) in reduced enzyme. *Biochem J* **219**(3): 985-90.

Blackburn, N. J., S. S. Hasnain, G. P. Diakun, P. F. Knowles, N. Binsted and C. D. Garner (1983). An Extended X-ray Absorption Fine Structure study of the copper and zinc sites of freeze-dried bovine superoxide dismutase. *Biochem J* **213**(3): 765-8.

Blackburn, N. J., M. Ralle, E. Gomez, M. G. Hill, A. Pastuszyn, D. Sanders and J. A. Fee (1999). Selenomethionine-substituted *Thermus thermophilus* cytochrome ba_3: Characterization of the Cu_A site by Se and Cu k-EXAFS. *Biochemistry* **38**(22): 7075-84.

Blackburn, N. J., R. W. Strange, J. Reedijk, A. Volbeda, A. Farooq, K. D. Karlin and J. Zubieta (1989). X-ray absorption edge spectroscopy of copper(I) complexes. Coordination geometry of copper(I) in the reduced forms of copper proteins and their derivatives with carbon monoxide. *Inorg Chem* **28**: 6433 - 6422.

Boden, N., M. C. Holmes and P. F. Knowles (1979). Properties of the cupric sites in bovine superoxide dismutase studied by nuclear magnetic relaxation measurements. *Biochem J* **177**(1): 303-9.

Bordo, D., K. Djinovic and M. Bolognesi (1994). Conserved patterns in the Cu,Zn superoxide dismutase family. *J Mol Biol* **238**(3): 366-86.

Boswell, J. S., B. J. Reedy, R. Kulathila, D. Merkler and N. J. Blackburn (1996). Structural investigations on the coordination environment of the active-site copper centers of recombinant bifunctional peptidylglycine alpha-amidating enzyme. *Biochemistry* **35**(38): 12241-50.

Brenner, A. J. and E. D. Harris (1995). A quantitative test for copper using bicinchoninic acid. *Anal Biochem* **226**(1): 80-4.

Bronner, F. and J. H. Yost (1985). Saturable and nonsaturable copper and calcium transport in mouse duodenum. *Am. J. Physio. Gastrointext. Liver Physio.* **249**(1): G108 - G112.

Brown, K. R., G. L. Keller, I. J. Pickering, H. H. Harris, G. N. George and D. R. Winge (2002). Structures of the cuprous-thiolate clusters of the Mac1 and Ace1 transcriptional activators. *Biochemistry* **41**(20): 6469-76.

Brown, N. M., A. S. Torres, P. E. Doan and T. V. O'Halloran (2004). Oxygen and the copper chaperone CCS regulate posttranslational activation of Cu,Zn superoxide dismutase. *Proc Natl Acad Sci U S A* **101**(15): 5518-23.

Buchman, C., P. Skroch, J. Welch, S. Fogel and M. Karin (1989). The Cup2 gene product, regulator of yeast metallothionein expression, is a copper-activated DNA-binding protein. *Mol Cell Biol* **9**(9): 4091-5.

Butt, T. R., E. J. Sternberg, J. A. Gorman, P. Clark, D. Hamer, M. Rosenberg and S. T. Crooke (1984). Copper metallothionein of yeast, structure of the gene, and regulation of expression. *Proc Natl Acad Sci U S A* **81**(11): 3332-6.

Byrd, J., R. M. Berger, D. R. McMillin, C. F. Wright, D. Hamer and D. R. Winge (1988). Characterization of the copper-thiolate cluster in yeast metallothionein and two truncated mutants. *J Biol Chem* **263**(14): 6688-94.

Cai, D. and J. P. Klinman (1994). Evidence of a self-catalytic mechanism of 2,4,5-trihydroxyphenylalanine quinone biogenesis in yeast copper amine oxidase. *J Biol Chem* **269**(51): 32039-42.

Calabrese, L., M. Carbonaro and G. Musci (1989). Presence of coupled trinuclear copper cluster in mammalian ceruloplasmin is essential for efficient electron transfer to oxygen. *J Biol Chem* **264**(11): 6183-7.

Carr, H. S., G. N. George and D. R. Winge (2002). Yeast Cox11, a protein essential for cytochrome *c* oxidase assembly, is a Cu(I)-binding protein. *J Biol Chem* **277**(34): 31237-42.

Carr, H. S. and D. R. Winge (2003). Assembly of cytochrome *c* oxidase within the mitochondrion. *Acc Chem Res* **36**(5): 309-16.

Carroll, M. C., J. B. Girouard, J. L. Ulloa, J. R. Subramaniam, P. C. Wong, J. S. Valentine and V. C. Culotta (2004). Mechanisms for activating Cu- and Zn-containing superoxide dismutase in the absence of the CCS Cu chaperone. *Proc Natl Acad Sci U S A* **101**(16): 5964-9.

Carter, P. (1987). Improved oligonucleotide-directed mutagenesis using M13 vectors. *Methods Enzymol* **154**: 382-403.

Casareno, R. L., D. Waggoner and J. D. Gitlin (1998). The copper chaperone CCS directly interacts with Copper, Zinc superoxide dismutase. *J Biol Chem* **273**(37): 23625-8.

Chong, S., F. B. Mersha, D. G. Comb, M. E. Scott, D. Landry, L. M. Vence, F. B. Perler, J. Benner, R. B. Kucera, C. A. Hirvonen, J. J. Pelletier, H. Paulus and M. Q. Xu (1997). Single-column purification of free recombinant proteins using a self-cleavable affinity tag derived from a protein splicing element. *Gene* **192**(2): 271-81.

Cobine, P. A., L. D. Ojeda, K. M. Rigby and D. R. Winge (2004). Yeast contain a non-proteinaceous pool of copper in the mitochondrial matrix. *J Biol Chem* **279**(14): 14447-55.

Cordano, A. (1998). Clinical manifestations of nutritional copper deficiency in infants and children. *Am. J. Clin. Nut.* **67**(5): 1012S - 1016S.

Cordano, A., J. M. Baertl and G. G. Graham (1964). Copper deficiency in infancy. *Pediatrics* **34**: 324 - 336.

Cotton, F. A. and G. Wilkinson (1980). *Advanced inorganic chemistry: A comprehensive text*. New York, John Wiley & Sons.

Crampton, R. F., D. M. Matthews and R. Poisner (1965). Observation on the mechanisms of absorption of copper by the small intestines. *J. Physio.* **178**(1): 111-126.

Culotta, V. C., W. R. Howard and X. F. Liu (1994). Crs5 encodes a metallothionein-like protein in *Saccharomyces cerevisiae*. *J Biol Chem* **269**(41): 25295-302.

Culotta, V. C., L. W. Klomp, J. Strain, R. L. Casareno, B. Krems and J. D. Gitlin (1997). The copper chaperone for superoxide dismutase. *J Biol Chem* **272**(38): 23469-72.

Dancis, A., D. Haile, D. S. Yuan and R. D. Klausner (1994). The *Saccharomyces cerevisiae* copper transport protein (Ctr1p). Biochemical characterization, regulation by copper, and physiologic role in copper uptake. *J. Biol. Chem.* **269**(41): 25660 - 25667.

Dancis, A., D. G. Roman, G. J. Anderson, A. G. Hinnebusch and R. D. Klausner (1992). Ferric reductase of *Saccharomyces cerevisiae*: Molecular characterization, role in iron uptake, and transcriptional control by iron. *Proc Natl Acad Sci U S A* **89**(9): 3869-73.

Dash, S. C. (1989). Copper sulphate poisoning and acute renal failure. *Int J Artif Organs* **12**(10): 610.

Dawkes, H. C. and S. E. Phillips (2001). Copper amine oxidase: Cunning cofactor and controversial copper. *Curr Opin Struct Biol* **11**(6): 666-73.

di Guan, C., P. Li, P. D. Riggs and H. Inouye (1988). Vectors that facilitate the expression and purification of foreign peptides in *Escherichia coli* by fusion to maltose-binding protein. *Gene* **67**(1): 21-30.

Eipper, B. A. and R. E. Mains (1988). Peptide alpha-amidation. *Annu Rev Physiol* **50**: 333-44.

Eisses, J. F. and J. H. Kaplan (2002). Molecular characterization of hCtr1, the human copper uptake protein. *J Biol Chem* **277**(32): 29162-71.

Engelberg-Kulka, H., Z. Liu, C. Li and M. Reches (2001). An extended *Escherichia coli* "selenocysteine insertion sequence" (secis) as a multifunctional RNA structure. *Biofactors* **14**(1-4): 61-8.

Evans, T. C., Jr. and M. Q. Xu (1999). Intein-mediated protein ligation: Harnessing nature's escape artists. *Biopolymers* **51**(5): 333-42.

EXAFSPAK. Revised: April 20, 2001. G. George, Stanford Synchrotron Radiation Laboratory. Available: http://ssrl.slac.stanford.edu/exafspak.html [Viewed: December 10, 2005]

Farrell, R. A., J. L. Thorvaldsen and D. R. Winge (1996). Identification of the Zn(II) site in the copper-responsive yeast transcription factor, Amt1: A conserved Zn module. *Biochemistry* **35**(5): 1571-80.

Farrell, S. R. and C. Thorpe (2005). Augmenter of liver regeneration: A flavin-dependent sulfhydryl oxidase with cytochrome *c* reductase activity. *Biochemistry* **44**(5): 1532-41.

Fenton, H. J. H. (1896). Constitution of a new dibasic acid, resulting from the oxidation of tartaric acid. *J. Chem. Soc. Trans.* **69**: 546 - 562.

Fridovich, I. (1983). Superoxide radical: An endogenous toxicant. *Annu Rev Pharmacol Toxicol* **23**: 239-57.

Fridovich, I. (1986). Biological effects of the superoxide radical. *Arch Biochem Biophys* **247**(1): 1-11.

Fridovich, I. (1989). Superoxide dismutases. An adaptation to a paramagnetic gas. *J Biol Chem* **264**(14): 7761-4.

Furst, P., S. Hu, R. Hackett and D. Hamer (1988). Copper activates metallothionein gene transcription by altering the conformation of a specific DNA binding protein. *Cell* **55**(4): 705-17.

Furukawa, Y., A. S. Torres and T. V. O'Halloran (2004). Oxygen-induced maturation of SOD1: A key role for disulfide formation by the copper chaperone CCS. *Embo J* **23**(14): 2872-81.

Garcia-Vasquez, J. A., J. Romero, R. Castro, A. Sousa, D. J. Rose and J. Zubieta (1997). Electrochemical synthesis and crystal structure of (3-trimethylsilylpyridine-2-thiolato) copper(I), $[Cu_4(3\text{-}Me_3Sipyt_4)_4]$ *Inorg. Chim. Acta* **260**: 221-223.

Gerdemann, C., C. Eicken and B. Krebs (2002). The crystal structure of catechol oxidase: New insight into the function of type-3 copper proteins. *Acc Chem Res* **35**(3): 183-91.

Getzoff, E. D., D. E. Cabelli, C. L. Fisher, H. E. Parge, M. S. Viezzoli, L. Banci and R. A. Hallewell (1992). Faster superoxide dismutase mutants designed by enhancing electrostatic guidance. *Nature* **358**(6384): 347-51.

Getzoff, E. D., J. A. Tainer, P. K. Weiner, P. A. Kollman, J. S. Richardson and D. C. Richardson (1983). Electrostatic recognition between superoxide and Copper, Zinc superoxide dismutase. *Nature* **306**(5940): 287-90.

Glerum, D. M., A. Shtanko and A. Tzagoloff (1996). Characterization of Cox17, a yeast gene involved in copper metabolism and assembly of cytochrome *c* oxidase. *J Biol Chem* **271**(24): 14504-9.

Glerum, D. M., A. Shtanko and A. Tzagoloff (1996). Sco1 and Sco2 act as high copy suppressors of a mitochondrial copper recruitment defect in *Saccharomyces cerevisiae*. *J Biol Chem* **271**(34): 20531-5.

Greenough, M. A., L. B. Pase, I. Voskoboinik, M. J. Petris, A. L. Wilson-O'Brien and J. Camakaris (2004). Signals regulating trafficking of the menkes (MNK; Atp7a) copper translocating p-type ATPase in polarized mdck cells. *Am J Physiol Cell Physiol* **Epub**.

Gunshin, H., B. Mackenzie, U. V. Berger, Y. Gunshin, M. F. Romero, W. F. Boron, S. Nussberger, J. L. Gollan and M. A. Hediger (1997). Cloning and characterization of a mammalian proton-coupled metal-ion transporter. *Nature* **388**(6641): 482-8.

Gurman, S. J., N. Binsted and I. Ross (1984). A rapid, exact, curved-wave theory for EXAFS calculations. *J. Phys. C* **17**: 143 - 151.

Gurman, S. J., N. Binsted and I. Ross (1986). A rapid, exact, curved-wave theory for EXAFS calculations. 2. The multiple-scattering contributions. *J. Phys. C* **19**: 1845 - 1861.

Haber, F. and J. Weiss (1932). Uber die einwirkung des hyrdoperoxydes. *Naturwiss* **51**: 948 - 950.

Harris, Z. L., L. W. Klomp and J. D. Gitlin (1998). Aceruloplasminemia: An inherited neurodegenerative disease with impairment of iron homeostasis. *Am. J. Clin. Nut.* **67**(5): 972 - 977.

Hassett, R. and D. J. Kosman (1995). Evidence for Cu(II) reduction as a component of copper uptake by *Saccharomyces cerevisiae*. *J Biol Chem* **270**(1): 128-34.

Haywood, S. and M. Loughran (1985). Copper toxicosis and tolerance in the rat. II. Tolerance--a liver protective adaptation. *Liver* **5**(5): 267-75.

Heaton, D., T. Nittis, C. Srinivasan and D. R. Winge (2000). Mutational analysis of the mitochondrial copper metallochaperone Cox17. *J Biol Chem* **275**(48): 37582-7.

Heaton, D. N., G. N. George, G. Garrison and D. R. Winge (2001). The mitochondrial copper metallochaperone Cox17 exists as an oligomeric, polycopper complex. *Biochemistry* **40**(3): 743-51.

Hellman, N. E. and J. D. Gitlin (2002). Ceruloplasmin metabolism and function. *Annu. Rev. Nut.* **22**: 439 - 458.

Hiser, L., M. Di Valentin, A. G. Hamer and J. P. Hosler (2000). Cox11p is required for stable formation of the Cu_B and magnesium centers of cytochrome *c* oxidase. *J Biol Chem* **275**(1): 619-23.

Holm, R. H., P. Kennepohl and E. I. Solomon (1996). Structural and functional aspects of metal sites in biology. *Chem Rev* **96**(7): 2239-2314.

Horng, Y. C., P. A. Cobine, A. B. Maxfield, H. S. Carr and D. R. Winge (2004). Specific copper transfer from the Cox17 metallochaperone to both Sco1 and Cox11 in the assembly of yeast cytochrome *c* oxidase. *J Biol Chem* **279**(34): 35334-40.

Inoue, T., H. Sugawara, S. Hamanaka, H. Tsukui, E. Suzuki, T. Kohzuma and Y. Kai (1999). Crystal structure determinations of oxidized and reduced plastocyanin from the *Cyanobacterium synechococcus* sp. Pcc 7942. *Biochemistry* **38**(19): 6063-9.

Jakubowski, W., T. Bilinski and G. Bartosz (2000). Oxidative stress during aging of stationary cultures of the yeast *Saccharomyces cerevisiae*. *Free Radic Biol Med* **28**(5): 659-64.

Jaron, S. and N. J. Blackburn (1999). Does superoxide channel between the copper centers in peptidylglycine monooxygenase? A new mechanism based on carbon monoxide reactivity. *Biochemistry* **38**(46): 15086-96.

Janssen, M. D., A. L. Spek, D. M. Grove and G. van Koten (1996). A mixed (arenethiolato)copper(I)/copper bromide aggregate: X-ray structure of octanuclear $[Cu_8\{Sc_6H_3(Ch_2NMe_2)_2\text{-}2,6\}_3Br_5]$. *Inorg Chem* **35**(13): 4078-4081.

Jensen, L. T., W. R. Howard, J. J. Strain, D. R. Winge and V. C. Culotta (1996). Enhanced effectiveness of copper ion buffering by Cup1 metallothionein compared with Crs5 metallothionein in *Saccharomyces cerevisiae*. *J Biol Chem* **271**(31): 18514-9.

Josephs, H. W. (1931). Treatment of anemia in infants with iron and copper. *Bull. John Hopkins Hosp.* **49**: 246-254.

Jungmann, J., H. A. Reins, J. Lee, A. Romeo, R. Hassett, D. Kosman and S. Jentsch (1993). Mac1, a nuclear regulatory protein related to Cu-dependent transcription factors is involved in Cu/Fe utilization and stress resistance in yeast. *Embo J* **12**(13): 5051-6.

Kagan, H. M. and W. Li (2003). Lysyl oxidase: Properties, specificity, and biological roles inside and outside of the cell. *J Cell Biochem* **88**(4): 660-72.

Kagi, J. H. and A. Schaffer (1988). Biochemistry of metallothionein. *Biochemistry* **27**(23): 8509-15.

Kau, L. S., D. J. Spira-Solomon, J. E. Penner-Hahn, K. O. Hodgson and E. I. Solomon (1987). X-ray absorption edge determination of the oxidation state and coordination number of copper. Application to the type 3 site in *Rhus vernicifera* laccase and its reaction with oxygen. *J. Amer. Chem. Soc.* **109**(21): 6433-6442.

Keele, B. B., Jr., J. M. McCord and I. Fridovich (1970). Superoxide dismutase from *Escherichia coli* b. A new manganese-containing enzyme. *J Biol Chem* **245**(22): 6176-81.

Keen, C. L., J. Y. Uriu-Hare, S. N. Hawk, M. A. Jankowski, G. P. Daston, C. L. Kwik-Uribe and R. B. Rucker (1998). Effect of copper deficiency on prenatal development and pregnancy outcome. *Am. J. Clin. Nut.* **67**(5): 1003S - 1011S.

Kille, P., A. Hemmings and E. A. Lunney (1994). Memories of metallothionein. *Biochim Biophys Acta* **1205**(2): 151-61.

Klinman, J. P. (1996). Mechanisms whereby mononuclear copper proteins functionalize organic substrates. *Chem. Rev.* **96**(7): 2541 - 2562.

Klinman, J. P. (2003). The multi-functional topa-quinone copper amine oxidases. *Biochim Biophys Acta* **1647**(1-2): 131-7.

Klinman, J. P. (2005). The copper-enzyme family of dopamine beta -monooxygenase and peptidylglycine alpha -hydroxylating monooxygenase: Resolving the chemical pathway for substrate hydroxylation. *J Biol Chem*.

Klomp, L. W., S. J. Lin, D. S. Yuan, R. D. Klausner, V. C. Culotta and J. D. Gitlin (1997). Identification and functional expression of HAH1, a novel human gene involved in copper homeostasis. *J Biol Chem* **272**(14): 9221-6.

Kono, Y. and I. Fridovich (1983). Inhibition and reactivation of Mn-catalase. Implications for valence changes at the active site manganese. *J Biol Chem* **258**(22): 13646-8.

Kronig, R. (1931). *Z. Phys* **70**: 317 - 323.

Kronig, R. (1932). *Z. Phys* **75**: 190 - 210.

Kuhlbrandt, W. (2004). Biology, structure and mechanism of p-type ATPases. *Nat Rev Mol Cell Biol* **5**(4): 282-95.

Kuo, Y. M., B. Zhou, D. Cosco and J. Gitschier (2001). The copper transporter Ctr1 provides an essential function in mammalian embryonic development. *Proc Natl Acad Sci U S A* **98**(12): 6836-41.

Lamb, A. L., A. S. Torres, T. V. O'Halloran and A. C. Rosenzweig (2001). Heterodimeric structure of superoxide dismutase in complex with its metallochaperone. *Nat Struct Biol* **8**(9): 751-5.

Lamb, A. L., A. K. Wernimont, R. A. Pufahl, V. C. Culotta, T. V. O'Halloran and A. C. Rosenzweig (1999). Crystal structure of the copper chaperone for superoxide dismutase. *Nat Struct Biol* **6**(8): 724-9.

Lamb, A. L., A. K. Wernimont, R. A. Pufahl, T. V. O'Halloran and A. C. Rosenzweig (2000). Crystal structure of the second domain of the human copper chaperone for superoxide dismutase. *Biochemistry* **39**(7): 1589-95.

Land, E. J., C. A. Ramsden and P. A. Riley (2003). Tyrosinase autoactivation and the chemistry of ortho-quinone amines. *Acc Chem Res* **36**(5): 300-8.

Leary, S. C., B. A. Kaufman, G. Pellecchia, G. H. Guercin, A. Mattman, M. Jaksch and E. A. Shoubridge (2004). Human Sco1 and Sco2 have independent, cooperative functions in copper delivery to cytochrome *c* oxidase. *Hum Mol Genet* **13**(17): 1839-48.

Lepock, J. R., L. D. Arnold, B. H. Torrie, B. Andrews and J. Kruuv (1985). Structural analyses of various Cu^{2+}, Zn^{2+}-superoxide dismutases by differential scanning calorimetry and raman spectroscopy. *Arch Biochem Biophys* **241**(1): 243-51.

Lescure, A., D. Fagegaltier, P. Carbon and A. Krol (2002). Protein factors mediating selenoprotein synthesis. *Curr Protein Pept Sci* **3**(1): 143-51.

Lewis, E. A. and W. B. Tolman (2004). Reactivity of dioxygen-copper systems. *Chem. Rev.* **104**(2): 1047 - 1076.

Lin, S. J., R. A. Pufahl, A. Dancis, T. V. O'Halloran and V. C. Culotta (1997). A role for the *Saccharomyces cerevisiae* Atx1 gene in copper trafficking and iron transport. *J Biol Chem* **272**(14): 9215-20.

Linder, M. C. (1991). *Biochemistry of copper*. New York, Plenum Publishing.

Liochev, S. I. and I. Fridovich (2000). Copper- and Zinc-containing superoxide dismutase can act as a superoxide reductase and a superoxide oxidase. *J Biol Chem* **275**(49): 38482-5.

Longo, V. D., E. B. Gralla and J. S. Valentine (1996). Superoxide dismutase activity is essential for stationary phase survival in *Saccharomyces cerevisiae*. Mitochondrial production of toxic oxygen species *in vivo*. *J Biol Chem* **271**(21): 12275-80.

Lonnerdal, B. (1998). Copper nutrition during infancy and childhood. *Am. J. Clin. Nut.* **67**(5): 1046S - 1053S.

Lutsenko, S., R. G. Efremov, R. Tsivkovskii and J. M. Walker (2002). Human copper-transporting atpase Atp7b (the Wilson's disease protein): Biochemical properties and regulation. *J Bioenerg Biomembr* **34**(5): 351-62.

Lutsenko, S. and J. H. Kaplan (1995). Organization of p-type ATPases: Significance of structural diversity. *Biochemistry* **34**(48): 15607-13.

Lutsenko, S., K. Petrukhin, M. J. Cooper, C. T. Gilliam and J. H. Kaplan (1997). N-terminal domains of human copper-transporting adenosine triphosphatases (the Wilson's and Menkes disease proteins) bind copper selectively *in vivo* and *in vitro* with stoichiometry of one copper per metal-binding repeat. *J Biol Chem* **272**(30): 18939-44.

Maina, C. V., P. D. Riggs, A. G. Grandea, 3rd, B. E. Slatko, L. S. Moran, J. A. Tagliamonte, L. A. McReynolds and C. D. Guan (1988). An *Escherichia coli* vector to express and purify foreign proteins by fusion to and separation from maltose-binding protein. *Gene* **74**(2): 365-73.

Mason, H. S. (1948). The chemistry of melanin. Mechanism of the oxidation of dihydroxyphenylalanine by tyrosinase. *J. Biol. Chem.* **172**(1): 83 - 92.

Mattatall, N. R., J. Jazairi and B. C. Hill (2000). Characterization of YPMq, an accessory protein required for the expression of cytochrome *c* oxidase in *Bacillus subtilis*. *J Biol Chem* **275**(37): 28802-9.

McAdam, M. E., E. M. Feilden, F. Lavelle, L. Calabrese, D. Cocco and G. Rotilio (1977). The involvement of the bridging imidazolate in the catalytic mechanism of action of bovine superoxide dismutase. *Biochem J* **167**(1): 271-4.

McCord, J. M. and I. Fridovich (1968). The reduction of cytochrome *c* by milk xanthine oxidase. *J Biol Chem* **243**(21): 5753-60.

McCord, J. M. and I. Fridovich (1969). Superoxide dismutase. An enzymic function for erythrocuprein (hemocuprein). *J Biol Chem* **244**(22): 6049-55.

McGuirl, M. A. and D. M. Dooley (1999). Copper-containing oxidases. *Curr Opin Chem Biol* **3**(2): 138-44.

Mercer, J. F. (1998). Menkes syndrome and animal models. *Am J Clin Nutr* **67**(5 Suppl): 1022S-1028S.

Messerschmidt, A. and R. Huber (1990). The blue oxidases, ascorbate oxidase, laccase and ceruloplasmin. Modelling and structural relationships. *Eur J Biochem* **187**(2): 341-52.

Muramatsu, Y., T. Yamada, D. H. Moralejo, Y. Suzuki and K. Matsumoto (1998). Fetal copper uptake and a homolog (ATP7b) of the Wilson's disease gene in rats. *Res Commun Mol Pathol Pharmacol* **101**(3): 225-31.

Nittis, T., G. N. George and D. R. Winge (2001). Yeast Sco1, a protein essential for cytochrome *c* oxidase function is a Cu(I)-binding protein. *J Biol Chem* **276**(45): 42520-6.

Odajima, T. and I. Yamazaki (1972). Myeloneperoxidase of the leukocyte of normal blood. 3. The reaction of ferric myeloperoxidase with superoxide anion. *Biochim Biophys Acta* **284**(2): 355-9.

Olivares, M. and R. Uauy (1996). Copper as an essential nutrient. *Am J Clin Nutr* **63**(5): 791S-6S.

Oury, T. D., J. D. Crapo, Z. Valnickova and J. J. Enghild (1996). Human extracellular superoxide dismutase is a tetramer composed of two disulphide-linked dimers: A simplified, high-yield purification of extracellular superoxide dismutase. *Biochem J* **317 (Pt 1)**: 51-7.

Outten, C. E. and T. V. O'Halloran (2001). Femtomolar sensitivity of metalloregulatory proteins controlling zinc homeostasis. *Science* **292**(5526): 2488-92.

Palmer, A. E., L. Quintanar, S. Severance, T. P. Wang, D. J. Kosman and E. I. Solomon (2002). Spectroscopic characterization and O_2 reactivity of the trinuclear cu cluster of mutants of the multicopper oxidase Fet3p. *Biochemistry* **41**(20): 6438-48.

Paret, C., K. Ostermann, U. Krause-Buchholz, A. Rentzsch and G. Rodel (1999). Human members of the Sco1 gene family: Complementation analysis in yeast and intracellular localization. *FEBS Lett* **447**(1): 65-70.

Percival, S. S. (1998). Copper and immunity. *Am. J. Clin. Nut.* **67**(5): 1064S - 1068S.

Petrukhin, K., S. Lutsenko, I. Chernov, B. M. Ross, J. H. Kaplan and T. C. Gilliam (1994). Characterization of the Wilson disease gene encoding a p-type copper transporting ATPase: Genomic organization, alternative splicing, and structure/function predictions. *Hum Mol Genet* **3**(9): 1647-56.

Pickering, I. J., G. N. George, C. T. Dameron, B. Kurz, D. R. Winge and I. G. Dance (1993). X-ray apsorption spectroscopy of cuprous- thiolate clusters in proteins and model systems. *J. Am. Chem. Soc* **115**: 9498-9505.

Portnoy, M. E., P. J. Schmidt, R. S. Rogers and V. C. Culotta (2001). Metal transporters that contribute copper to metallochaperones in *Saccharomyces cerevisiae*. *Mol Genet Genomics* **265**(5): 873-82.

Prigge, S. T., A. S. Kolhekar, B. A. Eipper, R. E. Mains and L. M. Amzel (1997). Amidation of bioactive peptides: The structure of peptidylglycine alpha-hydroxylating monooxygenase. *Science* **278**(5341): 1300-5.

Prigge, S. T., A. S. Kolhekar, B. A. Eipper, R. E. Mains and L. M. Amzel (1999). Substrate-mediated electron transfer in peptidylglycine alpha-hydroxylating monooxygenase. *Nat Struct Biol* **6**(10): 976-83.

Puig, S., J. Lee, M. Lau and D. J. Thiele (2002). Biochemical and genetic analyses of yeast and human high affinity copper transporters suggest a conserved mechanism for copper uptake. *J Biol Chem* **277**(29): 26021-30.

Rae, T. D., P. J. Schmidt, R. A. Pufahl, V. C. Culotta and T. V. O'Halloran (1999). Undetectable intracellular free copper: The requirement of a copper chaperone for superoxide dismutase. *Science* **284**(5415): 805-8.

Rae, T. D., A. S. Torres, R. A. Pufahl and T. V. O'Halloran (2001). Mechanism of Cu, Zn-superoxide dismutase activation by the human metallochaperone hCCS. *J Biol Chem* **276**(7): 5166-76.

Ralle, M., M. J. Cooper, S. Lutsenko and N. J. Blackburn (1998). The Menkes disease protein binds copper via novel 2 coordinate Cu(I)-cysteinates in the N-terminal domain. *J. Am. Chem. Soc* **120**: 13525 - 13526.

Ralle, M., S. Lutsenko and N. J. Blackburn (2003). X-ray absorption spectroscopy of the copper chaperone HAH1 reveals a linear two-coordinate Cu(I) center capable of adduct formation with exogenous thiols and phosphines. *J Biol Chem* **278**(25): 23163-70.

Ralle, M., S. Lutsenko and N. J. Blackburn (2004). Copper transfer to the N-terminal domain of the Wilson disease protein (ATP7b). X-ray absorption spectroscopy of reconstituted and chaperone-loaded metal binding domains and their interaction with exogenous ligands. *J. Inorg. Biochem.* **98**: 765-779.

Ralle, M., M. L. Verkhovskaya, J. E. Morgan, M. I. Verkhovsky, M. Wikstrom and N. J. Blackburn (1999). Coordination of Cu_B in reduced and co-liganded states of cytochrome bo_3 from *Escherichia coli*. Is chloride ion a cofactor? *Biochemistry* **38**(22): 7185-94.

Richardson, J., K. A. Thomas, B. H. Rubin and D. C. Richardson (1975). Crystal structure of bovine Cu, Zn superoxide dismutase at 3 Å resolution: Chain tracing and metal ligands. *Proc Natl Acad Sci U S A* **72**(4): 1349-53.

Roat-Malone, R. M. R. (2002). *Bioinorganic chemistry: A short course*. Hoboken, John Wiley & Sons.

Rosenzweig, A. C., D. L. Huffman, M. Y. Hou, A. K. Wernimont, R. A. Pufahl and T. V. O'Halloran (1999). Crystal structure of the Atx1 metallochaperone protein at 1.02 Å resolution. *Structure Fold Des* **7**(6): 605-17.

Rucker, R. B., T. Kosonen, M. S. Clegg, A. E. Mitchell, B. R. Rucker, J. Y. Uriu-Hare and C. L. Keen (1998). Copper, lysyl oxidase, and extracellular matrix protein cross-linking. *Am. J. Clin. Nut.* **67**(5): 996S - 1002S.

Salmi, M. and S. Jalkane (2002). Enzymatic control of leukocyte trafficking: Role of Vap-1. *Adv Exp Med Biol* **512**: 57-63.

Sandstead, H. H. (1995). Requirements and toxicity of essential trace elements, illustrated by zinc and copper. *Am J Clin Nutr* **61**(3 Suppl): 621S-624S.

Sarkar, B. (1981). Transport of copper. in *Properties of copper*. (H. Seigel). New York, Marcel Dekker, Inc. **12:** 233 - 277.

Sayers, D. E., E. A. Stern and F. W. Lytle (1971). *Phys. Rev. Letters* **27**: 1204 - 1209.

Schmidt, P. J., T. D. Rae, R. A. Pufahl, T. Hamma, J. Strain, T. V. O'Halloran and V. C. Culotta (1999). Multiple protein domains contribute to the action of the copper chaperone for superoxide dismutase. *J Biol Chem* **274**(34): 23719-25.

Senoo, Y., K. Katoh, Y. Nakai, Y. Hashimoto, K. Bando and S. Teramoto (1988). Activity and stability of recombinant human superoxide dismutase in buffer solutions and hypothermic perfusates. *Acta Med Okayama* **42**(3): 169-74.

Shriver, D. F., P. W. Atkins and C. H. Langford (1990). *Inorganic chemistry*. New York, W. H. Freeman and Company.

Smith-Mungo, L. I. and H. M. Kagan (1998). Lysyl oxidase: Properties, regulation and multiple functions in biology. *Matrix Biol* **16**(7): 387-98.

Srinivasan, C., M. C. Posewitz, G. N. George and D. R. Winge (1998). Characterization of the copper chaperone Cox17 of *Saccharomyces cerevisiae*. *Biochemistry* **37**(20): 7572-7.

Stenlund, P., D. Andersson and L. A. Tibell (1997). Subunit interaction in extracellular superoxide dismutase: Effects of mutations in the N-terminal domain. *Protein Sci* **6**(11): 2350-8.

Stenlund, P. and L. A. Tibell (1999). Chimeras of human extracellular and intracellular superoxide dismutases. Analysis of structure and function of the individual domains. *Protein Eng* **12**(4): 319-25.

Stohs, S. J. and D. Bagchi (1995). Oxidative mechanisms in the toxicity of metal ions. *Free Radic Biol Med* **18**(2): 321-36.

Strange, R. W., S. V. Antonyuk, M. A. Hough, P. A. Doucette, J. S. Valentine and S. S. Hasnain (2005). Variable metallation of human superoxide dismutase: Atomic resolution crystal structures of Cu-Zn, Zn-Zn and as-isolated wild-type enzymes. *J Mol Biol*.

Stern, E. A. (1975). *Phys. Rev.* **B10**: 3027 - 3037.

Sturtz, L. A., K. Diekert, L. T. Jensen, R. Lill and V. C. Culotta (2001). A fraction of yeast Cu,Zn-superoxide dismutase and its metallochaperone, CCS, localize to the intermembrane space of mitochondria. A physiological role for SOD1 in guarding against mitochondrial oxidative damage. *J Biol Chem* **276**(41): 38084-9.

Tainer, J. A., E. D. Getzoff, K. M. Beem, J. S. Richardson and D. C. Richardson (1982). Determination and analysis of the 2 Å structure of Copper, Zinc superoxide dismutase. *J Mol Biol* **160**(2): 181-217.

Tainer, J. A., E. D. Getzoff, J. S. Richardson and D. C. Richardson (1983). Structure and mechanism of Copper, Zinc superoxide dismutase. *Nature* **306**(5940): 284-7.

Tanzi, R. E., K. Petrukhin, I. Chernov, J. L. Pellequer, W. Wasco, B. Ross, D. M. Romano, E. Parano, L. Pavone, L. M. Brzustowicz and et al. (1993). The Wilson disease gene is a copper transporting ATPase with homology to the Menkes disease gene. *Nat Genet* **5**(4): 344-50.

Tao, T. Y. and J. D. Gitlin (2003). Hepatic copper metabolism: Insights from genetic disease. *Hepatology* **37**(6): 1241-7.

Telenti, A., M. Southworth, F. Alcaide, S. Daugelat, W. R. Jacobs, Jr. and F. B. Perler (1997). The *Mycobacterium xenopi gyra* protein splicing element: Characterization of a minimal intein. *J Bacteriol* **179**(20): 6378-82.

Thiele, D. J. (1988). Ace1 regulates expression of the *Saccharomyces cerevisiae* metallothionein gene. *Mol Cell Biol* **8**(7): 2745-52.

Thorvaldsen, J. L., A. K. Sewell, A. M. Tanner, J. M. Peltier, I. J. Pickering, G. N. George and D. R. Winge (1994). Mixed Cu^{+} and Zn^{2+} coordination in the DNA-binding domain of the Amt1 transcription factor from candida glabrata. *Biochemistry* **33**(32): 9566-77.

Torres, A. S., V. Petri, T. D. Rae and T. V. O'Halloran (2001). Copper stabilizes a heterodimer of the yCCS metallochaperone and its target superoxide dismutase. *J Biol Chem* **276**(42): 38410-6.

Trumbo, P., A. A. Yates, S. Schlicker and M. Poos (2001). Dietary reference intakes: Vitamin A, vitamin D, arsenic, boron, chromium, copper, iodine, iron, manganese, molybdenum, nickel, silicon, vanadium, and zinc. *J. Am. Diet. Assoc.* **101**(2): 294 - 301.

Tsukihara, T., H. Aoyama, E. Yamashita, T. Tomizaki, H. Yamaguchi, K. Shinzawa-Itoh, R. Nakashima, R. Yaono and S. Yoshikawa (1995). Structures of metal sites of oxidized bovine heart cytochrome c oxidase at 2.8 Å. *Science* **269**(5227): 1069-74.

Ullrich, V. and M. Bachschmid (2000). Superoxide as a messenger of endothelial function. *Biochem Biophys Res Commun* **278**(1): 1-8.

Vanderwerf, S. M., M. J. Cooper, I. V. Stetsenko and S. Lutsenko (2001). Copper specifically regulates intracellular phosphorylation of the Wilson's disease protein, a human copper-transporting ATPase. *J Biol Chem* **276**(39): 36289-94.

Vulpe, C. D., Y. M. Kuo, T. L. Murphy, L. Cowley, C. Askwith, N. Libina, J. Gitschier and G. J. Anderson (1999). Hephaestin, a ceruloplasmin homologue implicated in intestinal iron transport, is defective in the sla mouse. *Nat Genet* **21**(2): 195-9.

Walsh, F. M., F. J. Crosson, M. Bayley, J. McReynolds and B. J. Pearson (1977). Acute copper intoxication. Pathophysiology and therapy with a case report. *Am J Dis Child* **131**(2): 149-51.

Walshe, J. M. (1962). Wilson's disease. The presenting symptoms. *Arch Dis Child* **37**: 253-6.

Watts, D. L. (1989). The nutritional relationships of copper. *J. Orthomol. Med.* **4**(2): 99 - 108.

Weisiger, R. A. and I. Fridovich (1973). Mitochondrial superoxide dismutase. Site of synthesis and intramitochondrial localization. *J Biol Chem* **248**(13): 4793-6.

Whittaker, J. W. (1999). Oxygen reactions of the copper oxidases. *Essays Biochem* **34**: 155-72.

Wijmenga, C. and L. W. Klomp (2004). Molecular regulation of copper excretion in the liver. *Proc Nutr Soc* **63**(1): 31-9.

Winge, D. R., J. A. Graden, M. C. Posewitz, L. J. Martins, L. T. Jensen and J. R. Simon (1997). Sensors that mediate copper-specific activation and repression of gene expression. *JBIC* **2**: 2 - 10.

Xiao, Z. and A. G. Wedd (2002). A C-terminal domain of the membrane copper pump Ctr1 exchanges copper(I) with the copper chaperone Atx1. *Chem Commun (Camb)*(6): 588-9.

Yost, F. J., Jr. and I. Fridovich (1973). An iron-containing superoxide dismutase from *Escherichia coli*. *J Biol Chem* **248**(14): 4905-8.

Youn, H. D., E. J. Kim, J. H. Roe, Y. C. Hah and S. O. Kang (1996). A novel nickel-containing superoxide dismutase from *Streptomyces spp*. *Biochem J* **318 (Pt 3)**: 889-96.

Young, S. D. and P. P. Tamburini (1989). Enzymatic peptidyl alpha-amidatioin proceeds through formation of an alpha-hydrosyglycine intermediate. *J. Am. Chem. Soc* **111**(5): 1933 - 1934.

Zabinsky, S. I., J. J. Rehr, A. L. Ankudinov, R. C. Albers and M. J. Eller (1995). FEFF6: Multiple scattering calculations of X-ray absorption spectra. *Phys. Rev. B* **52**: 2995 - 3009.

Zelko, I. N., T. J. Mariani and R. J. Folz (2002). Superoxide dismutase multigene family: A comparison of the Cu, ZnSOD (SOD1), MnSOD (SOD2), and ECSOD (SOD3) gene structures, evolution, and expression. *Free Radic Biol Med* **33**(3): 337-49.

Zerounian, N. R., C. Redekosky, R. Malpe and M. C. Linder (2003). Regulation of copper absorption by copper availability in the caco-2 cell intestinal model. *Am J Physiol Gastrointest Liver Physiol* **284**(5): G739-47.

Zhou, B. and J. Gitshier (1997). Hctr1: A human gen for copper uptake identified by complementation in yeast. *Proc. Nat. Sci. USA* **94**(14): 7481 - 7486.

Zhu, H., E. Shipp, R. J. Sanchez, A. Liba, J. E. Stine, P. J. Hart, E. B. Gralla, A. M. Nersissian and J. S. Valentine (2000). Cobalt(2+) binding to human and tomato copper chaperone for superoxide dismutase: Implications for the metal ion transfer mechanism. *Biochemistry* **39**(18): 5413-21.

BIOGRAPHICAL SKETCH

I was born on November 10, 1971 in Baton Rouge, Louisiana. I began college at the Western College of Liberal Arts at Miami University in Oxford, Ohio, where I majored in chemistry and was a member of the Honor Society. My junior year of college, I transferred to The Evergreen State College where I continued my studies in chemistry and was awarded a Bachelor's of Science. At Evergreen, my senior presentation was entitled "Structure and Function of the Metal Centers in Nitrogenase" (Advisor: Dr. Darshi Bopegedra) and my senior research project was entitled "GC/MS Studies of Organic Pollutants in the Union River" (Advisor: Dr. Fred Tabutt), the latter receiving grants from both the Evergreen Fund and The Mason County, Washington DEO. After college, I first worked at the Hoodsport Winery, Hoodsport, Washington, as the laboratory technician. I then moved to New York City where I worked in the Department of Pediatrics Hematology-Oncology of the Columbia Presbyterian Medical Center of Columbia University as a Laboratory Assistant.

After Columbia, I accepted a position as a graduate student in the Blackburn lab at what was the Department of Biochemistry and Molecular Biology at the Oregon Graduate Institute, and would become the Department of Environmental and Biomolecular Systems at the Oregon Graduate Institute School of Science and Engineering of the Oregon Health and Science University. I began my studies using EPR spectroscopy to probe azide binding to peptidylglycine α-hydroxylating monooxygenase and then changed to preforming EXAFS on the human copper chaperone to superoxide dismutase, the latter of which would become

the topic for my thesis. While undertaking my graduate studies, I taught Introduction to Chemistry laboratories at both the University of Portland and the Portland Community College.

Publications

J.P. Stasser, J.F. Eisses, A.N. Barry, J.H. Kaplan,N.J. Blackburn, "Cysteine-to-serine mutants of the human copper chaperone for superoxide dismutase reveal a copper cluster at a domain III dimer interface" *Biochemistry*, **2005**,44(9):3143-52.

R.A Ghiladi, H.W. Huang, P. Moenne-Loccoz, **J. Stasser**, N.J. Blackburn, A.S. Woods, R.J. Cotter, C.D. Incarvito, A.L. Rheingold, K.D. Karlin, "Heme-copper/dioxygen adduct formation relevant to cytochrome c oxidase: spectroscopic characterization of [(6L)FeIII-(O2(2-))-CuII]+", J Biol Inorg Chem,. **2005**, 10(1):63-77.

N.M. Okeley, M. Paul, **J.P. Stasser**, N. Blackburn, W.A. van der Donk,"SpaC and NisC, the cyclases involved in subtilin and nisin biosynthesis, are zinc proteins", *Biochemistry,* **2003**, 42(46):13613-24.

J.F. Eisses, **J.P. Stasser**, M. Ralle, J.H. Kaplan, N.J. Blackburn,"Domains I and III of the human copper chaperone for superoxide dismutase interact via a cysteine-bridged Dicopper(I) cluster", *Biochemistry*, **2000**, 39(25):7337-42.